2007-03-22

Continuous Co-Separation by Liquid Absorption in Aqueous Cuprous Chloride (CuCl) and Magnesium Chloride (MgCl2) Solution

Paul J. Foster
Brigham Young University - Provo

CONTINUOUS CO SEPARATION BY LIQUID ABSORPTION IN

AQUEOUS CUPROUS CHLORIDE (CuCl) AND MAGNESIUM

CHLORIDE (MgCl$_2$) SOLUTION

by

Paul J. Foster

A thesis submitted to the faculty of

Brigham Young University

in partial fulfillment of the requirements for the degree of

Master of Science

Department of Chemical Engineering

Brigham Young University

April 2007

BRIGHAM YOUNG UNIVERSITY

GRADUATE COMMITTEE APPROVAL

of a thesis submitted by

Paul J. Foster

This thesis has been read by each member of the following graduate committee and by majority vote has been found to be satisfactory.

Date	John L. Oscarson, Chair

Date	Thomas H. Fletcher

Date	Kenneth A. Solen

BRIGHAM YOUNG UNIVERSITY

As chair of the candidate's graduate committee, I have read the thesis of Paul J. Foster in its final form and have found that (1) its format, citations, and bibliographical style are consistent and acceptable and fulfill university and department style requirements; (2) its illustrative materials including figures, tables, and charts are in place; and (3) the final manuscript is satisfactory to the graduate committee and is ready for submission to the university library.

_____   _____
Date   John Oscarson
                                                Chair, Graduate Committee

Accepted for the Department

                                              _____
                                              Larry L. Baxter
                                              Graduate Coordinator

Accepted for the College

                                              _____
                                              Alan R. Parkinson
                                              Dean, Ira A. Fulton College of Engineering
                                              and Technology

ABSTRACT

CONTINUOUS CO SEPARATION BY LIQUID ABSORPTION IN

AQUEOUS CUPROUS CHLORIDE (CuCl) AND MAGNESIUM

CHLORIDE (MgCl$_2$) SOLUTION

Paul J. Foster

Department of Chemical Engineering

Master of Science

The purpose of the research was to design, build, test, and recommend a process

to economically separate CO from a gas mixture of CO, CO$_2$, and O$_2$. The general

method considered in this research to accomplish the separation was liquid absorption in

a packed column. Several experiments were performed to identify the best process

solution to use in a prototype. The experiments, based on the COSORB process,

consisted of CuCl mixed with a complexing agent (metal tri-chloride) and a solvent

(metal tetra-chloride, toluene, ethanol, etc.). The best method consisted of an aqueous

solution of CuCl and MgCl$_2$, which has previously been used for CO absorption

experiments reported in the literature. The absorption takes place at elevated pressure (30

psig) and ambient temperature, and the stripping occurs at approximately 75 ºC.

Using the apparatus at approximate design conditions, the highest removal of CO was 88% with a product composition of 48%. The highest product composition achieved was 84%; in this case CO removal was 66%. Product composition was low because a significant amount of CO_2 physically absorbed into solution (which also decreased the pH of the solution to about 4, according to calculation). The removal of CO should increase with a taller column and higher liquid flow through the column; however, this might decrease the product composition. Advantages of this process are that the raw materials used are relatively cheap, heating and cooling requirements are lower than similar processes, and operation is relatively simple.

ACKNOWLEDGEMENTS

TABLE OF CONTENTS

LIST OF TABLES

LIST OF FIGURES

NOMENCLATURE

A   a constant, depends on nominal packing size
a   specified dumped packing surface area, ft^{-1}
a`   interfacial area, ft^{-1}
A^0_{Cu+} total Cu^+ concentration, mol/L
A_{CO} area of CO peak
A_{CO} CO absorption into solution (Section 4.1), mol/L
A_{CO2} area of CO_2 peak
A_{CS} absorber column cross-sectional area, ft^2
a_P same as a
a_{Ph} specified dumped packing surface area of gas-liquid interface, ft^{-1}
Ca_L capillary number
C_{Cl} Cl^- concentration, mol/L
C_{Cu+} Cu^+ concentration, mol/L
C_{CuCl} CuCl concentration, mol/L
C_L packing specific constant related to the liquid
C_{Mg++} Mg^{++} concentration, mol/L
C_P liquid heat capacity, J/kg·K
Cu^0 elemental copper
C_V packing specific constant related to the gas
D_G gas diffusion coefficient, ft^2/s
d_h hydraulic absorber column diameter, ft
D_L liquid diffusion coefficient, ft^2/s
d_P nominal packing size, ft
D_T absorber column diameter, inches
D^V same as D_G
e_i coefficients used in solution density equation (i = 0 to 3)
f   flooding factor
Fr_L liquid Froude number
g   gravitational acceleration, ft/s^2
G   molar gas flow rate, mol/s
H   height of packed section in absorber column, ft
H(T)   Henry's constant as a function of temperature, atm
h_L liquid holdup
k_1 absorption coefficient (dilute solutions), Pa^{-1}
k_2 absorption coefficient (concentrated solutions), Pa^{-1}
k_{CO2_CO} proportionality constant relation y_{CO2} to y_{CO}
k_Ga gas mass-transfer coefficient, s^{-1}
k^L liquid mass-transfer coefficient, ft/s

k_La liquid mass-transfer coefficient, s^{-1}

k^V vapor mass-transfer coefficient, ft/s

K_xa overall liquid, volumetric mass-transfer coefficient, $mol/ft^3 \cdot s$

L liquid molar flow rate, mol/s

σ liquid surface tension, dyne/cm

l_T absorber column length/height, ft

$\dot{m}$ liquid mass flow rate, kg/s

MW_G average gas molecular weight in absorber column

P^*_{CO} threshold pressure of CO

P_{CO} CO gas partial pressure, Pa

P_i partial pressure of component i, atm

Q energy, watts

Re'_L Reynolds number based on interfacial area

Re_V Reynolds number for vapor phase

Sc_L Schmidt number for liquid phase

Sc_V Schmidt number for vapor phase

T temperature, ºC

u'_L mean effective liquid velocity, ft/s

u_0 superficial gas velocity at flooding, in/s

u_G superficial gas velocity, ft/s

We_L liquid Weber number

x bulk CO liquid mole fraction

x_{eq} CO mole fraction that would be in equilibrium with the CO gas mole fraction

x_i mole fraction composition of component i in solution

y_{CO} mole fraction of CO in gas

y_{CO2} mole fraction of CO_2 in gas

ΔT temperature difference between hot and cold streams, K

ε void fraction

μ_L liquid viscosity, $g/ft \cdot s$

ν_G gas kinematic viscosity, ft^2/s

ν_L liquid kinematic viscosity, ft^2/s

ρ_G average gas density in column, g/mL

ρ_L solution density, g/mL

ρ^L_t liquid r, g/ft^3

σ_C packing critical surface tension, dyne/cm

σ_L liquid surface tension, N/m

Additional subscripts

c   refers to cooled liquid stream

F   feed stream

h   refers to heated liquid stream

G   product stream

g   gas

i   component i

l   liquid

1 INTRODUCTION

1.1 Overview

At high temperatures, CO_2 partially dissociates to form a gas mixture of CO_2, CO, and O_2. Jensen and Traynor have shown this can be achieved by using solar energy.[1] In their project, this mixture is then quenched to prevent complete recombination of the CO and O_2 (currently they have achieved ~12 mole % conversion of CO_2 to CO in the quenched stream). The steam generated from the quenching process can be used to produce electricity, while the CO is separated from the gas mixture and reacted with steam to form H_2 gas. The production of H_2 is the primary goal of the project.   The H_2 is then used as a fuel source while the primary byproduct, CO_2, is recycled to the start of the process.   The focus of research for this thesis is separating the CO from the $CO_2/CO/O_2$ gas mixture. To determine if the process would work, a laboratory prototype capable of continuously separating the CO from this stream was constructed.

1.2 Approach

The objective was to separate the CO from the CO_2 and O_2. The general approach to accomplish this consisted of the following steps:

1. Choose separation technique (pressure swing adsorption vs liquid absorption).

2. Conduct preliminary experiments to select the best option.

3. Design a process for the separation.

4. Construct prototype to achieve separation.

5. Test prototype to determine practicality.

6. Reconcile results with design predictions and make recommendations for scale up to a commercial process.

Sections 3 through 7 discuss these steps in detail as they were followed during the research.

1.3   Application

Although the primary objective of this project is to separate the CO for H_2 production, the process also has potential application in industrial processes which use CO as a raw material.   These include the production of olefins through hydroformylation,[2] as an intermediate in numerous processes involving C_1 chemistry,[3] and as a raw material in the production of methanol, formaldehyde, acetic acid, isocyanates, aldehydes, formic acid, pesticides, herbicides, polyurethanes, oxalic acid, dimethyl formamide, ethylene glycol, and solvents.[4, 5, 6]

2 LITERATURE REVIEW

Two methods were considered to obtain the desired separation: pressure swing adsorption (PSA) and liquid absorption. The technology involved in these two methods is generally well developed; both methods have been successfully used to separate and purify various gas mixtures.

2.1 Liquid Absorption

In 1850 Leblanc, Stas, and Doyère discovered that copper salts in HCl and ammoniacal solutions bind CO.[7, 8] Since that time, cuprous chloride (CuCl), the primary agent in binding the CO, has been used in many processes to separate and purify CO from gas mixtures. Some of these processes are summarized below.

Both solvents discovered by Leblanc in 1850 have been further developed. Of the two he discovered, the ammoniacal cuprous chloride[9] process has been used industrially, and, although not developed on an industrial scale (probably because of corrosion problems associated with the concentrated acid solution), the HCl solvent has been the object of further studies. Numerous studies discuss the use of CuCl in HCl and/or NaCl solutions to selectively bind CO, and discuss the absorption and effects of O_2 in the mixture (i.e., oxidation of Cu^+ to Cu^{++}).[10, 11, 12, 13, 14, 15, 16]

In the ammoniacal process, CO is absorbed in a solution of CuCl in NH_4Cl or aqueous NH_3, forming a carbonyl. Absorption of CO occurs at ambient temperature and elevated pressure, and decomplexation occurs at decreased pressure and elevated temperature.[9]

One study[9] reports the effects of mass-transfer and kinetics in the ammoniacal cuprous chloride solution. Not many data on this reaction and associated kinetics were previously reported. The absorption reaction in the ammoniacal process was found to be controlled by mass-transfer because of its dependence on the agitation in the experiments. It was also found that absorption rate decreased with increasing temperature (after passing through a maximum) and increased with increasing CO partial pressure and CuCl concentration.

A more economical process than its competitors, the COSORB process was developed by Tenneco Chemicals, Inc. in the 1970's.[5, 6] It was later sold to KTI, from whom much information on the COSORB process was gathered during this study. In this process[3, 20] an equimolar amount of CuCl and $AlCl_3$ are added to an excess of distilled toluene (or other organic solvent), forming a $CuAlCl_4$-toluene complex. When a gas mixture containing CO contacts the solution, the complex binds the CO while allowing the other gases to pass through. Both recovery and purity have been shown to be >98 mole % (where the pressure was 32.5 bar and the CO composition was anywhere from 14 to 70 mole % of the streams).[4, 5] The solvent absorbs CO at practical operating pressures and ambient temperature, and desorbs upon boiling.[3, 18] Although some of the components of COSORB are extremely reactive, the COSORB units are usually built with mild carbon steel, but can also be made from certain

stainless steels, copper-nickel alloys, and brass.[3] As of 1982, 14 COSORB units had

been licensed, with 7 in operation at the time.[3] The COSORB process has been used

to treat numerous types of feed streams from processes such as reforming of LPG,

coal, petroleum, and iron and steel, and typical feed streams to the COSORB process

are composed of CO, CO_2, CH_4, H_2, N_2, and O_2 (although O_2 is uncommon and

composes a very small fraction when present).[3, 17]

The literature states that the absorption of CO in COSORB is a fast reaction,[a]

resulting in the need to consider mass-transfer effects. However, not much kinetic or

mass-transfer data have been reported.[3] Similar to the ammoniacal solvent, the

absorption reaction in the COSORB process was found to be controlled by mass-

transfer because of its dependence on the agitation in the experiments.[3] Absorption

rate also decreased with increasing temperature and increased with increasing partial

pressure of CO and concentration of Cu-Al.[3] The decrease in absorption rate with

increased temperature is due to the reverse reaction having a higher activation energy

than the forward reaction.[3]

Due to environmental issues in disposing of the spent solvent, COSORB has

decreased in popularity[18] while pressure swing adsorption has increased in

popularity.[19] Challenges in the production and use of COSORB now make it a less

attractive alternative for separating and purifying CO. Stringent requirements are

necessary since COSORB reacts irreversibly with water,[18] methanol, ammonia,

hydrogen sulfide, and olefins.[4,5] The presence of even small amounts of moisture[20]

---

[a] Verified by private communications with Stan Che of KTI, 2005.[18]

(and oxygen[18, 21]) can irreversibly degrade the solvent, requiring the solvent to be replaced; the frequency of replacement depending on the rate of degradation. The quality and life of the solvent is extremely sensitive to the quality of raw materials used in its production,[20] as well as the ability to keep degrading components away from the mixture during use. Two studies present possible solutions to the problem of moisture in the solvent. In one, polystyrene[22] is introduced into the solvent, and in the other, activated carbon[23] is introduced. Both of these make the solvent water resistant. If components that cause degradation are prevented from contacting the solvent, it can last 5 years.[4]

Experiments performed in Japan reveal a number of $CuCl-MCl_n$ solutions that successfully bind CO.[24] The MCl_n compounds used included $MgCl_2$, HCl, LiCl, NaCl, NH_4Cl, KCl, $CaCl_2$, $SrCl_2$, $CoCl_2$, and $NiCl_2$. This study focused on the $CuCl-MgCl_2$ system since it behaved differently from the others, and absorbed more CO. At higher concentrations of CuCl and MCl_n, a flake, believed to be CuCl-CO, was formed in most cases except with the $MgCl_2$. At higher concentrations in the $MgCl_2$ system a fine particle, believed to be $CO{\cdot}CuMgCl_3{\cdot}nH_2O$, was formed. This compound decomposed (releasing the CO)[a] at approximately 70ºC (the temperatures at which the CO was released from the other solutions in this experiment were not reported).[24] The COSORB solution requires that it be heated to boiling (111ºC for toluene) to release the CO, accelerating the loss of toluene[23] and other solution components.

---

[a] In their work the maximum CO pressure was 101,000 Pa. It is not known how the increased overall pressure in this process affects the temperature at which CO is released.

6

Finally, an additional source summarizes several chemicals used in the separation of carbon monoxide from industrial gases, but very little process information is reported.[25] These different methods involve compounds such as $NH_4Na_2[Fe(CN)_5NH_3] \cdot 3H_2O$, $K_2Ni(CN)_3$, $CuCN$, $CuCNS$, $HOCH_2CO_2Cu$, $HOCH_2CH_2NH_2$ (I), C_5H_5N, C_6H_6-$PhNH_2$, $EtOH$, $PhOH$, $PhNH_2$, $PhMe$, cresol, and $PhNO_2$. No further details or data were included.

To summarize, several solvents employing cuprous chloride to reversibly bind CO have proven successful in separating CO from gas mixtures. Of those discussed, little is known about the rate of degradation of solutions due to the oxygen in the system.

2.2   Pressure Swing Adsorption (PSA)

Pressure swing adsorption (PSA) is also a commonly used technology in the purification of off-gas products from processes such as steam methane reforming and refineries.[26] As stated in Sircar and Golden's work,[26] "the research and development activities in this field have been very extensive during the last thirty years."

The PSA study most similar to the proposed research involved the recovery of CO from a mixture of CO and CO_2.[2] In this study, the experimenters used an activated carbon, NC30, as the adsorbent. The CO_2 was adsorbed, allowing the CO to pass through the column. Two columns, used in parallel, cycled through a pressurization stage, product recovery stage, depressurization stage, and purge. While product recovery occurred in one column, the other column was purged. The study does not include the presence of O_2 in the gas mixture.

Currently in industry, PSA is increasing in popularity. Developments in adsorption technology allow separations that would be difficult for other well-known technologies;[27] PSA is also becoming more economical,[28] and may be preferred when large flow rates are not required.[2]

2.3 Chemistry

This section summarizes studies relating to the chemistry involved with CO absorption in copper solution. A key issue is that the cuprous ion is the species that absorbs the CO. In the presence of O_2 and/or water, the cuprous ion (Cu^+) can oxidize or disproportionate to the cupric ion (Cu^{++}) and elemental copper (Cu). The following summaries of the studies (paraphrased directly from the articles) address some of these issues.

As mentioned previously, the ability of the cuprous ion to preferentially absorb CO was discovered as early as 1850.[8] These and later experiments involved Cu^+ in HCl and ammoniacal solutions. Upon absorption, the resulting compound was thought to be $Cu_2Cl_2 \cdot 2CO \cdot 4H_2O$, the ratio of CO to CuCl being 1:1.

In chemical abstracts,[25] 1931, it is reported that cuprous chloride can be formed from copper metal and cupric chloride. This reaction alone is slow, but the addition of small amounts of CO greatly speeds up the reaction. This led to the conclusion that the deterioration of the absorbent due to air oxidation can be slowed or stopped with the presence of copper metal.

In 1955, Nord[13] published some studies of Cu^+ oxidation rate in HCl solution. They determined that the rate of oxidation is proportional to the concentration of O_2

and Cu^+, and also that the rate increases as H^+ is increased (with H^+ concentration >
0.1). The proposed stoichiometry for the reaction is shown below:

$$4Cu^+ + 4H^+ + O_2 \rightarrow 4Cu^{++} + 2H_2O \qquad \text{(2-1)}$$

They proposed a several step kinetic mechanism, not shown here, and also reported
that Cu^+ in a salt solution is in the form $CuCl_2^-$.

Jhaveri and Sharma[14] published their results in 1967 on the kinetics of O_2
absorption in both neutral and acidic aqueous solutions of CuCl. They found that the
reactions were 1st and 2nd order with respect to O_2 and CuCl, respectively. They
reported the following reactions, the first under neutral conditions and the second
under acidic conditions:

$$6CuCl + 3/2O_2 + 3H_2O = (3CuO \cdot CuCl_2 \cdot 3H_2O) + 2CuCl_2 \qquad \text{(2-2)}$$

$$4CuCl + 4HCl + O_2 = 4CuCl_2 + 2H_2O \qquad \text{(2-3)}$$
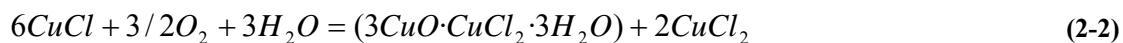
In the first case, copper oxychloride is formed along with cupric chloride,
while cupric chloride is the main product in the second case (see Equation (2-1). They
reported that the information available on oxidation in CuCl aqueous solutions is
limited, and that both diffusion and reaction kinetics may be important. Their data
show an example in which the oxidation rate is relatively slow. In a 100 mL solution

of 5M HCl at 30 ºC and a partial pressure of O_2 of 0.10 atm, the initial concentration of CuCl was 0.494M, and the final concentration of CuCl was 0.406M. The elapsed time was 15,000 seconds. This represents a conversion of Cu^+ to Cu^{++} of 18% in approximately 4 hours.

In 1970, Ahrland and Rawsthorne[31] published a study on the stability of cuprous chloride complexes. They stated that chemistry involving Cu^+ is of "special interest" but that it is difficult to experiment with because of its tendency to disproportionate (see Equation (2-4) and because of air oxidation.

$$2Cu^+ \leftrightarrow Cu^{++} + Cu^o \tag{2-4}$$

In Equation (2-4 the Cu^o represents metallic copper. Because of these difficulties, the information known about simple Cu^+ systems involving halides is limited. They report that in solution, the primary species formed from Cu^+ and chloride ions are $CuCl_2^-$ and $CuCl_3^{2-}$, and that very little $CuCl_4^{3-}$ is found. This is true for a wide range of chloride concentrations. At low concentration (< 0.01 M), CuCl might be formed. In their experiments, copper powder was added to reduce traces of Cu^{++}.

In 1970 Bruce[12] reported that there have been many claims in the literature that copper carbonyls have been formed, but that these claims are not based on sound observations, except for maybe one case. Evidence is given in his paper that showed that at high pressure, Cu(CO)Cl was formed with CO and fine CuCl powder. When CO was contacted with an HCl solution containing CuCl complexes, white, flaky crystalline deposits of Cu(CO)Cl·2H$_2$O were formed. When O_2 was present, the

uptake of O_2 competed with CO uptake, resulting in rapid oxidation of Cu^+ to Cu^{++} compounds. Absorption could be improved by addition of $SnCl_2$ or $PdCl_2$. According to his study, the absorption of CO in CuCl and H_2O solution was slow, forming $CuCl·CO·2H_2O$. In the case of the HCl solution, the absorption of CO depended on concentration (the best ratio of CuCl:HCl is 1:9), pressure, and temperature. He suggested the possibility of using other solvents such as ethanolamine and pyridine, but reported that there is no economic advantage. Among other solvents that he reported are various KCl and $MgCl_2$ solutions. The affinity of copper halides for CO is as follows: $Cu_2I_2 \ll Cu_2Br_2 < Cu_2Cl_2$.

In 1979, a study by Backén and Vestin[30] brought into question some previous studies by claiming that in aqueous HCl and KCl (with CuCl) solutions, the solid compounds formed only contained CO and CuCl—they did not contain H_2O. Their findings that the ratio of $CO:Cu^+$ is 1:1 is consistent with previous studies.

In 1981, Levy et al.[15] focused on a kinetic study of Cu^+ oxidation in concentrated NaCl solutions since few experimental data were available. The reaction shown in Equation (2-1 involves gas-liquid mass-transfer and a chemical reaction. In these experiments, large amounts of NaCl were added so there would be sufficient Cl^- ions to form complexes with Cu^+. It was found that the oxidation rate did not depend on Cu^+ or total Cu concentrations, but that it depended on the partial pressure of O_2, with a first-order dependence. Temperature also affected the rates, a maximum rate possibly occurring between 30 and 40 °C. They also showed that the rate increased a little as pH decreased and was much slower as Cl^- increased. The rate also increased

11

as the volume of the reaction vessel decreased. Experiments were performed with a starting Cu^+ concentration around 0.1M.

In 1984, Papassiopi et al.[16] studied Cu^+ oxidation in concentrated NaCl solutions. This study took place at constant temperature (22 ºC) and pH, and concentrations of Cu^+ ranging from 0.0009 to 0.0062 M. The oxidation rate was found to depend on O_2 concentration (first order) and Cu^+ concentration (order of 1.5). They report that others have found the dependence of the rate on Cu^+ concentration to be second order.

In 1985, Tran and Swinkels[11] found the dependence of $CuCl_4^{3-}$ oxidation in NaCl—HCl solutions to be first order. The dependence on O_2 was also first order, and the rate expression was also a function of H^+ concentration and temperature.

One particular study, published in 1984 by Katsumoto et al.[24] contains data on the absorption of CO in a number of $CuCl$—MCl_n solutions, the focus being on the $CuCl$—$MgCl_2$ solution. This solution demonstrated unique properties compared to the others—at higher concentrations of CuCl and $MgCl_2$ this solution formed a particle (as opposed to flakes in other systems) and absorbed more CO than the others. The data presented in their work are included here, since the solution used in their work is the focus for the current research project.

The ternary diagram for the $CuCl$-$MgCl_2$-H_2O system presented by Deringer is shown in Figure 1 (used by permission of CHIMIA, January 15, 2007).[29]

The majority of $CuCl$-$MgCl_2$ solutions in Katsumoto's work existed in the liquid region of the ternary diagram. For concentrated solutions, this system absorbed 8 times the amount of CO as did the CuCl-HCl system. Figure 2 (taken directly from

12
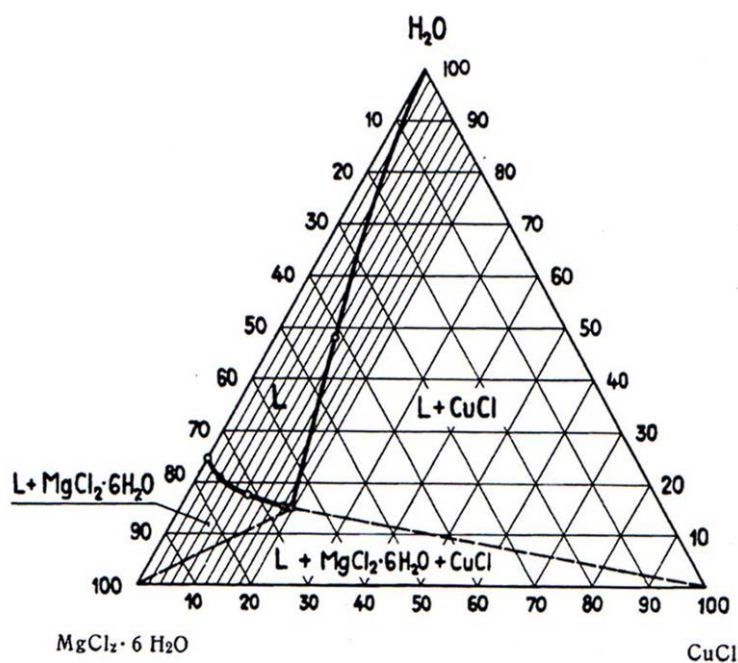
Figure 1. Ternary diagram for CuCl - MgCl₂·6H₂O - H₂O (from Deringer[29]).

Katsumoto's work) shows the absorption of CO (mol/L) versus partial pressure of CO for a number of solution concentrations (A – G). These concentrations are listed in Table 1.

The points in the figure correspond to the experimental data and the solid lines correspond to his model of the data. Lines F and G represent dilute (Cl^- < 10 mol/L) solutions. The absorption reaction is shown in Equation (2-5.

$$Cu(I) \cdot chloro - complex + CO \rightarrow CO \cdot Cu(I) \cdot chloro - complex \qquad \text{(2-5)}$$
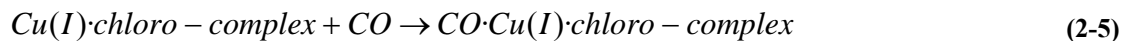
The authors describe the absorption with the following equation:
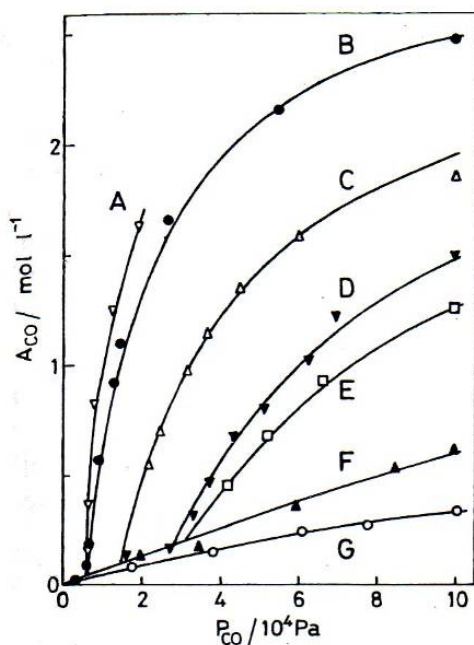
Figure 2. CO absorbed vs partial pressure at 30 ºC (from Katsumoto, et. al. [24]).

Table 1. Solution concentrations and absorption coefficients (Katsumoto) at 30 ºC.

Solution	CuCl (mol/L)	MgCl$_2$ (mol/L)	P$^*_{CO}$ (Pa)	k$_1$ (Pa^{-1})	k$_2$ (Pa^{-1})
A	3	4.8	5000	NA	$8.86(10)^{-5}$
B (s)^a	3	5	5000	NA	$5.196(10)^{-5}$
C	2.8	3.9	11600	NA	$2.625(10)^{-5}$
D (s)	3	4.0	23300	NA	$1.26(10)^{-5}$
E	2.7	3.7	24300	NA	$1.191(10)^{-5}$
F	2.2	3.3	NA	$3.725(10)^{-6}$	NA
G	0.8	2.0	NA	$6.771(10)^{-6}$	NA

^{a} s represents a suspension

$$A_{CO} = \frac{k_1 P_{CO} A^{\circ}_{Cu+}}{1 + k_1 P_{CO}} \tag{2-6}$$

where k_1 is a coefficient that depends on composition and temperature (Pa^{-1}), $A_{Cu+}^{\,o}$ is

the total Cu$^+$ concentration (mol/L), P_{CO} is the CO gas partial pressure (Pa), and A_{CO} is

14

CO absorption into solution (mol/L). The absorption of CO in these dilute solutions is similar to absorption in other types of solutions. When the solution is more concentrated (lines A – E), the absorption initially follows the same mechanism, then reaches a threshold pressure, P^*_{CO}, above which absorption increases dramatically. He suggests the following reaction as a possibility to describe the chemistry:

$$CO \cdot Cu(I) \cdot chloro-complex + Mg^{2+} + mCl^- + nH_2O \rightarrow$$
$$CO \cdot CuMgCl_3 \cdot nH_2O$$

(2-7)
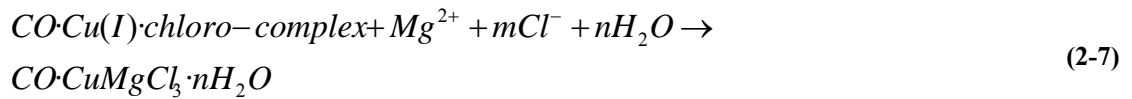
The expression for absorption in this region as a function of pressure is shown below:

$$A_{CO} = \frac{k_2(P_{CO} - P^*_{CO})A^\circ_{Cu+}}{1 + k_2(P_{CO} - P^*_{CO})}$$

(2-8)

where k_2 is a coefficient similar to k_1 and depends on composition and temperature. The solution concentrations, along with reported values of k_1, k_2, and P^*_{CO} are shown in Table 1.

It appears that, depending on the solution concentration, there is a threshold pressure above which the absorption of CO increases dramatically, due to the formation of the suggested compound, $CO \cdot CuMgCl_2 \cdot nH_2O$, which precipitates out of solution. However, exactly what causes this compound to form, and when the threshold pressure occurs, is unknown. It is also not clear whether CO absorption takes place according to both mechanisms (Equations (2-5 through (2-8) above the

threshold pressure or just one mechanism. Some of their results suggest that the formation of the $CO \cdot CuMgCl_2 \cdot nH_2O$ compound requires the presence of Cu^+ and Mg^{2+}, but there is no clear indication of their required concentrations. They observed that in the cases where Cl^- concentration exceeded 10 mol/L and where there was Cu^+ and Mg^{2+}, the compound was formed.

In their work, Katsumoto et. al. also show the temperature dependence of CO absorption in solution B (see Figure 3). As can be seen in the figure, regardless of the CO partial pressure, all CO desorbs at temperatures $\geq$ approximately 70 °C for concentrated solutions. The temperature required to release CO from dilute solutions was not reported.
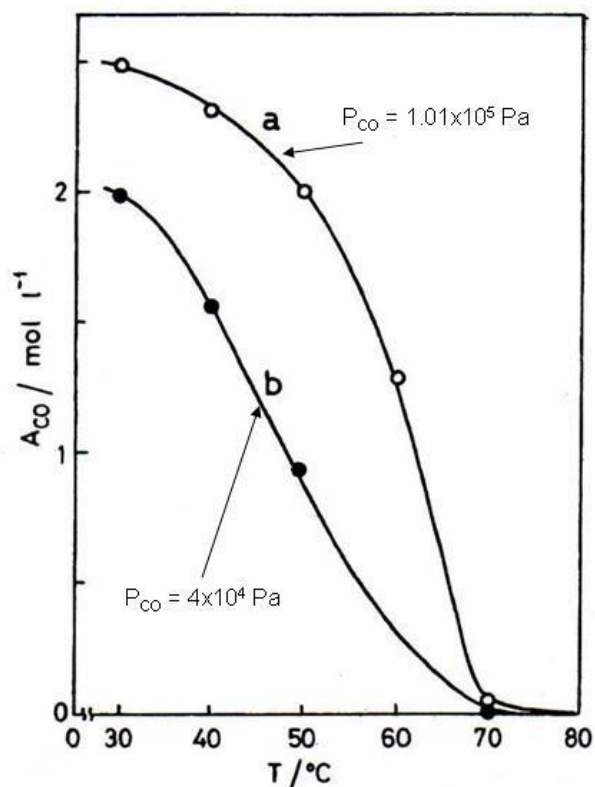
Figure 3. Absorption of CO vs temperature (from Katsumoto et. al.[24]).

To summarize the literature presented above, the copper complexes and CO compounds formed in solutions do not appear to be well known, and published reports are even contradictory in the literature. Some references indicate that copper carbonyls are certainly formed,[8, 24, 30] whereas others report no carbonyl formation.[12, 18]

In the presence of O_2 and H^+, Cu^+ is oxidized to Cu^{++}, which does not assist in the binding of CO. The rate of oxidation increases as pH decreases, and decreases as Cl^- concentration increases. Some references are made to adding metallic copper,[25] either in the form of powder[31] or small amounts of copper wire[18] to the solution to keep the Cu^+ from disproportionating or oxidizing to Cu^{++}, but not much additional detail is given. All of the literature appears to be consistent with the fact that CuCl solutions absorb CO, that it is the Cu^+ that does the absorbing, and that Cu^+ can be difficult to stabilize against disproportionation and oxidation to Cu^o and Cu^{++}. The Cu^+ is generally stabilized by having a complexing agent in the solution to form complexes with the Cu^+. Complexing agents are commonly chlorides, of the form MCl_n. It should be noted that when mixing a solution, the complexing agent should be mixed in first, allowing the Cu^+ to form a complex immediately upon entering solution. The literature is not consistent about the mechanism of absorption or compounds formed.

2.4   Project Contribution

The general techniques for separating gases are not new technologies. However, unique to this research are variations on the components of the COSORB process. Although CO has been separated from various mixtures, the separation of

CO from CO_2 and significant amounts of O_2 using liquid absorption appears to be unique to this research, as is the particular process used, as there is no known continuous separation process for CO using a CuCl-MgCl$_2$ solution.

3   STAGE ONE: PROCESS IDENTIFICATION

The work performed was divided into two stages. Ideas for the research (based on industrial practices and work reported in the literature) were developed in the first stage. This stage also consisted of preliminary experiments to narrow down the possibilities for accomplishing the separation to one preferred method. Sections 4 and 5 discuss the second stage—taking the process identification results from the first stage and building a prototype to test the separation.

3.1   Original Proposals

Originally, studying both PSA and liquid absorption was considered. Due to complexities and cost of a PSA separation, and because of ideas already formulated for liquid absorption, the scope was narrowed to liquid absorption. Complexity in a PSA separation arises from using multiple columns and having to reverse the flow during various stages to achieve the separation. This leads to a costly setup and complex operation. Table 2 shows the substrates that were considered for preliminary experiments with PSA.   No more mention of PSA will be made in this report.

On the other hand, liquid absorption has proven successful for industrial gas separations, and was adaptable to the lab and time constraints, and would be applicable to small processes such as the one proposed by Jensen.[1] Because of its

19

Table 2. Column substrates considered for preliminary tests.

Expt.	Substrate Type	Substrate
1	Zeolites	Molecular Sieve 5A
2		Molecular Sieve 13X
3	Carbon Molecular	Carboxen 1000
4	Sieves	Carboxen 1004
5		Porapak N
6	Poropak	Porapak Q
7		Porapak T
8	Silica Gels	Silica Gels
9	Activated Carbon	BPL Carbon

economic advantages, as well as its ability to absorb CO from gas mixtures with a recovery and purity of >98 % and >99 % respectively,[4] COSORB was used as a starting point for this research. However, its degradation in the presence of O_2 and stringent requirements with regard to moisture, necessitated modifying this process to better suit the needs of the present research. It was thought that replacing one or more components of the COSORB mixture with a suitable alternative might slow or eliminate the degradation from O_2 and moisture, extending the life of the solvent. Table 3 summarizes variations considered for process identification experiments. Experiment 1 utilized basic components of COSORB, experiments 2-13 consisted of variations similar to the COSORB process, and experiments 14-16 incorporated replacements for COSORB, discovered after initial stages of research.

Table 3. Liquid absorption experiments.

Expt.		Complexing Agent	Solvent
COSORB Variations			
1	CuCl	AlCl$_3$	Toluene
2	CuCl	AlCl$_3$	TiCl$_4$
3	CuCl	AlCl$_3$	VCl$_4$
4	CuCl	AlCl$_3$	SnCl$_4$
5	CuCl	AlCl$_3$	Ethanol
6	CuCl	AlCl$_3$	Acetone
7	CuCl	FeCl$_3$	Toluene
8	CuCl	InCl$_3$	Toluene
9	CuCl	GaCl$_3$	Toluene
10	CuCl	LaCl$_3$	Toluene
11	CuCl	None	TiCl$_4$
12	CuCl	None	VCl$_4$
13	CuCl	None	SnCl$_4$
COSORB Replacements			
14	CuCl	HCl	Water
15	CuCl	NaCl	Water
16	CuCl	MgCl$_2$	Water

3.2   Experimental Methodology and Results

Experiments 1 − 13 of Table 3 were performed to determine the solubility of the CuCl and complexing agents in the solvent, their compatibility with each other, and the effects of O$_2$ and small amounts of moisture.   Since a number of these chemicals are hygroscopic, experiments were performed in a glove box, shown in Figure 4.

HCl fumes and any other gas in the process were vented directly to the laboratory hood. A relative humidity sensor and de-humidifier were used inside the glove box to measure and maintain a dry environment. Relative humidity in general was maintained below 1%. Purging the glove box with nitrogen minimized oxygen

Figure 4. Glove box used in some preliminary experiments.

content. Details such as amounts of chemicals added and detailed observations upon mixing are not reported here; only a summary of results, as follows.

Upon mixing, the chemicals used in experiments 2, 5-6, and 9 reacted to form a white mist (thought to be HCl), or in the case of experiment 7, a polymer. Experiment 1 showed little solubility of $AlCl_3$ in toluene, and experiment 2 showed little solubility of both CuCl and $AlCl_3$ (separately and together) in $TiCl_4$. These options were ruled out, as well as all others involving $TiCl_4$ due to its extreme reactivity with small amounts of moisture or oxygen. Although the chemicals in experiment 9 appeared to be somewhat reactive (forming some white mist, believed to be HCl), the $GaCl_3$ was very soluble in toluene (approx. 34.7 grams $GaCl_3$ in 10 mL toluene), while the CuCl was not as soluble (addition of CuCl caused the formation of

what appeared to be metallic solids). Before trying experiments 5-6, 8, and 12-13, other alternatives were discovered which proved to be potentially more economical and less complex than the previously considered alternatives. These are shown in Table 3 as experiments 14 - 15.

Aqueous solutions of CuCl in concentrated HCl and NaCl have been found to absorb CO as reported in the literature.[7,8,24] Both were confirmed by experiments performed in the laboratory. These alternatives proved potentially useful due to the relatively inexpensive chemicals involved, as well as the fact that the components appear to be less sensitive to O_2 and moisture (the solution are aqueous) than the COSORB components. However, concentrated HCl would require handling by special materials.   These chemicals are also more benign to the environment than the COSORB chemicals.

Experiments were similar for both the NaCl and HCl process. The solution was poured into a glass tube (~1/2 inch diameter, ~1 foot long) with a septum plugging one end. Some experiments also involved adding glass beads or inert chips to help with mixing. All experiments were performed at ambient pressure. Once the tube was completely filled, a septum was inserted into the open end. To test separation, a known amount of gas sample was injected with a syringe into one end while liquid was withdrawn through a syringe from the other end to avoid pressure buildup. Shaking the tube allowed the gas to come to equilibrium with the liquid. Using a gas tight syringe, a sample of the gas was then withdrawn (while inserting liquid back into the tube to avoid pulling atmospheric air into the tube and diluting the sample) and injected immediately into a Gow-Mac Instrument Co. Series 600 Gas

Chromatograph (GC) to test composition. The GC column used was a Carboxen 1000 column, obtained from Supelco (part of Sigma-Aldrich located in Pennsylvania). A typical chromatogram of the source gas used is shown in Figure 5.
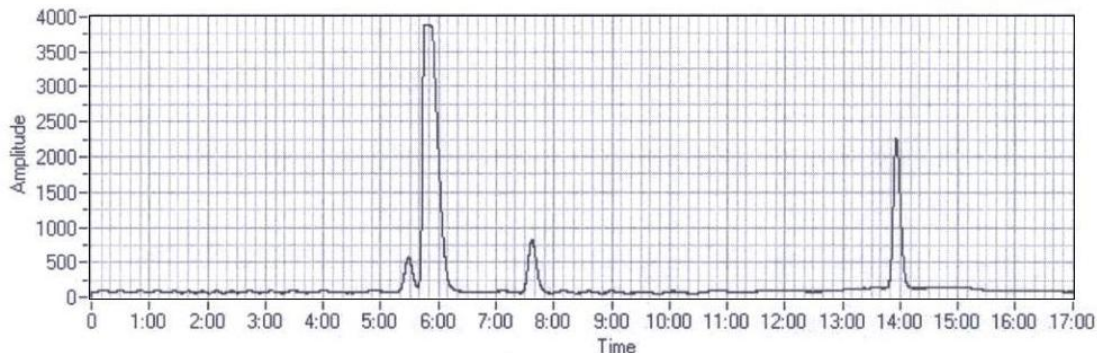
Figure 5. Typical chromatogram: O_2, N_2, CO, CO_2 from left to right.

The temperature program used started at 35 ºC, and was then ramped up to 200 ºC at 20 ºC/min, with injection sample sizes generally ranging from 200 to 400 μL.

The purpose of these experiments was to verify that the solutions separate CO from the gas mixture. To determine separation, a ratio of the CO_2 peak area to the CO peak area was compared to the same ratio of the gas standard. A typical chromatogram of the effluent gas is shown in Figure 6.

The absence of the CO peak indicates the CO was absorbed by the solution. As the experiment was repeated with the same fluid, the presence of a CO peak began to appear and increased in size with each successive experiment, indicating the saturation of CO in the solution. Note that the O_2 and N_2 peaks in Figure 6 are larger than in Figure 5 while the CO_2 peak is smaller. This was caused by dilution with

24
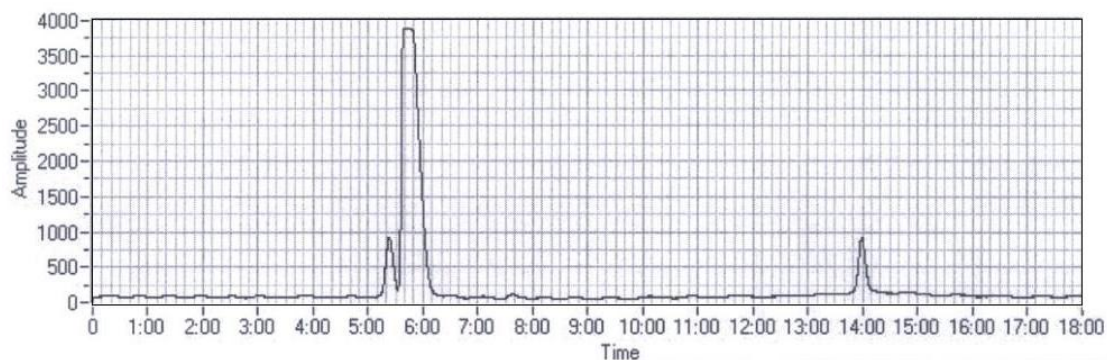
Figure 6. Chromatogram showing separation (NaCl solution): O_2, N_2, CO_2 from left to right.

atmospheric air, which was not completely eliminated during filling and which may have leaked in if positive pressure was not maintained. It is unclear how much gas was physically absorbed into solution, but was probably small since pressure was low.

To determine the reversibility of the CO absorption in solution, the saturated solution was boiled to release the CO. The solution was then cooled, and the above experiment was repeated. Again, the solution indicated absorption of CO. This was a necessary quality, as the actual process will operate continuously, the solution being cooled and heated repeatedly to absorb and release the CO.

To determine whether the solution would absorb CO after a period of aging, the solution was left in the sealed glass tube for several days. Following this period, the solution continued to absorb the CO. This is an important result for the actual process, since the separation process will be more economical if solution does not need to be replaced after a short time period. This simple glass experiment gives only a partial indication of this ability, since the solution remained stagnant in the glass tube and out of contact with gas. In the actual process, gas will be in contact with the

solution, while the solution will also be cooled, heated, and cycled through other materials continuously.

An alternate solution capable of absorbing CO was discovered in the literature[24] and involved CuCl and $MgCl_2$ (experiment 16; see also Section 2.3). The same experiments were performed with the $CuCl/MgCl_2$ solution as with the CuCl/HCl and CuCl/NaCl solutions. In these experiments, low concentrations of CuCl and $MgCl_2$ were used, so no precipitate containing CO was formed (refer to Section 2.3). These experiments showed results similar to those of the HCl and NaCl systems.

Additional tests were performed to verify the solubility of $CuCl/MgCl_2$ in aqueous solutions as shown in Figure 1 of Section 2.3. A point was chosen in the liquid region near the point of highest CuCl and $MgCl_2 \cdot 6H_2O$ concentrations, and a solution of this composition was mixed. Contrary to what is indicated by Figure 1 (this should have been the liquid region), some CuCl remained insoluble in solution. A possible explanation could be that the remaining insoluble particles in solution were impurities in the CuCl (which was 97% pure) rather than being CuCl itself.

3.3 Process Identification: Conclusion

Of all options considered or tested in the preliminary experiments, the last three discussed (CuCl/HCl, CuCl/NaCl, $CuCl/MgCl_2$) were the most feasible. Experiments confirmed that these aqueous solutions absorb CO. Both the CuCl/HCl system and $CuCl/MgCl_2$ system continued to absorb CO for long periods of time, even after being heated and releasing the CO. The HCl and $MgCl_2$ are readily available and relatively inexpensive. However, $MgCl_2$ has the additional advantage of not being as

corrosive as HCl, and CO absorption capacity of the $CuCl/MgCl_2$ system is greater than other systems when it is at high concentrations (absorption capacity may be similar at lower concentrations). A concentrated $CuCl/MgCl_2$ system releases almost all CO when heated to a temperature of about 70 - 75 ºC. The temperature at which the other aqueous solutions (as well as dilute $CuCl/MgCl_2$ solutions) release the CO is unknown, but the COSORB process requires the solution to be heated to boiling (approximately 111 ºC). This is a significant advantage since operating costs are reduced by the reduced heating and cooling requirements. Due to these significant advantages, the solution consisting of CuCl and $MgCl_2$ became the solution of choice. The next stage of the project was the design of an absorber and construction of a prototype to test separation in a practical process.

4   STAGE TWO: PROTOTYPE DESIGN

After determining the method (liquid absorption) and solution (CuCl/MgCl$_2$) to use for the separation, the next step was to design and build a prototype to test the separation in a practical process. Following a description on how CO absorption into solution was accounted for, this section describes the general design of the absorber as well as required heat exchangers. Other equipment used in the prototype, such as pumps, tubing, variacs, vessels, etc. are described in the appendix.

4.1   Equilibrium Model for CO Absorption

The CO absorption data were presented in Section 2.3. Katsumoto[24] developed a model (see Equations (2-6 and (2-7) which matches his reported data. The reported absorption coefficients and threshold pressures are shown in Table 1. However, no explanation of the derivation of his model was included, and efforts to contact him for details were unsuccessful. Since no model could be derived from theory that followed his data, and since it was necessary to have a model that could estimate CO absorption into liquid as a function of CO partial pressure and CuCl and MgCl$_2$ concentrations in solution, the following method was used.

The absorption coefficients and threshold pressures (as shown in Table 1) for each solution were plotted versus concentration of CuCl or Cl$^-$ and a line was fitted

through the data. A linear line was used for the absorption coefficients, and a power law was used for the threshold pressures. Unfortunately, there were only two points to use for the dilute cases and three for the concentrated cases. For these particular cases, the fit was very good, as would be expected. Following are the equations of the lines:

$$k_1 = -2.18 \cdot 10^{-6} C_{CuCl} + 8.51 \cdot 10^{-6} \qquad \text{(4-1)}$$

$$k_2 = 3.08 \cdot 10^{-5} C_{Cl} - 3.00 \cdot 10^{-4} \qquad \text{(4-2)}$$

$$P_{CO}^* = 4.62 \cdot 10^{10} \left(C_{CuCl} \right)^{-14.64} \qquad \text{(4-3)}$$

where subscript 1 refers to dilute solutions (C_{Cl^-} < 10 mol/L), 2 refers to concentrated solutions (C_{Cl^-} > 10 mol/L), C is concentration (mol/L), and k has units of Pa^{-1}.

Application of these equations gives coefficients that are used in Katsumoto's model to predict CO absorption. As these coefficients are based on limited data, this model should only be used for solutions if they are very close to the reported values.

4.2 Absorber

The absorber was a cylindrical, packed column in which the liquid and gas contacted each other countercurrently, providing as much contact as possible between the gas and liquid phases to promote mass-transfer of CO from the gas to the liquid, while allowing the gas and liquid to flow at reasonable rates through the column. The primary parameters needed to build the prototype absorber were the diameter and height. Numerous attempts have been made by scientists and engineers to formulate correlations that can be used in the design of gas-liquid, counter-current, packed

columns. An ideal correlation for the packed column in consideration was not known to exist, and different diameters and heights were estimated.

The general method followed for estimating diameter and height is outlined in Separation Process Principles.[32] Based on gas and liquid compositions, an estimate of the diameter and height of a commercial column were determined. Calculating gas and liquid compositions required experiments to determine the solution density. This section first describes how solution density was calculated, and then explains the basic theory used to determine the required column diameter and height. The appendix shows a sample of the Mathcad program which allows a user to input basic parameters such as: pressure, temperature, inlet and outlet gas composition, concentration of CuCl and $MgCl_2$ in the solution, packing characteristics, flooding factor, and minimum liquid flow rate factor, and which then calculates flow rates, diameter, height. This program was used to predict the size of a commercial column as well as the prototype column used in the laboratory. Experimental results obtained from the prototype were then used to more accurately estimate the required size of a commercial column.

4.2.1 Solution Density

Three different methods were used to estimate solution density. In the first method, individual volumes of the solids in solution were determined from their solid densities and experimental concentrations, and water volume was found by difference. Individual component masses (including water) in one liter of solution were then found, which led to solution density. The second method involved measuring several densities and deriving a correlation based on a factorial analysis. Method 3 combined densities of individual CuCl and $MgCl_2$ solutions reported in Perry's Handbook.[33] A

31

comparison of these methods compared to the measured densities is shown in Figure 7 and Figure 8.
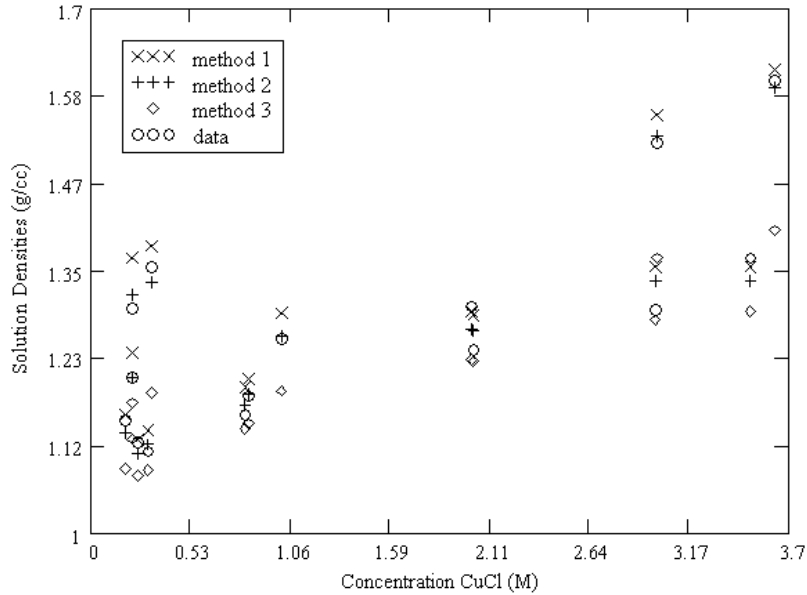
Figure 7. Solution densities as a function of CuCl concentration.   These points are also at different MgCl₂ concentrations.

As can be seen, method one in general predicted a high solution density, method three predicted a slightly low solution density, and method two correlates best with the data. Method 2 was used in the design and uses the following equation:

$$\rho_L = e_0 + e_1 C_{Cu+} + e_2 C_{Mg++} + e_3 C_{Cu+} C_{Mg++}$$

(4-4)

where ρ_L is the solution density (g/mL), the e's are coefficients (0.9949, 0.0673,

0.0635, and 0.0023 respectively) derived from the factorial analysis, and C is concentration (mol/L).
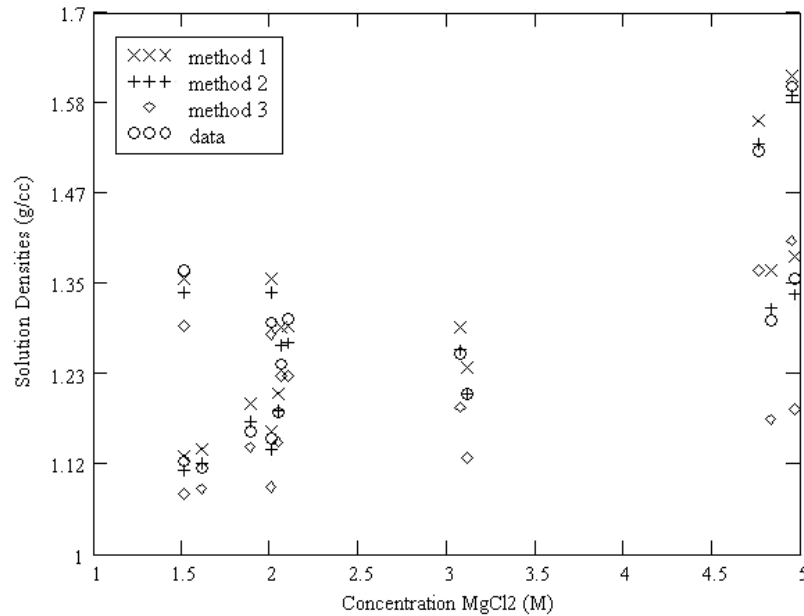
Figure 8. Solution densities as a function of MgCl$_2$ concentration. These points are also at different CuCl concentrations.

4.2.2 Column Diameter

The following equation was used to calculate the column diameter:[32]

$$D_T = \left(\frac{4 \cdot G \cdot MW_G}{f \cdot u_o \cdot \pi \cdot \rho_G} \right)^{1/2}$$
(4-5)

where D_T is the column diameter (inches), G is the molar gas flow rate, MW_G is the average gas molecular weight in the column, f is the flooding factor, u_o is the superficial gas velocity at flooding (in/s), and ρ_G is the average gas density in the

column (g/in^3). The flooding factor is usually chosen to be in the range of 0.5 to 0.7,[32] ensuring that the column will operate in the preloading region. Numerous calculations were performed to obtain the variables in this equation, most of which can be seen in the appendix and the original reference.[32] Some details unique to this research are presented here.

Figure 9 shows the calculated equilibrium plot (at 30 psi). The absorber operating line, representing the equation derived from a material balance around the absorber, is also plotted. The operating line (whose slope is a ratio of the liquid flow rate to the gas flow rate) lies above the equilibrium line, indicating transfer of the solute from the gas phase to the liquid phase. The steepness of the operating line indicates the large liquid flow rate compared to the gas flow rate.

Once all factors in Equation (4-5 were estimated, the diameter could be calculated. The predicted diameter of the column for Jensen's proposed process was approximately 12 inches (seeTable 4).

4.2.3   Column Height

As with the diameter, the general procedure followed for calculating column height is described primarily in reference 32. The procedure involved performing a material balance on a differential height of the column with a simplified model for mass-transfer between phases. Once the overall expression for the height was obtained, the overall mass-transfer coefficient was estimated from correlations. This was a significant challenge since no ideal correlation exists—this led to variation in its value, and therefore variation in the predicted column height. A number of methods
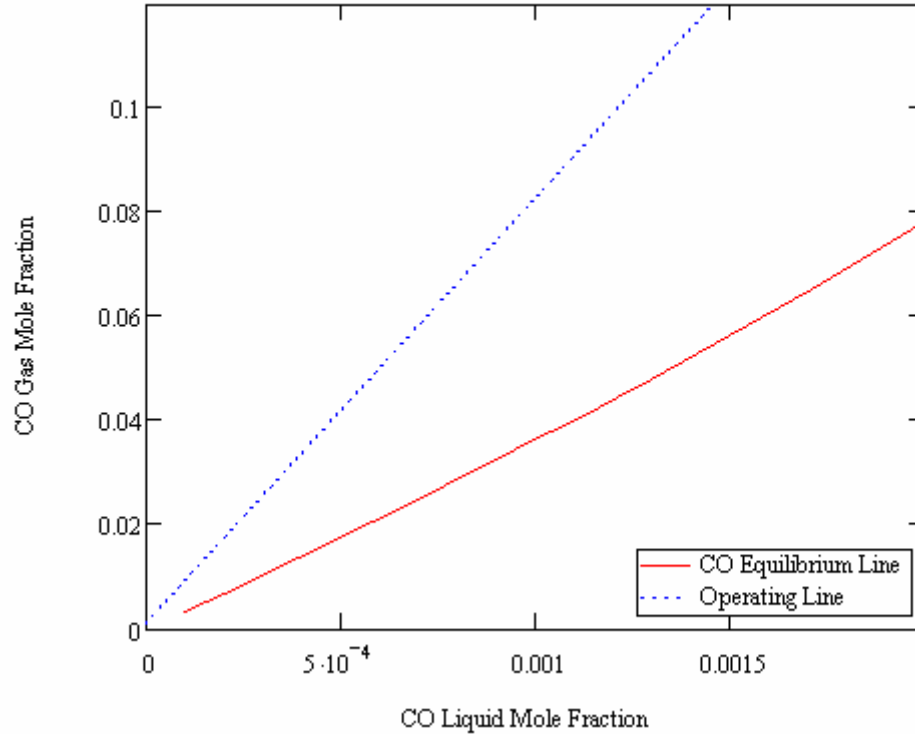
Figure 9. Equilibrium of CO in a dilute solution (0.8 M CuCl, 2.0 M MgCl₂).

were used in this project to predict mass-transfer coefficients, including that of Billet and Schultes,[34] Bravo and Fair,[35] and Onda.[36] The latter two are presented by Taylor and Krishna in Multicomponent Mass-transfer.[37]

The model used in the material balance is that of a liquid phase passing down the column and in contact with a gas phase rising through the column, with transfer of CO from the gas phase to the liquid phase across the interface. Details are included in the appendix and in reference 32. The final equation for calculating the column height is:

$$l_T = \left(\frac{L}{K_x a \cdot A_{CS}} \right) \cdot \left(\int \frac{dx}{x_{eq} - x} \right) \qquad \text{(4-6)}$$

where l_T is the column height, L is the liquid molar flow rate, dx is the differential mole fraction of CO across a differential length dl, $K_x a$ is the overall volumetric mass-transfer coefficient based on the liquid, x_{eq} is the liquid mole fraction that would be in equilibrium with the gas mole fraction, x is the bulk liquid mole fraction, and A_{CS} is the cross sectional area of the column. The first quantity on the right hand side is referred to as H_{OL}, the overall height of a mass-transfer unit based on the liquid phase, and the second quantity is referred to as N_{OL}, the overall number of mass-transfer units based on the liquid phase.[32]

Assuming the solution is dilute and that the equilibrium curve is approximately linear, the overall mass-transfer coefficient based on the liquid, $K_x a$, can be described in terms of individual coefficients of the gas and liquid phases. These can be determined from correlations found in the literature, and, for this research, three sets of correlations are presented. The first set presented is by Billet and Schultes,[34] the general equations being shown in Equations (4-7 and (4-8. These correlations are based on 3500 measurements, and take into account the physical characteristics of the system for over 70 arranged and random packings.[34] The liquid mass-transfer coefficient, $k_L a$ (s^{-1}), is defined in Equation (4-7).

$$k_L a = C_L \cdot 12^{1/6} \cdot u_L^{'\,1/2} \cdot \left(\frac{D_L}{d_h}\right)^{1/2} \cdot a \cdot \frac{a_{Ph}}{a} \tag{4-7}$$

where C_L is a packing-specific constant (related to the liquid) found in a table in references 32 and 34, $u_L^{'}$ is mean effective liquid velocity (ft/s), D_L is the liquid diffusion coefficient (ft^2/s), d_h is the hydraulic diameter (ft), a is specified dumped

36

packing surface area (ft^{-1}), and a_{Ph} is the specified dumped packing surface area at the interface (ft^{-1}). The gas mass-transfer coefficient, k_Ga (s^{-1}), is defined in Equation (4-8).

$$k_Ga = C_V \cdot \frac{1}{(\varepsilon - h_L)^{1/2}} \cdot \frac{a^{3/2}}{d_h^{1/2}} \cdot D_G \cdot \left(\frac{u_G}{a \cdot \nu_G}\right)^{3/4} \cdot \left(\frac{\nu_G}{D_G}\right)^{1/3} \cdot \left(\frac{a_{Ph}}{a}\right) \tag{4-8}$$

where C_V is a packing-specific constant (related to the gas) found in a table in references 32 and 34, ε is the void fraction, h_L is the liquid holdup, u_G is the superficial gas velocity (ft/s), D_G is the gas diffusion coefficient (ft^2/s), and ν_G is the kinematic viscosity of the gas (ft^2/s). In the above correlations, a_{Ph} was found from an additional correlation which depends on d_h, a (dumped packing surface area), u_L, ν_L (kinematic viscosity of the liquid), ρ_L, σ_L (surface tension of the liquid, taken as water at ambient temperature), and g, gravitational acceleration.

Diffusion coefficients for the gas were calculated from the Chapman-Enskog theory (using Lennard-Jones parameters),[38] which applies to low-density, low-pressure gas. The liquid diffusion coefficients were calculated from a method explained by Prausnitz.[39] The second method used to calculate mass-transfer coefficients is explained in <u>Multicomponent Mass-transfer</u>,[37] which presents a correlation by Onda.[36] Equation(4-9 shows the correlation for the gas mass-transfer coefficient:

$$k^V / (a_P D^V) = A \, Re_V^{0.7} \, Sc_V^{0.333} (a_P d_P)^{-2} \tag{4-9}$$

where k^V is the vapor mass-transfer coefficient (ft/s), a_P is the specific surface area of packing (ft²/ft³), D^V is the vapor diffusion coefficient (ft²/s), A is a constant that depends on d_P (ft), the nominal packing size, Re_V is the Reynolds number for the vapor phase, and Sc_V is the Schmidt number for the vapor phase. Similarly, the liquid mass-transfer coefficient was calculated from the following correlation:

$$k^L(\rho_t^L / \mu_L g)^{0.333} = 0.0051(Re'_L)^{0.667} Sc_L^{-0.5}(a_P d_P)^{0.4} \qquad \textbf{(4-10)}$$

where k^L is the liquid mass-transfer coefficient (ft/s), ρ_t^L is density (g/ft³), μ_L is viscosity (g/ft·s), $Re`_L$ is the Reynolds number for the liquid based on interfacial area, and Sc_L is the Schmidt number for the liquid.

The third method, presented in the same text,[37] was developed by Bravo and Fair.[35] They use the same method for the mass-transfer coefficients, but they calculate interfacial area density differently than does Onda. Onda's[36] correlation for interfacial area density is shown in Equation (4-11, and Bravo and Fair's[35] is shown in Equation (4-12).

$$a' = a_P[1 - \exp\{-1.45(\sigma_c / \sigma)^{0.75} Re_L^{0.1} Fr_L^{-0.05} We_L^{0.2}\}] \qquad \textbf{(4-11)}$$

where a' is the interfacial area density (ft⁻¹), σ_c is packing critical surface tension (dyne/cm), σ is liquid surface tension (dyne/cm), Fr_L is the Froude number for the liquid phase, and We_L is the Weber number for the liquid phase.

$$a' = 19.78 a_P (Ca_L \, Re_V)^{0.392} \sigma^{0.5} / H^{0.4}$$

(4-12)

where Ca_L is the capillary number, and H is the packed section height (ft).

Once individual mass-transfer coefficients $k_L a$ and $k_G a$ were calculated (calculated by solving for k^L and k^V and multiplying by a`), the ratio $k_G a/k_L a$ was taken. The large values obtained (~24) confirmed the relative insignificance of gas mass-transfer resistance when compared to the resistance to mass-transfer in the liquid phase. These resistances are large compared to the reversible reaction of CO with Cu^+, which is assumed very fast.

Once the diameter and height of the actual column were calculated for the full-scale process, it was necessary to scale it down to a size that could be experimented with in the laboratory. A column inner diameter of 1 inch was chosen for the prototype, and it was scaled down by taking a ratio of the cross-sectional area of the prototype to the full-scale column and adjusting the flow rates for the prototype by the same ratio, while leaving the height the same.

There were some implications associated with the scale-down of the actual column. For example, to minimize wall effects in the separation, the diameter of the packing particles should be no greater than $1/8^{th}$ of the column diameter. Upon reducing the diameter of the column to 1 inch, the packing particle diameter should have been no larger than $1/8^{th}$ of an inch (3.2 mm). Unfortunately, a search for a suitable packing material after construction of the column revealed that new generation packing material this size is rare and expensive. The only known readily available and inexpensive option was to use 3 mm glass beads. However, due to the

39

low void space and other issues, flow rates had to be reduced significantly to avoid complete entrainment. Due to practicality issues, 6 mm glass beads were used instead, probably making wall effects a significant factor in the separation since the beads were approximately 1/4th the column diameter. The design calculations use 6 mm beads.

A further implication is that the predicted diameter and height of the prototype column changed after it was built as adjustments were made to the calculation program, more applicable correlations were found, and different packing was used.

In conclusion, the height of the column, as constructed (4 feet), does not match the height as calculated by the changed design, and would predictably not separate according to design (>99% CO removal). However, it was still used to obtain results that were useful in understanding how well an actual full-scale absorber might behave. A summary of the calculated mass-transfer coefficients, diameters, and heights are shown in Table 4. The concentration of the solution used was 0.8 M CuCl and 2.0 M $MgCl_2$; feed gas composition was 11.1% CO, 29.99% CO_2, 2.647% O_2, balance N_2; feed gas temperature was 20 ºC; feed gas flow rate was 0.2 mol/sec;[a] feed gas pressure was 30 psig; and liquid temperature in the column was 15 ºC.[a] The feed gas composition differed from the original specified mixture in that the laboratory mixture had to contain significant N_2 due to safety issues. The presence of N_2 was not expected to significantly affect the design parameters of the column. Note that the

---

[a] This value comes from the original proposal.

Billet and Schultes correlation is not used for spherical packing—it was included here (using 15 mm ceramic Raschig rings) as a comparison.

Table 4. Predicted column mass-transfer coefficients, diameter, and height.

Correlation → Parameter ↓	Billet & Schultes[24]	Bravo & Fair[35]	Onda[36]
$k_L a\ (s^{-1})$	0.024	0.015	0.015
$k_G a\ (s^{-1})$	0.99	0.362	0.362
Diameter (in)	10.0	12.4	12.4
Height (ft)	4.45	5.12	5.05
L/G^a	90.9	91.8	91.8
$D_{Tower}/D_{Packing}$	16.8	52.3	52.3

[a] Solute free.

It should be noted that numerous correlations and assumptions throughout the design lead to inaccuracies in the predicted diameter and height of the column. These values are approximate.

4.3 Heat Exchangers

Once flow rates for the absorber were calculated, the required heat addition and removal were calculated, along with the heat-exchanger sizes. A sample Mathcad program that determines the heat-exchanger sizes is included in the appendix. General stream properties used in the calculations were obtained using the DIPPR[40] database, and in some cases pure water properties rather than solution properties were assumed to simplify the calculations.

---

[a] In the original proposal this temperature was closer to 20º C, but 15º C was used to more closer match what actually occurred in the experiments.

The first heat exchanger was used to heat the CO-containing liquid exiting the absorber from < 20 ℃ to approximately 75 ℃[a] to release the separated CO. The liquid was heated by wrapped electric heating ropes around the coiled process line. In all, five Omegalux® ropes (purchased from Omega Engineering, Inc.) were obtained, rated at 500 watts each with a 3/16 inch diameter and 10 foot length. The process line extended from the bottom of the absorber, formed a "p trap" (180° bend), then coiled upward toward the CO separation point (see Figure 10). This design allowed any CO coming out of solution prior to the separation point to travel toward the separation point, rather then re-enter the column. This arrangement also helped to prevent inlet gas from bypassing the column and traveling through the liquid exit line, which the original design failed to prevent.

The energy required to heat the solution was calculated from the following equation:

$$Q = \dot{m} \cdot C_P \cdot \Delta T \tag{4-13}$$

where Q is the energy (W), $\dot{m}$ is the liquid mass flow rate (kg/s), C_P is the liquid heat capacity (J/kg·K), and ΔT is the temperature increase required for the stream (K). This equation provided only an estimate as it neglected the heat of desorption of CO from the liquid. However, it still provided a conservative estimate since the actual flow rate decreased from the original maximum design value of 10 GPH to approximately 2 GPH. Using this flow rate, the energy requirement

---

[a] Katsumoto et. al.[24] report that this temperature applies to the decomposition of the solid CO compound. Since no information was given for releasing CO from dilute solutions, this value had to be

Figure 10. Heat exchanger used to heat liquid stream, E-101.

was calculated to be approximately 2300 watts, a conservative estimate. The ropes had the potential of providing 2500 watts; to mitigate heat loss to the surroundings, the entire portion containing the ropes was wrapped with high temperature insulation.[a]

The second heat exchanger, used to cool the liquid stream from 75 ºC back to < 20 ºC, was the largest of the three heat exchangers. It was a cylindrical shell-and-tube type exchanger, the main body being 8 inches outside diameter and 30 inches long (see Figure 11).

The shell, built by the Precision Machining Lab (PML) on BYU campus, was made of carbon steel, and consisted of a flange on one end to allow insertion of and

assumed for dilute solutions in this research.

Figure 11. Heat exchanger used to cool liquid stream, E-102.

maintenance on the copper tubing on the inside. The cooling water flowed through the

shell portion while the process stream flowed through the tube portion, which

consisted of approximately 40 feet of coiled ¼-inch copper tubing. The length of

copper tubing was calculated using typical heat-transfer correlations using the log

mean temperature difference. Details are shown in the appendix.

The third heat exchanger, also made by the PML on campus, was used to cool

the hot CO gas and condense water vapor. It was similar to the second heat

exchanger, but made of aluminum, and was 3 inches in diameter, and 18 inches long

(see Figure 12). The inside was later coated with high-temperature paint because of its

relatively close proximity to the solution, which was found to corrode aluminum. In

[a] This was later found to be unnecessary, as the actual flow rate was much smaller than design.

44

this case, the cooling water passed through the coil of ¼-inch copper tubing on the inside while the gas passed vertically upward through the main cavity. The bottom flange was sloped to allow condensed vapor to run out the bottom of the shell and back into the 1 inch diameter opening into the liquid. The spiraled ¼ inch tubing on the inside was approximately 3 feet long, much more conservative than necessary according to original calculations. Detailed calculations are included in the appendix. Cooling water was supplied in the lab and flowed first through E-103, and then through E-102.

Values calculated for required heat removal or heat addition based on a solution containing 0.8M CuCl and 2.0M MgCl$_2$ are shown in Table 5.

Figure 12. Heat exchanger (E-103) used to cool CO gas and condense water vapor.

Table 5. Heat requirement and heat exchanger size.

Heat Exchanger	Heat Requirement (W)	Tube Length (ft)
1	631	7
2	631	30.5
3	0.23	0.10

5 STAGE TWO: PROTOTYPE EXPERIMENTS

5.1 Basic Operation

A simple block diagram of how the industrial process would work is shown in Figure 13.
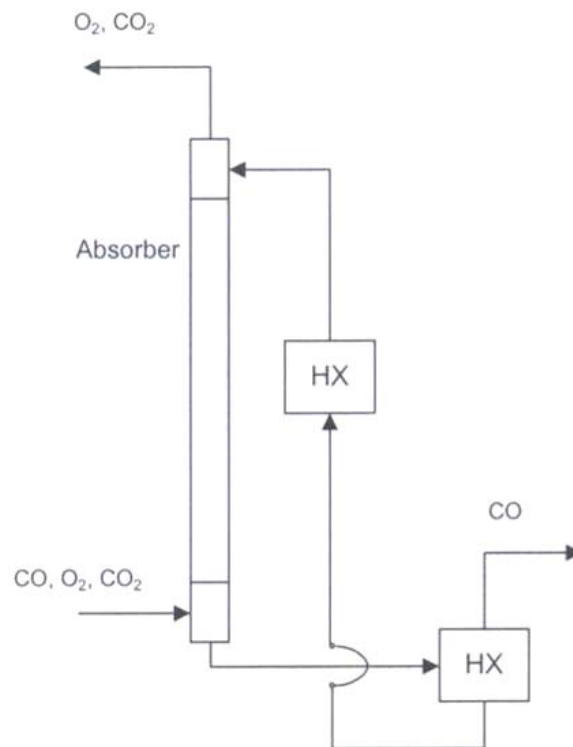

Figure 13. Simple block diagram of actual CO separation process.

In this ideal process, the feed stream enters the bottom of the column, with all O_2 and CO_2 passing through the column and all CO being absorbed by the solution passing down through the column. The CO-containing liquid is heated, releasing the CO, and then cooled prior to re-entry into the column.

Since the feed gas composition of the industrial process (13% CO, 6.5% O_2, balance CO_2) is combustible, an alternative gas mixture was used in the laboratory. Initially, this mixture contained 7% CO, 5% O_2, and 15% CO_2 (balance N_2). This safe mixture has all of the necessary components and was still safe to use in the research. However, due to the cost of this gas source, a modification was made to the prototype design in which the gas could be recycled. This basic process, hereafter referred to as Version 1, is shown in Figure 14.
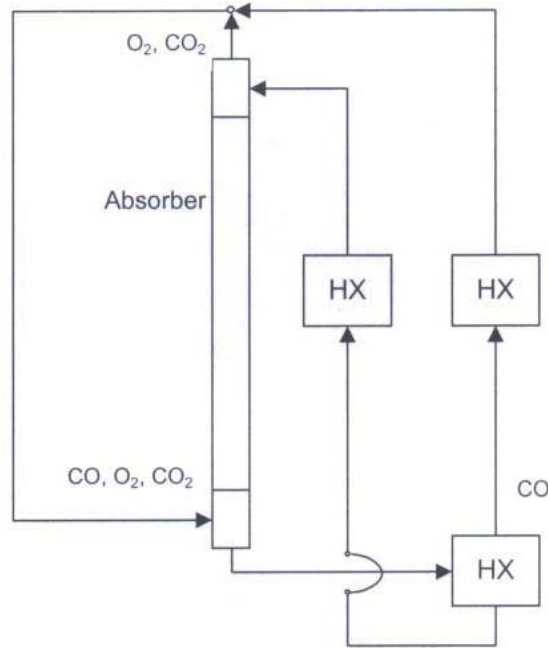

Figure 14. Simple block diagram of CO separation process with recycle.

In this process, the removed CO was cooled and recombined with the column offgas prior to re-entry into the column. (Note: although not shown in the figure, the system also contained nitrogen.) A simplified process flow and instrumentation diagram of Version 1 of the prototype is shown in Figure 15. See the appendix for additional details.
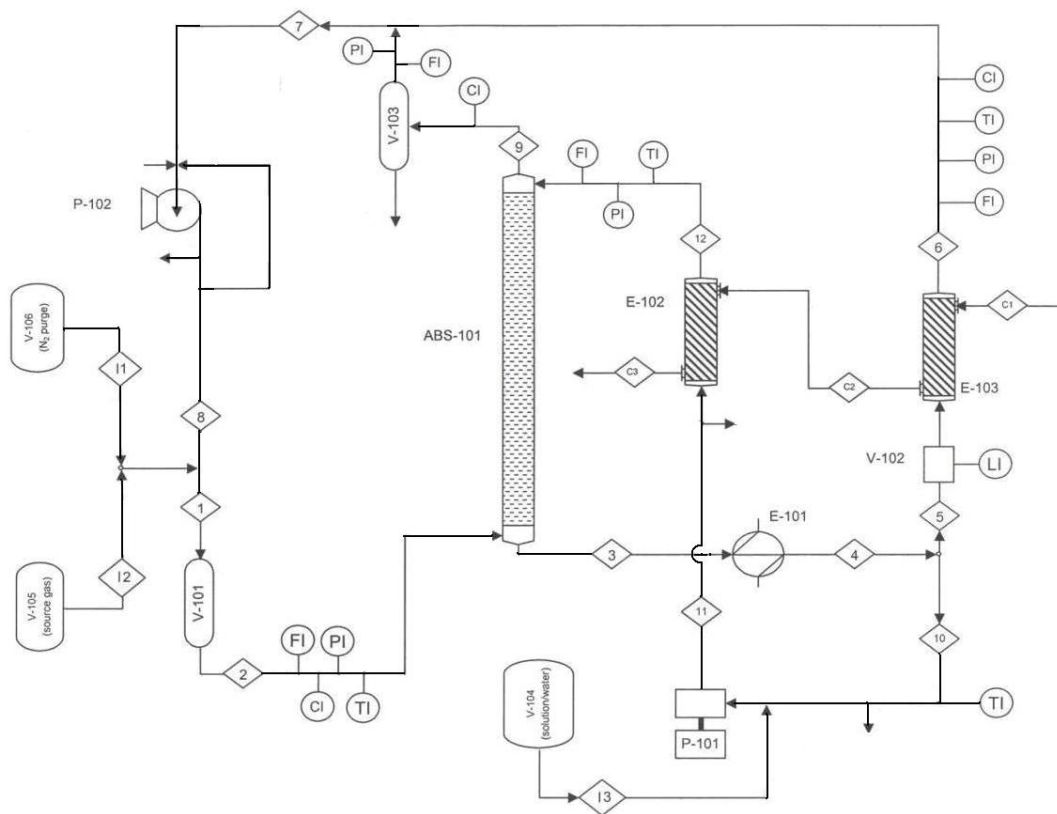

Figure 15. Process flow and instrumentation diagram, Version 1.

Following is an explanation of symbols used: FI, CI, PI, TI, and LI are flow, composition, pressure, temperature, and level indicators, respectively; ABS, E, V, and P represent absorber, heat exchanger, vessel, and pump respectively; and the

numbered diamonds refer to stream names (the numbers preceded by "I" or "c" are inlet and cooling streams, respectively).

The entire process was built onto a custom cart constructed of 2 x 4's and was approximately 2 feet wide by 3 ½ feet tall by 3½ feet long. The apparatus, shown in Figure 16, was built on a set of casters, which enabled the unit to be portable.
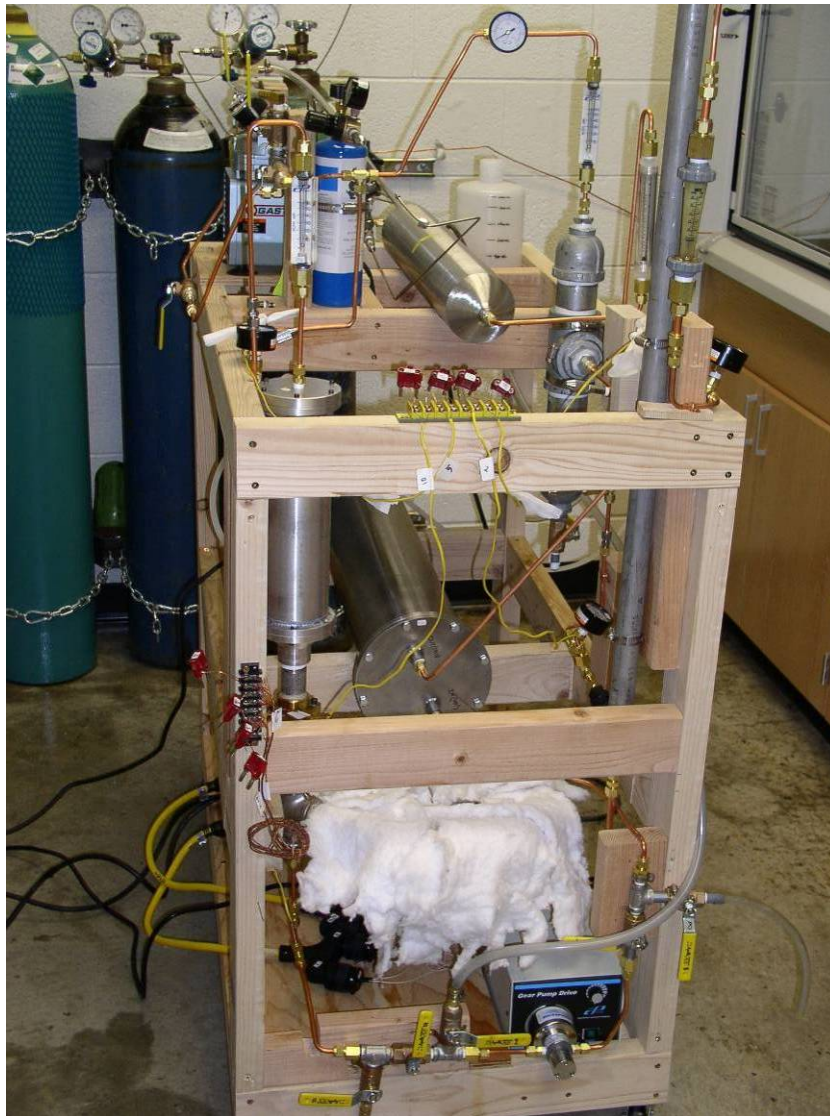

Figure 16. Constructed prototype, Version 1.

Three initial experiments were performed using this version of the prototype, during which much was learned, leading to modifications. Because of difficulties controlling the process during startup, and significant gas leaks from the recycle pump, this version of the prototype was modified to resemble the actual process, shown in Figure 13. A less expensive source of gas was also found and was used in the remaining experiments. This gas was composed of 11% CO, 2.6% O_2, and 30% CO_2 (balance N_2). This single-pass version of the prototype, Version 2, is shown in Figure 17.

As in Figure 15, symbols are as follows: FI, CI, PI, TI, and LI are flow, composition, pressure, temperature, and level indicators, respectively; ABS, E, V, and P represent absorber, heat exchanger, vessel, and pump respectively; and the numbered diamonds refer to stream names (the numbers preceded by "I" or "c" are inlet and cooling streams, respectively).

In this version, the separated CO and column offgas were vented to the hood rather than being recombined to be recycled to the gas inlet. Besides eliminating the gas pump portion of the prototype, a major difference included the addition of valves on the two gas outlet streams, which were used to control flow rates and maintain the proper system pressure (to achieve steady state flow rates and proper liquid levels in the apparatus, Streams 6 and 7 had to be connected). Although Version 1 could be used at lower pressures, Version 2 was used to obtain results at 30 psig, the original design specification.
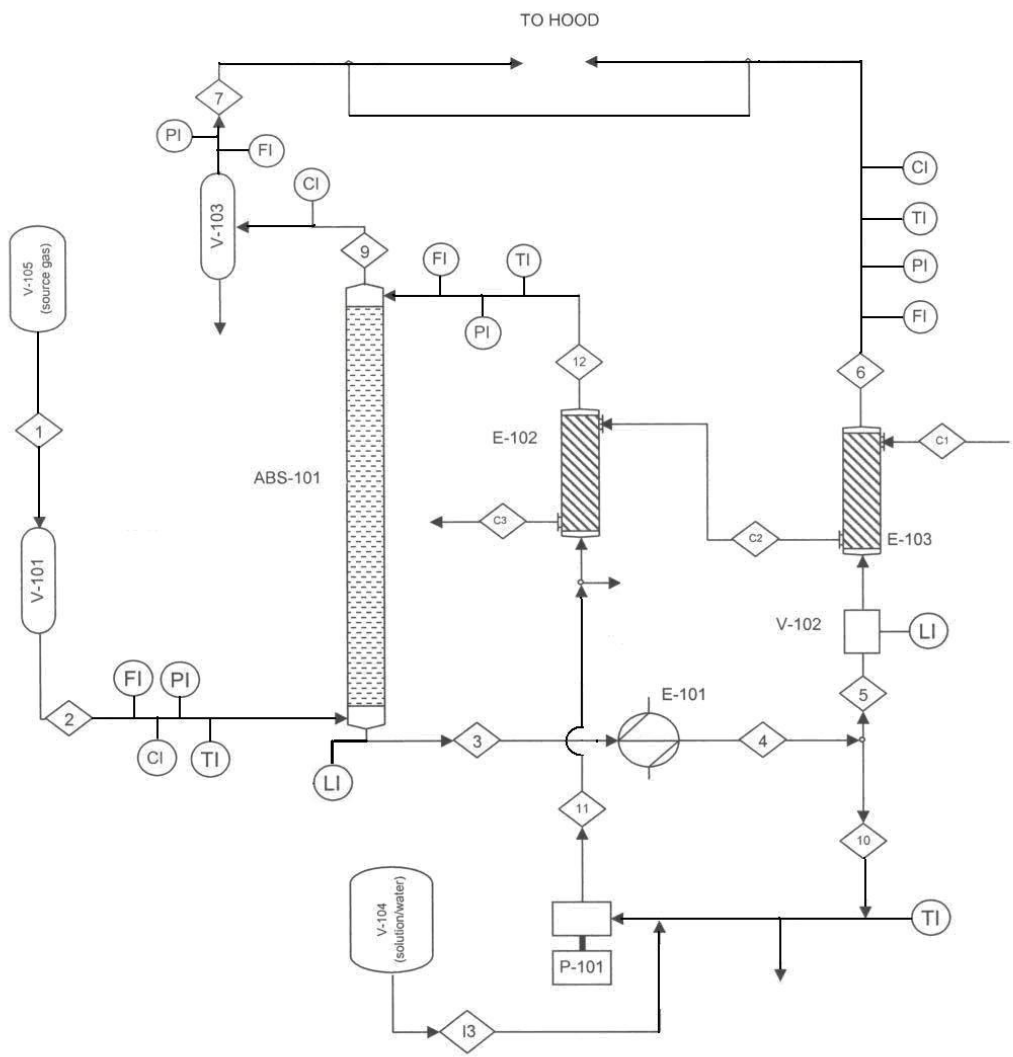
Figure 17. Process flow and instrumentation diagram, Version 2.

5.2 Detailed Operation

The apparatus was connected to a nitrogen gas cylinder, used to purge the equipment, both before (Version 1) and after the experiments. After the initial purge, the equipment was filled with solution, the liquid level being observed through the

sight glass (or sight tube) and maintained by adjusting flow rates with valves. The system was then pressurized with process gas to the desired pressure.

Once the system was pressurized and the gas and liquid were circulating at the desired flow rates, valves were adjusted so the system became closed (Version 1). However, in Version 1, gas had to be added continually to the system to maintain proper pressure since gas was lost through the gas pump. Version 2 (single-pass version) used a continuous fresh feed supply. Once the process reached "steady state," it operated continuously in this mode until shutdown.

While in continuous operation, the liquid level was monitored by watching the level through a sight glass or tube, and required constant monitoring, as a small perturbation in the process would significantly and quickly change the level. During continuous operation, the gas mixture entered the absorber at the bottom and exited from the top, while the cooled (< 20 ºC) liquid entered the top and absorbed the CO out of the gas while traveling to the bottom. This exiting liquid was then heated to approximately 75 ºC[a], releasing the CO; the liquid was then pumped through a heat exchanger where it was cooled back to < 20 ºC prior to re-entry into the absorber. The hot CO gas, along with some water vapor, traveled through a heat exchanger which cooled the gas (and condensed water vapor) to approximately 20 ºC prior to recombination with the offgas from the absorber. This recombined gas then passed through a gas pump and ballast tank and back to the gas inlet of the absorber. In

---

[a] Katsumoto et. al.[24] report that this temperature applies to the decomposition of the solid CO compound (formed in concentrated solution). Since no information was reported for the dilute solution cases, this temperature had to be assumed for the dilute cases in this research.

Version 2, the offgas and cooled CO were vented to the laboratory hood. During this continual operation, the following measurements were recorded periodically:

1. Pressure: inlet gas, column offgas, CO stream, solution inlet (streams 2, 9, 6, 12—see Figure 15 and Figure 17).

2. Temperature: inlet gas, CO stream, solution inlet, heated solution (streams 2, 6, 10, 12), and at 4 points on the surface of the solution heater (E-101).

3. Flow rate:[a] inlet gas, CO stream, offgas, liquid inlet (streams 2, 6, 9, 12).

4. Composition:[a] inlet gas, CO stream, offgas (streams, 2, 6, 9).

At the conclusion of the data collection, process shut down occurred as follows: the electric heater (used to heat the solution) was turned off while solution continued to flow until it was cool, gas was vented to the hood, and the system was purged with nitrogen. The cooled liquid was drained and disposed of into an appropriate waste container, and the system was flushed with deionized water to remove residual chemicals.

5.3 Experiments

Once the prototype was designed and built, the next step was to test it. Although experiments varied from case to case, three primary observations were considered throughout the cases:

- How well did the prototype separate the CO compared to design?

- How long did the process solution last?

---

[a] Streams 6 and 9 flow meters were not used in later experiments since they were out of range.

- How did CuCl and $MgCl_2$ concentrations (dilute vs. concentrated) affect the separation?

To determine whether the process actually worked, and to what extent, experiments were performed using the prototype at conditions close to those used in the prediction. The achieved separation was then compared to the predicted value.

The life of the process solution determines the practicality and economics of this process in an industrial version. A number of factors, including oxidation and disproportionation due to interaction with gas and process materials, can deplete the cuprous ion. Preliminary experiments showed that this system had potential, but the extent of disproportionation at large process times was unknown.

The third question led to useful insights about the column as well as economics of the process. In the work of Katsumoto,[24] it was found that the absorption of CO into solution was linearly proportional to CO partial pressure in the gas for dilute solutions (Cl^- < 10 mol/L). The absorption increased significantly in concentrated solutions, which should lead to increased separation at smaller flow rates. An improved separation would have to be weighed against the increased cost of additional raw materials. Further, it would be expected that if destabilization of Cu^+ occurs due to its contact with O_2, then a larger supply of Cu^+ available in a concentrated solution would extend the solution lifetime.

Table 6 shows basic information on six experiments performed with the prototype.

---

[a] For Version 2, the known inlet composition was constant. The CO stream measurement did not provide an accurate measurement—this was calculated as explained in a later section.

Table 6. Prototype experiments.

Experiment	Concentration (mol/L)		Prototype Version	Approximate Duration (min)
	CuCl	**MgCl$_2$**		
Case 1	0.81	1.30	One	10 min
Case 2	0.71	1.22	One	40 min
Case 3	0.65	2.92	One	120 min
Case 4	0.81	2.01	Two	190 min
Case 5[a]	0.52	1.12	Two	120 min
Case 6	3.00	4.78	Two	90 min

[a] Included 1.84 mol/L NaCl.

Each successive case differed from the previous case due to continual process improvements after each experiment. A detailed description of observations and improvements after each case is included in the appendix. Some common and significant challenges throughout the cases are mentioned here.

One challenge was making the solution. Raw materials were first mixed in a 1-liter beaker (the apparatus used about 800 mL solution per experiment), after which the solution was transferred to a 1-liter volumetric flask so more accurate concentrations could be measured. In most instances, insoluble particles remained in solution, the amount depending on concentrations and stirring method. When transferring the solution to the volumetric flask, some of these particles were inevitably left in the beaker, along with a residue on the glass. Attempting to rinse the remaining particles into the flask caused the particles to produce light green foam, much different from the normal brown solution, and not all particles could be transferred. The reported concentrations, therefore, are higher than the actual concentrations, but it is not clear by how much (see Section 5.7).

During most experiments, the solution eventually turned a reddish rust color. This was most notable in Case 1, when the apparatus was exposed to the process solution for the first time. When solution started flowing through the apparatus, large reddish brown flakes appeared in the sight glass and plugged up the equipment. It was realized that the zinc in the galvanized steel parts reacted with the copper solution according to the reaction(s):

$$2Cu^+ + Zn \Leftrightarrow Zn^{2+} + 2Cu^o \tag{5-1}$$

and/or

$$Cu^{2+} + Zn \Leftrightarrow Zn^{2+} + Cu^o \tag{5-2}$$

causing the copper in solution to precipitate. The solution also reacted with other materials in the process (brass fittings, aluminum floats in the flow meters, and aluminum heat exchanger), but not as rapidly as with the galvanized steel.

Another challenge stemmed from bubble formation in the first heat exchanger. As the solution containing absorbed CO was heated in the copper coils prior to separation, gas bubbles formed and traveled upwards through the coils. The formation of these bubbles may have contributed to varying flow rates through the coils, which may also have impacted heat transfer. This made it difficult to maintain a temperature of 75 ºC, particularly in Case 6 in which the solution was most viscous. This challenge may also have been related to the varying liquid levels in the separation region and at the bottom of the absorption column. It should be noted that since the column offgas stream and the product gas stream were connected (which helped to

maintain balanced pressures and therefore proper liquid levels in Version 2), and since the flow rate of the separated gas stream was significantly less than the column offgas stream, the separated gas stream contained a significant portion of the column offgas.

Although valuable information was learned from each experiment, the latter four experiments provided the most useful information on the separation. Of these four, Case 5 was more qualitative than quantitative. Case 5 was originally intended as a practice experiment, and the NaCl was only used to add extra chloride ions to solution. It turned out that it provided some results, but primarily qualitative. Therefore, Cases 3, 4, and 6 are the cases for which results are reported. These cases represent both versions of the prototype, as well as dilute and concentrated solutions.

5.4 Results

Numerous measurements were taken during the experiments, only a few of which are included in this section (see the appendix for raw data). The results presented below were obtained from a combination of measurements as well as calculations. Figure 18, a simplified schematic of the process, is included here to clarify notation used to report results.

Table 7 shows separation: the amount of CO (along with CO_2) that was removed from the gas inlet (or feed stream) and released in the product stream, as well as product composition. Small amounts of O_2 (approx. 0.3%, 2.2%, 3.2% for Cases 3, 4, and 6) and N_2 (approx. 0.1%, 1.1%, 1.7% for Cases 3, 4, and 6) were also removed and make up the balance of the product stream. The table also shows corresponding flow rates (actual liters per minute), pressures, and temperatures of the inlet gas (15%
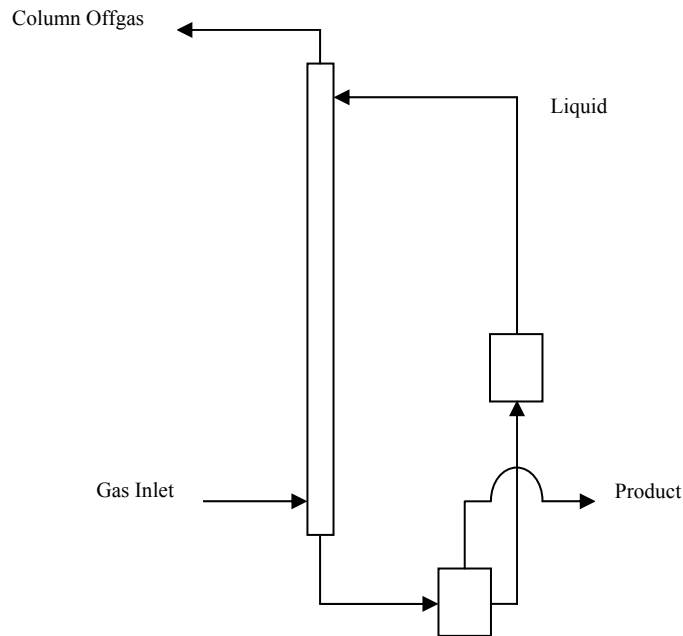
Figure 18. Simplified process schematic.

CO_2, 7% CO, 5% O_2, balance N_2 for Case 3, and 29.99% CO_2, 11.1% CO, 2.65% O_2, balance N_2 for Cases 4 and 6), as well as flow rates and temperatures of the liquid stream. The time refers to approximately how long the experiment had been running when measurements were taken.

Table 8 shows the ratio of the molar flow rate of the liquid to the molar flow rate of the solute-free gas through the column. The design value is based on the CO_2, O_2, and N_2 entering into the column,[a] while the measured value is based on the average CO_2, O_2, and N_2 in the column.[b]

---

[a] The design value uses the pressures that occurred in the experiments, showing what the L/G ratio should have been at the operating pressure.
[b] In practice, some CO_2, O_2, and N_2 is absorbed in the column, but this does not account for the large difference between the design and measured values of L/G—this difference arose from the need to adjust flow rates in the experiments to make the process run properly.

Table 7. Separation Results and Stream information.

Time	Gas Removed[a]		Product Comp.[a]		Gas Inlet			Liquid[b]		
	CO (%)	CO_2 (%)	CO (mole %)	CO_2 (mole %)	F (ALPM)	P (psig)	T^d (ºC)	F (LPM)	T_c (ºC)	T_h (ºC)
(min)[e]										
Case 3 (0.65M CuCl, 2.92M MgCl$_2$)										
52	56	4.5	83.8	14.2	1.05	6	25.8	0.095	15.8	75.2
118	66	5.0	84.2	13.8	0.93	4	23.7	0.095	16.2	78.0
Case 4 (0.81M CuCl, 2.01M MgCl$_2$)										
24	88	34	47.5	49.6	0.278	30	25.8	0.201	15.8	77.7
63	84	38	43.6	53.3	0.250	30	26.4	0.189	13.9	78.3
134	85	39	43.4	53.5	0.250	30	27.0	0.201	14.5	78.9
187	87	41	42.7	54.5	0.279	30	27.6[c]	0.201	14.5[c]	96.4
Case6 (3.0M CuCl, 4.8M MgCl$_2$)										
39	76	27	48.3	45.9	0.109	31	22.2	0.189	17.2	44.7
77	82	17	61.9	35.4	0.277	30	23.4	0.189	20.9	53.3

[a] From material balance calculations (not measured directly).
[b] Flow rate of cooled liquid; temperatures are cooled and heated liquid, respectively.
[c] Estimated.
[d] Ambient room temperature, measured above heat exchanger—temperature was probably smaller.
[e] Times are approximate. It took 1 or 2 minutes to collect an entire set of measurements manually.

Table 8. Liquid-to-gas molar flow ratios.

Time (min)	Design L/G	Measured L/G
Case 3 (0.65M CuCl, 2.92M MgCl$_2$)		
52	204	80
118	228	102
Case 4 (0.81M CuCl, 2.01M MgCl$_2$)		
24	91	332
63	91	351
134	91	373
187	91	337
Case6 (3.0M CuCl, 4.8M MgCl$_2$,)		
39	6	648
77	6	257

5.5   Discussion of Results: Measurements and Calculations

According to design, the prototype was originally equipped to measure pressure, temperature, flow rate, and composition of each gas stream, in addition to the

pressure, temperature, and flow rate of the liquid stream. These measurements would have provided all necessary information on the separation of CO and the product composition. However, because of difficulties with the equipment, the flow rate and composition of the product gas, and flow rate of the column offgas (see Figure 18) were not measured. These values were obtained by performing a material balance on the column, combined with the measurements from the experiments. Following is an explanation of material balance calculations as well as some general assumptions used.

The material balance calculations consisted of balancing the components (using moles per time) entering and exiting the absorber, the separator (the point where the solution was heated and gas was desorbed from solution), and the combination of both. The resulting equations were combined with additional relationships and substitutions, such as the ideal gas law. An example of a final equation used in the calculation, in its general form is:

$$n_{i.G} = \frac{P_{i.F} \cdot \dfrac{n_{H2O}}{H(T_c)}}{1 - \dfrac{P_{i.F}}{H(T_c)}} - \frac{n_{i.G} \cdot \dfrac{P_G}{n_G} \cdot \dfrac{n_{H2O}}{H(T_h)}}{1 - \dfrac{P_G}{n_G} \cdot \dfrac{n_{i.G}}{H(T_h)}} \tag{5-3}$$

where n is molar flow rate, P is pressure, H is the Henry's law constant, T_c is the temperature of the solution in the column, T_h is the heated solution temperature, subscript i is the component, subscript G is the product stream, and subscript F is the feed stream. Other similar equations can be seen in the appendix.

61

The amounts of CO_2, O_2, and N_2 physically absorbed into the liquid in the column, as well as the amounts of these gases desorbed from the liquid upon heating the solution were estimated from Henry's Law, as follows:

$$x_i \cdot H_i(T) = P_i \qquad \textbf{(5-4)}$$

where x is the mole fraction of component i in solution, H(T) is the Henry's constant as a function of temperature, and P is the partial pressure of component i in the gas.

Henry's Law assumes the gases had achieved equilibrium with the gases dissolved in the liquid phase, giving a conservative estimate (equilibrium might not have been achieved). It was also assumed that the gases absorbed into pure water, not taking into account the salting out effect. This also resulted in a conservative estimate of the amount of gases physically absorbed into solution. The result of these assumptions is that the calculated amount of CO_2, O_2, and N_2 absorbed into solution could be higher than what actually absorbed, so that the reported removals are high and the reported CO in the product is low, but to what extent is unknown. In the case of N_2 and O_2, even the conservatively-high estimates were small in the product stream.

An additional relationship used to solve the material balance involved the composition measurement of the column offgas stream. The gas chromatograms showed distinct CO and CO_2 peaks, but the O_2 and N_2 peaks overlapped. This required using the ratio of the CO_2 to CO mole fractions rather than absolute values. This ratio of CO_2 to CO was calculated as follows:

$$\frac{y_{CO2}}{y_{CO}} = k_{CO2\_CO}\left(\frac{A_{CO2}}{A_{CO}}\right) \tag{5-5}$$

where y is mole fraction, A is area of the peak, and k is a proportionality constant. The constant, k_{CO2_CO}, was found by running 10 samples (varying in size from 200 μL to 1000 μL) of known composition through the GC column. With the ratio y_{CO2}/y_{CO} known and the ratio A_{CO2}/A_{CO} found from the chromatograms, an average k_{CO2_CO} was calculated to be 0.889 (with a standard deviation of 0.017). This average value was used in the material balance to calculate the molar ratio of CO_2 to CO.

One assumption made for the calculations of Case 3 was that the composition of the feed gas to the column was the same as the original gas supplied to the process (7% CO, 5% O_2, 15% CO_2, balance N_2). During this experiment, the column offgas and product streams were recombined prior to re-entry into the absorber.[a] The actual composition more closely resembled the column offgas in this case since the offgas streams were not well-mixed. These streams were not well mixed because the product stream was cooled and was located at a low point in the process, in addition to having a much smaller flow rate than the column offgas. The composition of the combined stream also would have deviated from the original supply gas composition if some of the absorbed gas remained in solution. This assumption would probably cause the reported value of CO removed from the feed stream to reflect a higher-than-actual value.

---

[a] Note that the column offgas was sampled prior to recombining the two streams.

An assumption in the material balance for Case 6 was that all CO was released from the heated solution—this is not a good assumption since the temperature was well below 75 ºC. However, it was not possible to determine how much was released at the lower temperatures in this case. This assumption would cause the reported value of CO removed from the feed stream to be higher than it actually was since solution entering the column would have still contained CO.

Combining the measurements from experiments with the material balance allowed information on each stream to be known, as presented in Section 5.4. For a detailed example of these calculations, refer to the appendix.

5.6   Discussion of Results: Observations

It should be noted that experimental conditions often deviated from desired conditions. This was due to laboratory constraints, as well as other factors (such as having only one operator to monitor and control more than 16 process parameters). In the practical process, adjustments were required for equipment and processes to work properly.

Experimental observations were based on three primary ideas, restated here: comparison of actual CO separation with predicted CO separation, process solution lifetime, and effect of concentrated solution versus dilute solution—these are discussed in detail in the next sections.

5.6.1   Comparison of actual CO separation with predicted CO separation

The column height was estimated to be approximately 5 feet to achieve 99% CO removal. Since the actual height of the prototype column was 4 feet, the predicted

CO removal would drop to approximately 98% (Case 4). However, separation was lower than this predicted value. In Case 4, CO removal was 10-14% lower than predicted, and lower for the other cases.

The difference might be explained in part by some of the following factors: pressure, the ratio of liquid to gas molar flow rates, temperature, solution concentration, wall effects, and column operating region.   The significance of each factor is not known, but is discussed below. An attempt to quantify the effect of some of these factors is also discussed. It should be noted that these calculations are limited by the assumption that the ratio of CO_2 to CO in the column offgas stream remains constant. This value, which is used in the material balance calculations, was measured during the experiments. When changing a parameter, such as pressure, in the calculations to test its effect on separation, it is not known how the change would affect this ratio in an actual experiment, so it must be assumed constant.   The calculated effects of various parameters on separation, shown below, are therefore approximate, but give some idea of their impact on separation.

Pressure played a role in the lower CO removal of Case 3. In this case, the pressure (4-6 psig) was significantly lower than the design pressure (30 psig). As mentioned previously, the low pressure was caused by loss through the vacuum/pressure pump. Increasing this pressure to 30 psig in the absorber design and material balance calculations increased the removal of CO from 66% to 67%, CO_2 from 5% to 8%, decreased CO in the product from 84% to 77%, and increased CO_2 from 14% to 20%. This change accounted for only a small part of the low separation. However, as noted previously, the change in pressure in the calculations does not

reflect the change that would have occurred in the ratio of CO_2 to CO in the column offgas, which may have been significant. (Note: This change in pressure also lowered the liquid to gas molar ratio from 228 to 95 (close to the measured value) and the required column diameter from 18 inches to 12 inches.)

The lower L/G ratio would predictably decrease absorption of CO (as well as CO_2) into solution. This ratio is significantly impacted by the pressure, as noted above for Case 3. In Case 4, the actual L/G exceeded 300, while it was only 91 according to design. To test the effect of L/G on removal of gas from the feed stream and on product composition, the actual liquid flow rate was decreased in the material balance until the ratio was ~91. The removal of CO from the feed stream only decreased from 88% to 84% while the recoveries of CO_2, O_2, and N_2 decreased from 34% to 14%, 2% to 0.6%, and 1% to 0.3%, respectively. This correspondingly increased CO product composition from 48% to 68%.

The temperature to which the solution was heated upon exiting the column played a role in the less-than-expected separation of Case 6. At the time of the measurements (see Table 7), the temperature of the heated solution was ~20-30 ºC less than the desired 75 ºC for decomposing any CO compound formed and releasing it from solution. This would predictably decrease the CO removed from the feed stream in this case, but to what extent is unknown. It should be noted that the column operated approximately 10 to 15 ºC lower than the 30 ºC used in the CO absorption equilibrium model. A lower column temperature would in theory, increase the amount of gases absorbed into solution. To test the effect of column temperature on separation, both the gas and liquid temperatures in Case 4 were changed to 30º C in

66

the calculations. This had the effect of decreasing CO removal from 88% to 86%, and CO_2 removal from 34% to 20%. This correspondingly changed the product composition from 48% CO to 59% CO and 50% CO_2 to 38% CO_2. This might suggest that at the lower temperatures of the column and the higher temperatures of the heated solution, physical absorption of CO_2, O_2, and N_2 into the solution might be more dependent on temperature than the chemical absorption of CO into solution.

It was thought that making the solution slightly acidic would reduce the amount of CO_2 dissolved into solution. This would be the case if the solution were neutral. However, calculations (see the appendix) using data for CO_2 and water[41] show that the amount of CO_2 that probably dissolved into solution dropped the pH of the solution to around 4, although this was not measured. Adding additional acid to a solution already below a pH of approximately 5 has a minimal effect on the amount of CO_2 that dissolves in solution.

Wall effects could have been a significant factor in reducing mass-transfer efficiency and lowering separation. Wall effects occur when the packing diameter is too large in relation to column diameter. The ratio of surface area of the wall to surface area of the packing (6 mm glass beads) in the prototype (1 inch diameter, 4 feet tall) was 25%. To neglect wall effects, the column diameter should have been a minimum of 1.9 inches (rather than 1 inch), giving a maximum acceptable ratio of wall surface area to packing surface area of approximately 13%. For an industrial column 12.4 inches in diameter and 4 feet tall (prediction for industrial column), the ratio of surface area of the wall to surface area of the packing would be 2%. However, in an industrial column, a more modern generation packing with a larger diameter

would be used to increase efficiency. The individual impact of wall effects on the separation is unknown.

Another factor that could have affected the difference between actual and predicted separation is the operating region of the column. In Case 6 the solution was more viscous than in the others and made it more difficult to maintain steady operation in the column. The changing liquid level immediately below the bottom of the column (see Figure 26 in the appendix) indicated that the liquid flow through the column fluctuated during operation. It is likely that not all packing was wetted at some points, while the column may have been partly flooded at other times. Because of the dark color of the liquid, it was difficult to see whether solid particles formed (as predicted for concentrated solutions). If there was precipitation of solids, they could have accumulated in the "p trap" below the absorber, restricting flow from the column through the heat exchanger. There was some difficulty in maintaining steady operation in the other cases as well as in Case 6.

The factors discussed above as well as any others can be accounted for by calculating the experimental overall mass-transfer coefficient based on the liquid. The value calculated from experiments for Case 4 is shown in Table 9. The solute free liquid to gas molar flow rate ratio is shown again for comparison. It can be seen that the experimental mass-transfer coefficient is much less than the expected mass-transfer coefficient. The coefficient based on the experiments was used to estimate the column height required to achieve ~99% CO removal if the column operated at identical conditions as in the experiments (same L/G, etc.). The newly predicted required height based on this mass-transfer coefficient is shown in the table.

Table 9. Comparison of expected and experimental mass-transfer coefficients and required column height.

Time (min)	Design L/G	Measured L/G	Expected K_xa (mol/m^3·sec)	Achieved K_xa (mol/m^3·sec)	Design Height [a, b] (ft.)	Predicted Height[b] (ft.)
24	90.9	332	530.1	73.8	4.8	8.9
63	90.9	351	515.5	55.1	4.8	10.7
134	90.9	373	523.7	58.7	4.8	9.9
187	90.9	337	526.5	70.7	4.7	9.2
Average	90.9	348	524.0	64.6	4.8	9.7

[a] Note that the experimental column was 4 feet.
[b] For ~99% CO removal.

An additional factor relevant to the CO separation has to do with the physical absorption of CO_2, O_2, and N_2 into solution. According to the assumptions in the design, all CO_2, O_2, and N_2 pass through the column without being absorbed. The small amount of N_2 absorbed would not present any problem in the commercial process since it would not be present. In the commercial process, partial pressures of O_2 (2 psig) and CO_2 (24 psig) would be larger than in these experiments (0.8 psig and 9 psig respectively for Version 2), which would increase the amount of these gases that would be absorbed. Using the composition of the commercial process in the design calculations (for Case 4) leads to an increase in both the predicted diameter and height for the commercial process of less than 1 inch. This value is much smaller than the variation in predicted diameter and height due to assumptions made in the calculations.

5.6.2 Process solution lifetime

No prediction was made as to the exact lifetime of the process solution. The lifetime corresponds to the depletion of the Cu^+ as would be indicated by a decrease in

separation. The longest experiment lasted approximately 3 hours. However, there was no noticeable decrease in separation in any of the experiments at the time of shutdown. In each case involving dilute solutions, the solution was observed to turn from light brown to red over time (the red being a precipitate—this is what eventually led to shutdown). The appearance of red precipitate may have been a combination of corrosion of the stainless steel parts due to the hot, acidic solution, as well as galvanic corrosion of brass fittings and other metals in contact with the copper solution. In each successive case, the appearance of red precipitate occurred more slowly, as would be expected. The fact that separation did not decrease over time might suggest that the rate of disproportionation of Cu^+ was slow, and/or there could have been an excess of Cu^+. This result is not surprising when compared to one study (see Section 2.3) in which ~18% of the Cu^+ (dilute concentration) in a concentrated acidic solution was converted to Cu^{++} in the presence of O_2 in approximately 4 hours.

It was originally believed that building the process primarily out of copper tubing would help to prevent disproportionation. Although the lifetime of the Cu^+ in solution (and hence CO removal) did not appear to be noticeably affected (decreased) over the duration of the experiments by the formation of red precipitate (disproportionation/corrosion), a set of experiments was performed to test the interaction of the solution with various materials. Approximately 20 mL of a solution of 0.85M CuCl and 2.33M $MgCl_2$ was added to each of 6 test tubes. Other materials were added to the test tubes as follows: copper tubing, copper wire, brass fitting, and stainless steel fitting. The four test tubes containing these materials, along with one test tube containing only solution, were heated in a water bath to 75 ºC for several

hours. The remaining test tube containing solution was the control sample. All solutions were originally brown and somewhat clear. Over time, a layer of light green insolubles collected on the bottom of each—this may have been impurity from the CuCl bottle (which appeared to be somewhat contaminated) that settled out. All heated solutions became clear. The solutions containing the copper tube and copper wire became colorless, while the copper turned slightly pinkish-red. The brass fitting turned pink (the zinc probably dissolved into solution leaving only copper), and the originally brown solution eventually became less intense. The solution containing the stainless steel remained brown, and red precipitate formed on the fitting (looked like rust). This red precipitate resembled the red precipitate that appeared during experiments with the prototype. The only difference between the heated solution with no other material in it and the unheated solution was that it became slightly clearer. It appears from the experiments that galvanic corrosion of the stainless steel may have contributed to the formation of red precipitate in the experiments, but this precipitate did not noticeably affect separation during the life of the experiments.

5.6.3 Effect of concentrated versus dilute solution on CO removal

It was expected that, of the dilute cases (Cases 3 and 4), the more concentrated solution (Case 4) would improve CO removal. It was also expected that the concentrated (Cl^- > 10 mol/L) solution (Case 6) would significantly improve CO separation. Results show that Case 4 (0.81 M CuCl) had a higher separation (88%) than Case 3 (0.65 M CuCl and 66% separation), and that the concentrated solution of Case 6 (3.0 M CuCl) actually resulted in a lower separation (82% compared to 88%).

The significant increase in separation of Case 4 compared to Case 3 has been discussed—factors such as the ratio of molar liquid to gas flow rates, different pressures, and different gas compositions hide the effect of the difference in solution concentration. The lower separation of Case 6 compared to Case 4 might be due to mass-transfer limitations in the column. It was mentioned that the column probably did not operate in the preloading region (could have ranged from the packing not all being wetted to the column being partially entrained) during Case 6, and that the temperature of the heated stream did not reach 75 ºC at the time of measurement (which was not accounted for in the material balance), again masking the true effect of the concentration difference. The true effect of solution concentration on separation in these experiments is unknown.

5.7   Discussion of Results: Uncertainty

A number of factors lead to uncertainty in the reported separation values (Table 7). Sources of uncertainty include correlations and fluid property estimations used in the column design and material balance calculations, Henry's Law assumptions used in the material balance, gas composition, raw chemical composition, lag time between measurements as well as the process not being at steady state at the time of measurement, some instability in material balance calculations (extremely small flow rates used with large flow rates), and the following measurements (monitored and controlled "simultaneously" by one operator): temperature, pressure, flow rate, gas composition (including chromatograph analysis), and solution

72

concentration. An attempt to quantify some of these follows. Approximate relative

uncertainties for measurements are shown in Table 10.

Table 10. Approximate Relative Uncertainties.

Measurement	Relative Uncertainty
Pressure[42]	± 2%
Temperature[43]	± 10%[a]
Gas Chromatograph Area	± 3%[b]
Gas Composition	± 2%
Flow[44,45]	± 5%
Solution Composition	± 10%[c]

[a] Absolute uncertainty is 2.2 °C, which is large at lower temperatures.
[b] Estimate. In one set of isolated measurements, it was 7% for CO.
[c] Estimated from experiments.

Based on Case 4, the measurements were varied by their uncertainties and the

effect on the calculated separation was observed. In all cases, the separation varied by

approximately ±1.5% or less (in some cases much less than 1%). To be conservative,

all factors were assumed to cause a 1.5% uncertainty in the separation value, and were

combined by taking the square root of the sum of the squares. The resulting overall

uncertainty was estimated to be ± 6%. This value is assumed for all cases.

One composition measurement from Case 5 helped to verify that the product

stream actually released and consisted of a significant amount of CO. In this case, the

molar ratio of CO_2 to CO was 0.6 (compared to 2.7 in the inlet gas). This particular

measurement provided mostly a qualitative comparison since the solution differed

from the other cases, and there was some inaccuracy in the measurement.

An additional calculation using Case 4 establishes a lower-bounding value for

the separation and helps show the reasonableness of the reported values. In this

calculation, it was assumed that only CO was absorbed into solution in the column, so that only CO was removed from the gas mixture. This significantly simplified the material balance calculation and resulted in a CO removal of approximately 83%. This is a lower-bounding value for this case, since an increase in the amounts of other gases absorbed into solution increases this value. The highest reported separation value in this case was 88%, a reasonable value based on the lower-bounding value.

It should be noted that each experiment performed differed from the previous experiment. Although it would be desirable to perform multiple experiments at identical conditions, perhaps on different days, this was not possible at the time due to changes and improvements to the process, as well as time and other constraints. However, reported results (derived from measurements and calculations) at different times during a given experiment were consistent.

6 CONCLUSIONS

Based on the results, the following conclusions were drawn. First, aqueous CuCl/MgCl$_2$ solutions separate CO from gas mixtures of CO, CO$_2$, O$_2$, and N$_2$. In addition to removing a significant portion of the CO (88% in Case 4) from the original gas mixture, a significant quantity of CO$_2$ (34% in Case 4) was also removed. Negligible amounts of O$_2$ and N$_2$ were removed. The absorption of CO$_2$, O$_2$, and N$_2$ into the solution occurred by physical absorption, assumed to follow Henry's Law, whereas the absorption of CO was a chemical (and reversible) process.

The significant amount of absorbed CO$_2$ was released upon heating, decreasing the fraction of CO in the product to approximately 50%. The fraction of CO in the product could be increased by decreasing the CO$_2$ absorbed. This could be accomplished by decreasing the pressure at which the column operates, thus lowering the partial pressure of CO$_2$ in the gas. Reducing the pressure could also decrease the CO absorbed (and therefore removed), but the impact would be much less than with the physically absorbed CO$_2$.

Another way to decrease the CO$_2$ absorbed and released with the separated CO would be to operate at less extreme temperatures (operate the column at a slightly higher temperature, i.e., 25-30 ºC rather than 15 ºC, and lower the separation temperature, i.e., from 75 ºC to 70 ºC). Since physical absorption is a function of

temperature, and absorption decreases with increasing temperature, less CO_2 would absorb into solution in the column, and less of this absorbed CO_2 would be released at the separation point. As with a reduction in pressure, these changes in temperature would also decrease the CO removed, but the effect might be less significant on CO than with the other gases (as shown in previous calculations), and the fraction of CO in the product would increase.

Another parameter that can be used to adjust CO removed from the feed stream as well as the product composition is the ratio of liquid molar flow rate to gas molar flow rate, L/G. This ratio has a much greater impact on the removal of CO_2, O_2, and N_2, than on the removal of CO (according to calculations discussed in Section 5.6.1). Adjusting this ratio, as well as the pressure and temperature, can be used to adjust CO removal and product composition, but there is a tradeoff with any of these methods. As the removal of CO from the feed stream increases, the fraction of CO in the product decreases, so the process would need to be optimized until the desired criteria are met.

Another conclusion from the experiments is that aqueous $CuCl/MgCl_2$ can be used in a *continuous* process to separate the CO for extended periods. The exact lifetime of the solution based on concentrations of $CuCl/MgCl_2$, gas compositions, and materials was not determined from the experiments. However, no notable decrease in separation had occurred after more than 3 hours of operation (Case 4). Although the exact lifetime could not be predicted, it appears that the process would have continued to separate, had it not been required to shut down for other reasons.

Another conclusion based on the experiments is that, in these particular experiments, the dilute solution (Cl^- < 10 mol/L) removed more CO than the concentrated solution (Cl^- > 10 mol/L), contrary to prediction. This was due to factors possibly including wall effects and fluctuating column operation, which could have contributed to lowering the mass-transfer efficiency. As discussed in the results, the experiment that used concentrated solution (Case 6) also did not achieve the desired separation temperature. These factors masked the effect of dilute vs concentrated solution on separation. The mass-transfer coefficient found from experiments (74 $mol/m^3 \cdot s$) was much smaller than the predicted value (530 $mol/m^3 \cdot s$). Given the same mass-transfer coefficient as in the experiments, a similar column would be required to be ~9 feet tall (rather than 4 feet) to remove 99% of the CO from the feed stream.

Finally, it was concluded that the $CuCl/MgCl_2$ solution was corrosive to many of the materials in this prototype. Corrosion stemmed from two sources: galvanic corrosion, and corrosion due to acidity from CO_2 absorption. The galvanic corrosion occurred upon contacting aqueous copper chloride solution with galvanized steel, aluminum, brass, and even stainless steel. The primary incompatible materials were aluminum and the zinc found in the galvanized steel and the brass.

7 RECOMMENDATIONS

Based on the results and conclusions from the experiments, the following recommendations for improvements and future work are made.

Materials: The solution was more corrosive than originally expected, and a commercial process would last longer if constructed with other materials such as pure copper, a more resistant metal alloy, plastic, and/or glass.

Solution: The benefit of using $MgCl_2$ as a complexing agent in this process rather than NaCl, KCl, and others was that, according to the literature, a concentrated solution would absorb much more CO than the other similar systems. However, a higher separation in these experiments was achieved with the dilute solution. The advantages of using dilute solution are that it is less corrosive, less viscous, does not form solid CO compounds, and it can achieve good separation with reasonable column height. Its disadvantages are that it requires a higher liquid flow rate, and the solution might not last as long, since there are fewer Cu^+ ions to start with. On the other hand, significantly lower flow rates would be required with a concentrated solution, lowering pumping costs, and it might last longer. The disadvantages of concentrated solution are that it is more corrosive, more viscous, and forms a solid compound as it absorbs CO (according to the literature). More experiments should be performed to ascertain the effect of concentration on separation. If it is determined that dilute

solution is preferred to concentrated solution, perhaps other complexing agents could be tested.

When first mixing a solution, water and $MgCl_2 \cdot 6H_2O$ should be mixed first, with CuCl being the last component added, and it should be added slowly while mixing. Solution should contain excess Cl^- to help stabilize the Cu^+. Exposure of the solution to O_2 during storage, transportation, etc., should be minimized. The process should contain elemental copper in contact with solution to assist in slowing disproportionation.

Carbon dioxide removal: If the amount of CO_2 physically absorbed into solution is unacceptable, methods for reducing the amount absorbed into solution and released upon heating solution will need to be considered. One option would be to operate at a lower column pressure—this would decrease CO removal, but might more significantly reduce the amount of CO_2 absorbed. Increasing column temperature, decreasing the temperature to which the solution is heated, and decreasing the L/G ratio may have similar effects. An increase in temperature, however, might increase the rate of Cu^+ oxidation in acidic solution, as reported in the literature. Additional experiments should be performed to explore this.

Physical process: Challenges associated with operating an absorption column at elevated pressure in a commercial process, which may also contain particles in the solution (particularly in the concentrated solution case), will require special consideration. The prototype in this research was unable to handle the concentrated solution well, and required constant monitoring. Although not necessary to state, automating the measurement and control of the process would improve the process.

Ratio of L/G: If it is desired to have a higher fraction of CO in the product, then the ratio L/G should be as low as feasible—this might significantly reduce the amount of CO_2, O_2, and N_2 physically absorbed compared to CO absorbed.

Additional experiments: Further studies to understand the mechanisms of CO absorption in $CuCl/MgCl_2$ solution, including pressure and temperature effects would be worthwhile. It would be helpful to know the temperature at which the CO is released from a dilute solution (which had to be assumed the same temperature as in a concentrated solution in these experiments)—if it were significantly different from 70 ºC, the heating and cooling requirements would change. This could also include a study of the mechanism and rate of Cu^+ oxidation to determine the lifetime of the solution. Additional experiments should be performed with the diameter of the commercial column (12 inch) and modern generation packing with a diameter less than 1/8 of the column diameter. These improvements would bring the experimental mass-transfer coefficient (74 mol/m³·sec) closer to the design mass-transfer coefficient (530 mol/m³·sec). This would also reduce the newly predicted column height (9 feet) closer to the originally predicted height (5 feet). Additional experiments would also provide more information on the accuracy of the data obtained in these experiments and their repeatability.

8 REFERENCES

[1] Traynor, A.J., Jensen, R.J. "Direct Solar Reduction of CO_2 to Fuel: First Prototype Results," *Industrial & Engineering Chemistry Research*, Vol. 41(8), 1935-1939, 2002.

[2] Battrum, M. J., Thomas, W. J. "Carbon Monoxide Recovery By Pressure Swing Adsorption," *Trans IChemE*, Vol. 69(A), March, 1991.

[3] Gholap, Raghuraj V., Chaudhari, Raghunath V. "Absorption of Carbon Monoxide with Reversible Reaction in CuAlCl$_4$-Toluene-Complex Solutions," *The Canadian Journal of Chemical Engineering*, Vol. 70, June, 1992.

[4] "The KTI-COSORB® Process: Recovery, Purification of Carbon Monoxide," Company Brochure, sent by Stan Che.

[5] Haese, D. J., Walker, D. G. "The COSORB Process," *Chemical Engineering Progress*, Vol. 70(5), May, 1974.

[6] Haase, D.J., Duke, P.M., Cates, J.W. "CO recovery and purification," *Hydrocarbon Processing*, March, 1982.

[7] Kohl, A.L., Nielsen, R.B. <u>Gas Purification</u>, 1st ed. McGraw Hill, 485-533, 1960.

[8] Jones, W. A. "A Contribution To Our Knowledge Of Dicarbonyl Cuprous Chloride," *Am. Chem. J.*, Vol. 22, 287-311, 1899.

[9] Gholap, Raghuraj V., Chaudhari, Raghunath V. "Absorption of Carbon Monoxide with Reversible Reaction in Cuprous Chloride Solutions," Ind. Eng. Chem. Res., Vol. 27, 2105-2110, 1988.

[10] Gaunand, A. "Oxidation of Cu(I) By Oxygen In Concentrated NaCl Solutions-III. Kinetics In A Stirred Two-Phase and Three-Phase Reactor," *Chemical Engineering Science*, Vol. 41(1), 1-9, 1987.

[11] Tran, T., Swinkels, D. A. J. "The Kinetics Of Oxidation Of Cu(I) Chloride By Oxygen In NaCl-HCl Solutions," *Hydrometallurgy*, Vol. 15, 281-295, 1986.

[12] Bruce, M. I. "Carbonyl Chemistry Of The Group IB Metals," *Journal of Organometallic Chemistry*, Vol. 44, 209-226, 1972.

[13] Nord, Hakon. "Kinetics of the Autoxidation of Cuprous Chloride in Hydrochloric Acid Solution," *Acta Chemica Scandinavica*, Vol. 9, 430-437, 1955.

[14] Jhaveri, A. S., Sharma, M. M. "Kinetics of absorption of oxygen in aqueous solutions of cuprous chloride," *Chemical Engineering Science*, Vol. 22, 1-6, 1967.

[15] Levy, Pierre Emmanuel, Baratin, Francois, Renon, Henri. "The Oxidation Of Cu(I) By Oxygen Gas In Concentrated NaCl Solutions: A Kinetic Study," *Chemical Engineering Science*, Vol. 36(9), 1475-1485, 1981.

[16] Papassiopi, N., Gaunand, A., Renon, H. "Oxidation Of Cu(I) By Oxygen In Concentrated NaCl Solutions—I. Homogeneous Kinetics Of Oxidation By Molecular Oxygen In Solution," *Chemical Engineering Science*, Vol. 40(8), 1527-1532, 1985.

[17] http://www.kobelco.co.jp/eneka/copsa/indexe.htm

[18] Private communication with Stan Che of KTI in Texas, May, 2005.

[19] Sircar, S., Golden, T. C. "Purification of Hydrogen by Pressure Swing Adsorption," *Separation Science and Technology*, Vol. 35(5), 667-687, 2000.

[20] Guide For COSORB® Solvent Manufacturing Procedure, KTI COSORB LTD., INC., Feb. 18, 1987.

[21] Toshima, N., Kanaka, K., Ishiyama, N., Hirai, H. "The Polymerization of Toluene and Its Analogs Catalyzed by a Copper (I) Chloride-Aluminum Chloride-Oxygen System," *Bulletin of the Chemical Society of Japan*, Vol. 62, 2201-2207, 1989.

[22] Hirai, Hidefumi, Komiyama, Makoto, Hara, Susumu. "Polystyrene/Copper Aluminium Tetrachloride as Water-Resistant Carbon Monoxide Absorbent," *Makromol. Chem., Rapid Commun.* Vol. 2, 495-498, 1981.

[23] Hirai, Hidefumi, Komiyama, Makoto, Wada, Keiichiro. "Active Carbon-Supported Aluminium Copper Chloride As Water-Resistant Carbon Monoxide Adsorbent," *Chemistry Letters*, 1025-1028, 1982. © The Chemical Society of Japan.

[24] Katsumoto, M., Kanehori, K., Kamiguchi, T. "Carbon Monoxide Absorption by Aqueous CuCl-MgCl$_2$ Absorbent," *Bull. Chem. Soc. Jpn.*, Vol. 57, 166-170, 1984.

[25] Engel, K. H. "Carbon monoxide from industrial gases," *Chemical Abstracts*, Vol. 26, 3626, 1932.

[26] Sircar, S., Golden, T. C. "Purification of Hydrogen by Pressure Swing Adsorption," *Separation Science and Technology*, Vol. 35(5), 667-687, 2000.

[27] Knaebel, K.S. "For Your Next Separation Consider Adsorption," *Chemical Engineering*, 92 – 102, November, 1995.

[28] LaCava, A.I., Shirley, A.I., and Ramachandran, R. "How to Specify Pressure-Swing Adsorption Units," Chemical Engineering, 110 – 118, June, 1998.

[29] Deringer, Von Dr. Hans. "Über ein Absorptionsmittel zur Auswaschung und Gewinnung von Kohlenoxyd aus Gasgemischen," *Chimia*, Vol. 1, 125-140, 1947.

[30] Backén, W., Vestin, R. "Solid Copper(I)carbonyl Complex. Composition and Equilibria," *Acta Chemica Scandinavica*, Vol. 33, 85-91, 1979.

[31] Ahrland, Sten, Rawsthorne, James. "The Stability of Metal Halide Complexes in Aqueous Solution VII. The Chloride Complexes of Copper(I)," *Acta Chemica Scandinavica*, Vol. 24, 157-172, 1970.

[32] Seader, J. D., Henley, E.J. Separation Process Principles. John Wiley & Sons, Inc., 1998.

[33] Perry, R.H., Green, D.W. Perry's Chemical Engineers' Handbook, 7th ed., McGraw-Hill companies, Inc., 1997.

[34] Billet, R., Schultes, M. "Prediction Of Mass-transfer Columns With Dumped And Arranged Packings: Updated Summary of the Calculation Method of Billet and Schultes," *Trans IChemE*, Vol. 77(A), 498-504, September, 1999.

[35] Fair, J.R, Bravo, J.L. "Generalized Correlation for Mass-transfer in Packed Distillation Columns," *Ind. Eng. Chem. Process Des. Dev.*, Vol. 21, 162-170, 1982.

[36] Onda, K., Takeuchi, H., Okumoto, Y. "Mass-transfer Coefficients Between Gas and Liquid Phases in Packed Columns," *Journal of Chemical Engineering of Japan*, Vol. 1(1), 56-62, 1968.

[37] Taylor, R., Krishna, R. Multicomponent Mass-transfer. John Wiley & Sons, Inc., 1993.

[38] Bird, R.B., Stewart, W.E., Lightfoot, E.N. Transport Phenomena, 2nd ed., John Wiley & Sons, Inc., 2002.

[39] Poling, B.E., Prausnitz, J.M., O'Connell, J.P. The Properties of Gases And Liquids, 5th ed., McGraw-Hill, 2001.

[40] DIPPR database.

[41] Cohen, P., Editor-in-Chief. The ASME Handbook on Water Technology For Thermal Power Systems, The American Society of Mechanical Engineers, 1989.

[42] http://www.grainger.com/Grainger/wwg/itemDetailsRender.shtml?ItemId=1612699484

[43] http://www.omega.com/toc_asp/frameset.html?book=Temperature&file=tc_colorcodes

[44] http://www.coleparmer.com/catalog/product_view.asp?sku=3247000&pfx=EW

[45] http://www.omega.com/ppt/pptsc.asp?ref=FL210_215&Nav=greb02

APPENDIX A: Absorber Design

The following program calculates diameter and height of a packed absorbtion column which uses a $CuCl/MgCl_2$ solution to separate CO from a gas mixture of CO, O_2, CO_2, and N_2.

Introduction: The primary parameters in designing a column are the diameter and height. The program proceeds as follows: Section 1 is where the user inputs all values to be specified, Section 2 contains definitions pertinent to Mathcad, as well as physical constants, Section 3 consists of a number of calculations such as flow rates and densities that are preliminary to the final calculation of the diameter, Section 4 contains the height calculation, Section 5 scales down the design to a laboratory prototype, and Section 6 consists of miscellaneous information. Each section contains assumptions that should be checked by the user, especially when inputs vary significantly from original values.

Section I: User-specified Values

User Inputs

$P_{atm} := 12.3 psi$ — (atmospheric pressure, BYU, ~4700 feet (BYU current conditions website))

$P_g := 30 psi$ — (gas inlet pressure (gauge))

$T_f := (25.8 + 273.15)K$ — (gas inlet temperature)

$T_L := (15.8 + 273.15)K$ — (liquid temperature in column)

$G := 0.2 \dfrac{mol}{s}$ — (gas inlet molar flow rate)

$y_{out} := 0.0012$ — (desired CO mole fraction in scrubber off-gas)

$y_{O2} := 0.02647$ — (inlet O_2 mole fraction in gas)

$y_{CO2} := 0.2999$ — (inlet CO_2 mole fraction in gas)

$y_{in} := 0.111$ — (inlet CO mole fraction in gas)

$y_{N2} := 0.563$ — (inlet N_2 mole fraction in gas; included for prototype--not present in actual)

$Sum := y_{CO2} + y_{O2} + y_{in} + y_{N2}$ — (check inlet mole fractions) — $Sum = 1$

$x_{in} := 0$ — (inlet CO mole fraction in liquid: *assumes all CO was desorbed upstream*)

$C_{CuCl} := 0.81 \dfrac{mol}{l}$ — (concentration of CuCl in solution, 0.2 - 3.0)

87

$C_{MH} := 2.01 \dfrac{mol}{L}$

(concentration of $MgCl_2 \cdot 6H_2O$ (MH) in solution, 1 - 4.8 (note: should be > CuCl)

$L_{factor} := 2.0$

(to find solute-free liquid flow rate: ranges from 1.1 to 2: Separations, 285)

$f := 0.7$

(flooding factor; typically 0.5 to 0.7 (Sep, 330); lower is more conservative)

Spherical Beads: glass, 6mm

$D_P := 6mm \quad SA := 4 \cdot \pi \cdot \left(\dfrac{D_P}{2}\right)^2 \quad Vol := \dfrac{4}{3}\pi \cdot \left(\dfrac{D_P}{2}\right)^3 \quad a_v := \dfrac{SA}{Vol} \quad a_v = 1 \times 10^3 \dfrac{m^2}{m^3} \quad \varepsilon := 0.37 \dfrac{m^3}{m^3}$

$a := a_v \cdot (1 - \varepsilon) \qquad a = 630 \dfrac{m^2}{m^3}$

$F_P := \dfrac{a}{\varepsilon^3} \qquad F_P = 3.791 \times 10^3 \dfrac{ft^2}{ft^3}$

Section 2: Definitions, Physical Constants

MathCAD Definitions

$ORIGIN \equiv 1 \qquad cP \equiv 0.01 poise \quad kmol \equiv 1000 mole \quad mol \equiv mole \quad J \equiv joule \quad Ang := 10^{-10}m$

$\qquad\qquad\qquad s \equiv sec \qquad\qquad L \equiv liter \qquad\qquad N \equiv newton \qquad kJ \equiv 1000J$

Physical Constants

$R_g := 0.08206 \dfrac{L \cdot atm}{mol \cdot K}$

(universal gas constant)

$MW_{CO} := 28.01 \dfrac{gm}{mol} \quad MW_{O2} := 31.999 \dfrac{gm}{mol}$

(gas molecular weights)

$MW_{CO2} := 44.01 \dfrac{gm}{mol} \quad MW_{N2} := 28.013 \dfrac{gm}{mol}$

$MW_{CuCl} := 99 \dfrac{gm}{mol} \quad MW_{MH} := 203.3 \dfrac{gm}{mol}$

(liq. molecular weights)

$MW_w := 18.02 \dfrac{gm}{mol} \qquad MW_{MgCl2} := 95.21 \dfrac{gm}{mol}$

88

$$\rho_{CuCl} := 3.53 \frac{gm}{mL} \qquad \rho_{MH} := 1.56 \frac{gm}{mL} \qquad \text{(densities (Perry's Handbook))}$$

$$T_c := 647.096K \qquad T_r(T) := \frac{T}{T_c} \qquad t(T) := 1 - T_r(T) \qquad \text{(critical and reduced temperatures are for water)}$$

(water molar density--correlation from DIPPR)

$$\rho_{wat}(T) := \left[(17.863) + 58.606 \cdot t(T)^{0.35} + -95.396 \cdot t(T)^{\frac{2}{3}} + 213.89 \cdot t(T) + -141.26 \cdot t(T)^{\frac{4}{3}}\right] \cdot \frac{kmol}{m^3}$$

$$\rho_w(T) := \rho_{wat}(T) \cdot MW_w \qquad \rho_w(T_f) = 0.995 \frac{gm}{cm^3} \qquad \text{(water density)}$$

Section 3: Diameter

Inlet Gas

$$P_{tot} := P_g + P_{atm} \qquad \qquad \text{(inlet gas absolute pressure)}$$

$$V_f := \frac{G \cdot R_g \cdot T_f}{P_{tot}} \qquad V_f = 102.275 \frac{L}{min} \qquad \text{(inlet gas volumetric flow rate)}$$

Assumption: Ideal Gas Law is valid at this elevated pressure and lower temperature.

Solute-free Flows and Compositions

Solute-free flows denoted with a prime (') and compositions with capital letters

$$G' := G \cdot (1 - y_{in}) \qquad G' = 640.08 \frac{mol}{hr} \qquad \text{(molar flow rate of gas, constant through column)}$$

$$Y_{in} := \frac{y_{in}}{1 - y_{in}} \qquad Y_{in} = 0.125 \qquad \text{(inlet CO mole fraction in gas)}$$

$$X_{in} := \frac{x_{in}}{1 - x_{in}} \qquad X_{in} = 0 \qquad \text{(inlet CO mole fraction in liquid)}$$

$$Y_{out} := \frac{y_{out}}{1 - y_{out}} \qquad Y_{out} = 1.201 \times 10^{-3} \qquad \text{(desired CO mole fraction in scrubber off-gas)}$$

Flow rates of CO

$$CO_{init} := Y_{in} \cdot G' \qquad CO_{init} = 1.332 \frac{mol}{min} \qquad \text{(initial CO in feed)}$$

$$CO_{trans} := \left(Y_{in} - Y_{out}\right) \cdot G' \qquad CO_{trans} = 1.319 \frac{mol}{min} \qquad \text{(CO transferred from gas to liquid)}$$

$$CO_{rem} := CO_{init} - CO_{trans} \qquad CO_{rem} = 0.013 \frac{mol}{min} \qquad \text{(CO remaining in gas)}$$

General Gas Stream Properties

$$MW_{G.in} := y_{in} \cdot MW_{CO} + y_{O2} \cdot MW_{O2} + y_{CO2} \cdot MW_{CO2} + y_{N2} \cdot MW_{N2} \qquad \text{(inlet gas MW)}$$

$$G_{out} := y_{O2} \cdot G + y_{CO2} \cdot G + CO_{rem} + y_{N2} \cdot G \qquad G_{out} = 10.685 \frac{mol}{min} \qquad \text{(molar flow rate of exiting gas)}$$

$$MW_{G.out} := y_{out} \cdot MW_{CO} + \frac{y_{O2} \cdot G}{G_{out}} \cdot MW_{O2} + \frac{y_{CO2} \cdot G}{G_{out}} \cdot MW_{CO2} + \frac{y_{N2} \cdot G}{G_{out}} \cdot MW_{N2} \qquad \text{(outlet gas MW)}$$

$$MW_G := \left(MW_{G.in} + MW_{G.out}\right) \cdot 0.5 \qquad \text{(average gas MW)}$$

$$\rho_G := \frac{P_{tot} \cdot MW_G}{R_g \cdot T_f} \qquad \rho_G = 3.898 \frac{kg}{m^3} \qquad \text{(average gas density)}$$

General Liquid Stream Properties

Viscosity

$$\mu_{wat}(T) := exp\left[-52.843 + \frac{3.7036 \times 10^3 \cdot K}{T} + 5.866 \cdot ln\left(\frac{T}{K}\right) + 0 \cdot \left(\frac{T}{K}\right)^{10}\right] \cdot Pa \cdot s$$

(liquid viscosity assumed to be water--correlation from DIPPR)

$$\mu_L := \mu_{wat}\left(T_L\right) \qquad \mu_L = 1.128 \, cP$$

$$\mu_w := \mu_{wat}\left(T_L\right) \qquad \mu_w = 1.128 \, cP$$

Solution Density and Moles

Correlation and corresponding coefficients from factorial analysis in Excel (coefficients were refined using solver)

$\rho_L = e_o + e_1 \cdot C_{Cu} + e_2 \cdot C_{Mg} + e_3 \cdot C_{Cu} \cdot C_{Mg}$ $e_o := 0.9949$ $e_1 := 0.0673$ $e_2 := 0.0635$ $e_3 := 0.0023$

$C_{MgCl2} := C_{MH}$

<u>Solution Density</u> (using correlation)

$$\rho_L := \left[\left[e_o + e_1 \cdot C_{CuCl} \cdot \frac{L}{mol} + e_2 \cdot C_{MgCl2} \cdot \frac{L}{mol} + e_3 \cdot C_{CuCl} \cdot C_{MgCl2} \cdot \left(\frac{L}{mol} \right)^2 \right] \right] \cdot \frac{gm}{mL}$$ $\rho_L = 1.181 \frac{gm}{mL}$

Note that all measurements for solution denisty were taken at room temperature (~22 °C).

<u>Total Moles in Solution</u>

$Vol_b := 1L$ (volume basis)

$n_{CuCl} := C_{CuCl} \cdot Vol_b$ $m_{CuCl} := n_{CuCl} \cdot MW_{CuCl}$ (moles and mass CuCl)

$n_{MgCl2} := C_{MH} \cdot Vol_b$ $m_{MgCl2} := n_{MgCl2} \cdot MW_{MgCl2}$ (moles and mass MgCl2)

$m_w := \rho_L \cdot Vol_b - m_{CuCl} - m_{MgCl2}$ (mass and moles of water)

$n_w := m_w \cdot MW_w^{-1}$ $n_w = 50.457 \, mol$ (moles of water in 1 liter of solution)

$n_{Tot} := n_{CuCl} + n_{MgCl2} + n_w$ $n_{Tot} = 53.277 \, mol$ (total moles in 1 liter of solution)

<u>Equilibrium</u>

The following equilibrium calculations are based on data presented by Katsumoto et. al. His data are used here to derive a model that will predict CO absorption into solution based on partial pressure of CO in the gas. He does not present details on how his own model was derived, and there are very few data points to work with--therefore, the model here is far from perfect, but gives a decent approximation. Note that his data are for a system at 30 °C, while the current design operates around 20 °C. Because the current design operates 10 °C lower than what the following model is based on, the amount of CO absorbed is underestimated in this case, and therefore provides a more conservative estimate. However, the amount of CO absorbed in this temperature range does not vary significantly--CO absorption varies significantly in the range from just beyond 30 °C up to 70 °C.

<u>Original Data</u> (k = absorption coefficient, $A_{Cu'}$ = total Cu^+ concentration, $P_{CO'}$ = threshold pressure above which absorption increases dramatically for concentrated solutions):

Dilute solutions, denoted by subscript 1 (Cl^- concentration < 10):

$k_1 := \begin{pmatrix} 3.725 \cdot 10^{-6} \\ 6.771 \cdot 10^{-6} \end{pmatrix} \cdot Pa^{-1}$ $A_{Cu'1} := \begin{pmatrix} 2.2 \\ 0.8 \end{pmatrix} \cdot \frac{mol}{L}$

Concentrated solutions, denoted by subscript 2 (Cl⁻ concentration >10):

$$k_2 := \begin{pmatrix} 8.860 \cdot 10^{-5} \\ 5.196 \cdot 10^{-5} \\ 2.625 \cdot 10^{-5} \\ 1.260 \cdot 10^{-5} \\ 1.191 \cdot 10^{-5} \end{pmatrix} \cdot Pa^{-1} \qquad A_{Cu'2} := \begin{pmatrix} 3.0 \\ 3.0 \\ 2.8 \\ 3.0 \\ 2.7 \end{pmatrix} \cdot \frac{mol}{L} \qquad P_{CO'} := \begin{pmatrix} 5000 \\ 5000 \\ 11600 \\ 23300 \\ 24300 \end{pmatrix} \cdot Pa$$

Define rages for this section:

$$i := 2 .. 101 \quad k := 1 .. 5 \qquad j := 1 .. 2$$

$$P_{CO_i} := [1000 \cdot (i - 1)] \cdot Pa \qquad\qquad \text{(CO partial pressures in gas)}$$

Katsumoto's absorption models (a_{CO} represents dilute concentrations, b_{CO} concentrated)

$$\alpha_{CO}(P_{CO}, i, j) := \frac{\overrightarrow{k_{1_j} \cdot P_{CO_i} \cdot A_{Cu'1_j}}}{1 + k_{1_j} \cdot P_{CO_i}} \qquad\qquad \beta_{CO}(P_{CO}, i, k) := \frac{\overrightarrow{k_{2_k} \cdot \left(P_{CO_i} - P_{CO'_k}\right) \cdot A_{Cu'2_k}}}{1 + k_{2_k} \cdot \left(P_{CO_i} - P_{CO'_k}\right)}$$

Plot of Katsumoto's model (note: concentrated lines do not actually extend below dilute lines and will be dealt with subsequently)

Katsumoto's CO Absorption Data

CO Absorption in Liquid (mol/L) vs CO Partial Pressure in Gas (Pa)

— A
···· B
— · C
— · D
— E
···· F
— · G
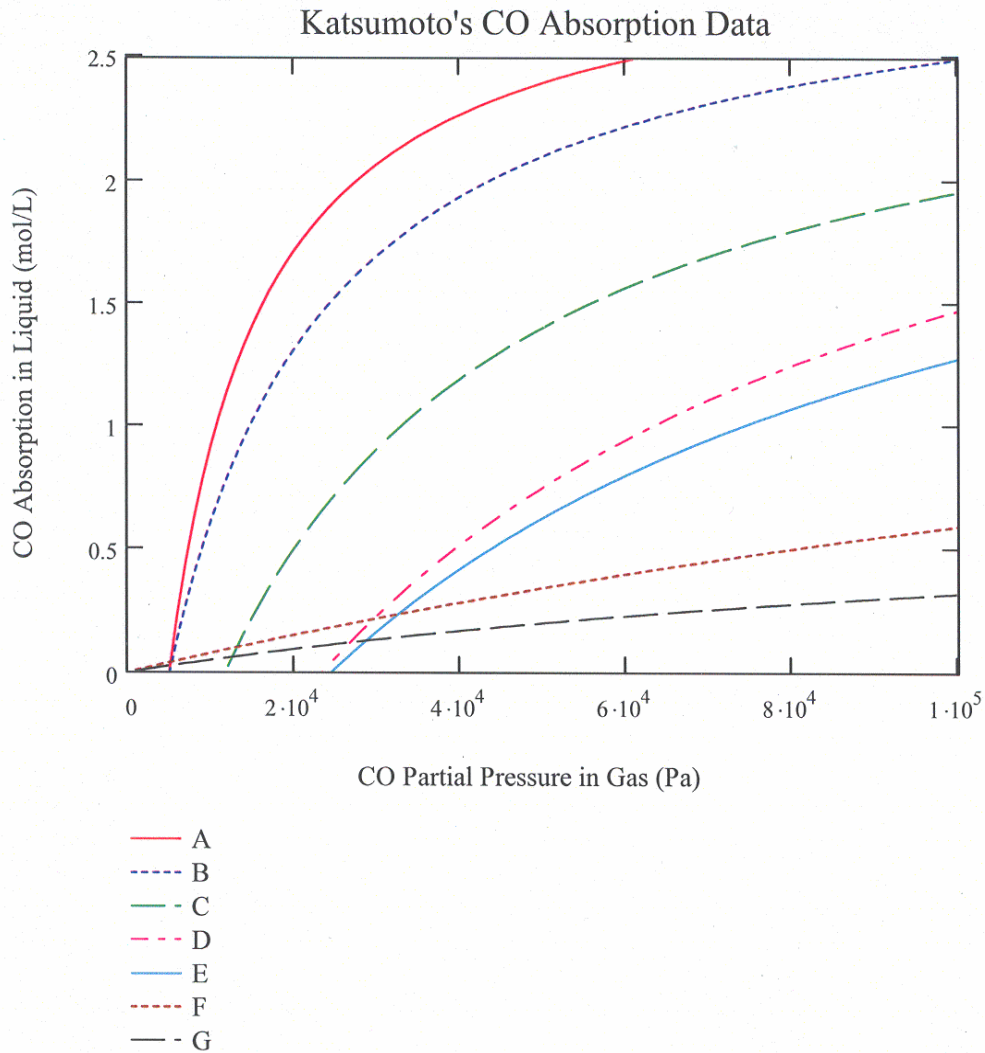
Derive a Model from Katsumoto's data that can be used to predict CO absorption of a solution with arbitrary CuCl and MgCl2 concentrations.

Dilute solutions: Only two absorption coefficients are presented with no details showing how they were derived. Although a major assumption, these two points are used to find an equation for the absorption coefficient for dilute cases.

$$k_1 := \left(-2.17571 \cdot 10^{-6} \cdot \frac{C_{CuCl}}{mol \cdot L^{-1}} + 8.51157 \cdot 10^{-6} \right) \cdot Pa^{-1} \quad \text{(absorption coefficient)}$$

93

Concentrated solutions: Of the five concentrated solutions, two are suspensions. If the remaining three solutions are used to plot k_2 and P_{CO}' versus the chloride concentration, a linear line fits the data well for k_2 ($R^2 = 0.9998$), while a power law was used for P_{CO}' ($R^2 = 0.9806$). The regressed values and associated equations are shown below.

Solution concentrations:
$$C_{CuCl} = 0.81 \frac{mol}{L} \quad C_{MgCl2} = 2.01 \frac{mol}{L} \quad C_{Cl} := C_{CuCl} + 2 \cdot C_{MH}$$

k_2:
$$s_{k2} := 3.0819 \cdot 10^{-5} \quad int_{k2} := 2.9983 \cdot 10^{-4} \quad k_2 := \left(s_{k2} \cdot C_{Cl} \cdot \frac{L}{mol} - int_{k2} \right) \cdot Pa^{-1}$$

P_{CO}':
$$aa := 4.617 \quad b := -14.64 \quad P_{CO'} := \left(aa \cdot 10^{10} \right) \cdot \left(C_{CuCl} \cdot \frac{L}{mol} \right)^{b} \cdot Pa$$

CO Absorption as a function of P_{CO} for an arbitrary concentration.

Define total Cu^+, and redefine dilute and concentrated CO absorption models using absorption coefficients based on arbitrary concentration:

$$A_{Cu} := C_{CuCl} \qquad \alpha(P_{CO}, i) := \frac{\overrightarrow{k_1 \cdot P_{CO_i} \cdot A_{Cu}}}{1 + k_1 \cdot P_{CO_i}} \qquad \beta(P_{CO}, i) := \frac{\overrightarrow{k_2 \cdot \left(P_{CO_i} - P_{CO'} \right) \cdot A_{Cu}}}{1 + k_2 \cdot \left(P_{CO_i} - P_{CO'} \right)}$$

Katsumoto's data suggest that CO absorption in concentrated cases increases linearly as dilute solutions until P_{CO}' is reached. The following relationship accounts for this, causing the absorption to follow the line for dilute solution F (as it appears to do in Katsumoto's work) when it would otherwise fall below it:

$$\beta_{CO}(P_{CO}, i, k) := if \left(\beta_{CO}(P_{CO}, i, k) > \alpha_{CO}(P_{CO}, i, 1), \beta_{CO}(P_{CO}, i, k), \alpha_{CO}(P_{CO}, i, 1) \right)$$

$$\beta(P_{CO}, i) := if \left(\beta(P_{CO}, i) > \alpha_{CO}(P_{CO}, i, 1), \beta(P_{CO}, i), \alpha_{CO}(P_{CO}, i, 1) \right)$$

The following correlation determines whether the solution is dilute or concentrated and calculates the CO absorption accordingly:

$$\gamma(P_{CO}, i) := if \left(C_{Cl} > 10 \frac{mol}{L}, \beta(P_{CO}, i), \alpha(P_{CO}, i) \right)$$

94

CO Absorption Model

(Legend: A, B, C, D, E, F, G, Predict)

Y-axis: CO Absorption in Liquid (mol/L)
X-axis: CO Partial Pressure in Gas (Pa)
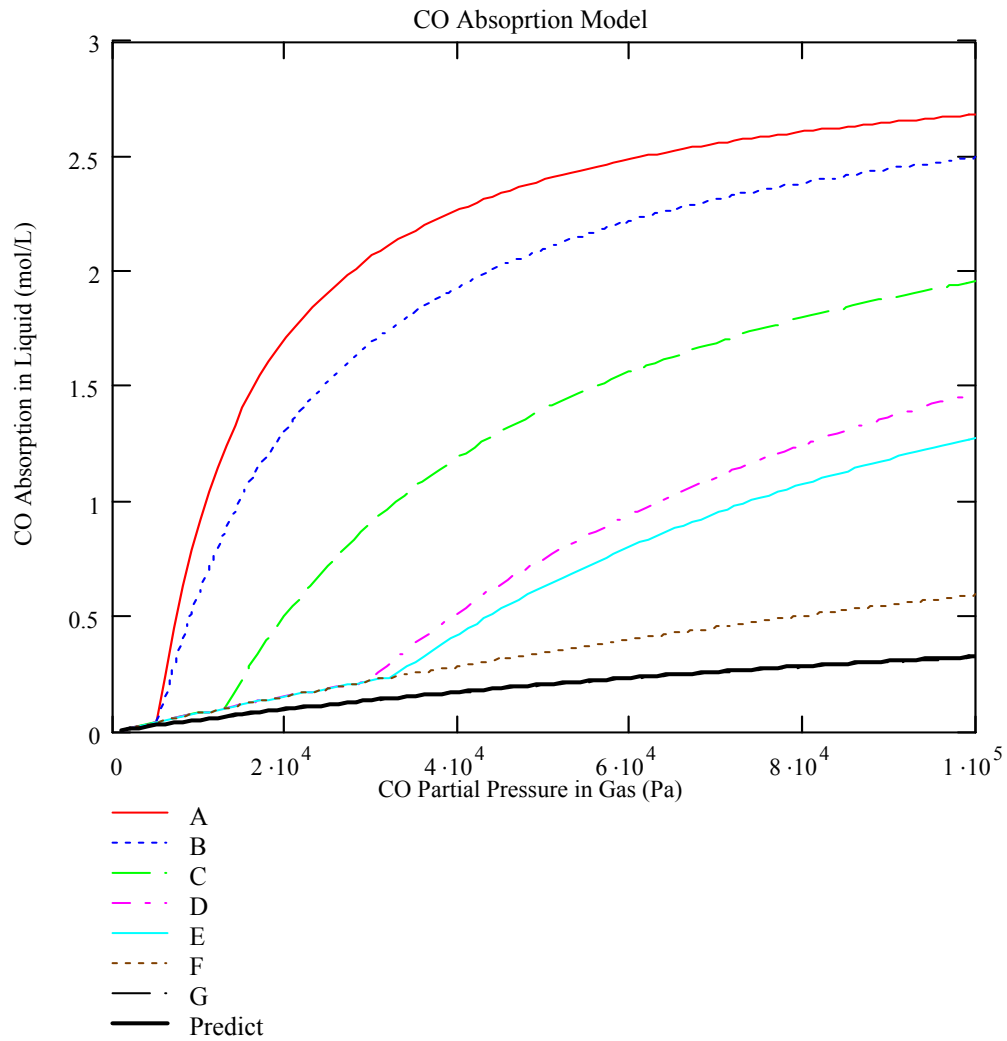
Calculate CO mole fration   in gas and in solution and   plot equilibrium curve :

$$A_{CO_i} := \gamma\left(P_{CO}, i\right)$$ (redefined absorbed CO)

$$n_{CO_i} := A_{CO_i} \cdot Vol_b$$ (moles CO in solution)

$$x_{CO_i} := \frac{n_{CO_i}}{n_{CO_i} + n_{Tot}}$$ (mole fraction CO in liquid)

$$y_{CO_i} := \frac{P_{CO_i}}{P_{tot}}$$ (mole fraction CO in gas)

CO Equilibrium
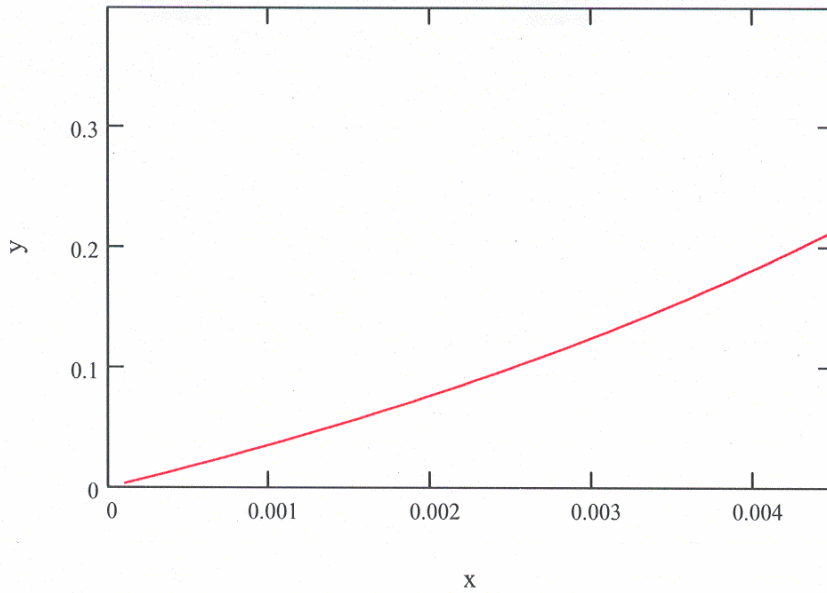
$$vs := cspline(y_{CO}, x_{CO})$$

(fits a cubic spline through equilibrium curve)

$$ff(xx) := interp(vs, y_{CO}, x_{CO}, xx) \quad ff(y_{in}) = 2.719 \times 10^{-3}$$

(the x that would be in equilibrium with y_{in})

Equilibrium ratio (K value)

$$KK_i := \frac{y_{CO_i}}{x_{CO_i}}$$

(K value)

$$K_N := \frac{y_{in}}{ff(y_{in})} \qquad K_N = 40.827$$

(K at bottom of scrubber: note - large K suggests liquid phase MT limited)

Equilibrium Ratio
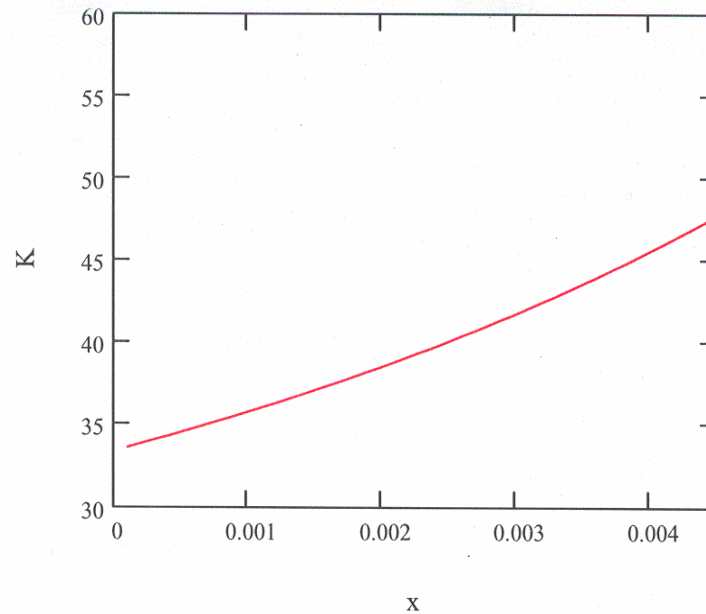
Liquid Flow Composition

$$L'_{min} := \frac{G' \cdot (Y_{in} - Y_{out})}{\dfrac{Y_{in}}{Y_{in} \cdot (K_N - 1) + K_N} - X_{in}}$$

$L'_{min} = 2.903 \times 10^4 \dfrac{mol}{hr}$

(minimum liquid flow rate; from material balance (operating line) and definition of K)

$$L'_{min1} := G' \cdot K_N \cdot \frac{CO_{trans}}{CO_{init}}$$

$L'_{min1} = 2.588 \times 10^4 \dfrac{mol}{hr}$

(assumes dilute solution, no solute entering in liquid stream: L'_{min} used below to be conservative)

$$L' := L'_{min} \cdot L_{factor}$$

$L' = 5.807 \times 10^4 \dfrac{mol}{hr}$

(solute-free liquid flow rate required)

Mole fraction CO in exiting liquid

$$X_{out} := \frac{CO_{trans}}{L'}$$

$X_{out} = 1.363 \times 10^{-3}$

(solute free)

$$x_{out} := \frac{X_{out}}{1 + X_{out}}$$

$x_{out} = 1.361 \times 10^{-3}$

(non-solute free)

Actual liquid flow rate (includes small CO amount)

$$LL := L' + CO_{trans}$$

$LL = 969.092 \dfrac{mol}{min}$

(small increase over L')

97

Liquid Mole Fraction, Molecular Weight, Volume

$$x_{CuCl} := \frac{n_{CuCl}}{n_{Tot}} \qquad x_{MgCl2} := \frac{n_{MgCl2}}{n_{Tot}} \qquad x_w := \frac{n_w}{n_{Tot}}$$

$$MW_L := MW_{CuCl} \cdot x_{CuCl} + MW_{MH} \cdot x_{MgCl2} + MW_w \cdot x_w \qquad \text{(doesn't include CO here)}$$

$$V_L := L' \cdot MW_L \cdot \rho_L^{-1} \qquad V_L = 21.507 \frac{L}{min} \qquad \text{(liquid flow rate through column)}$$

GPDC Factors

This calculates the liquid to gas kinetic energy ratio, which is then used to calculate Y, a factor on the generalized pressure drop correlation plot (flooding = 1). An equation for Y was regressed in Excel and is used below.

$$F_{LG} := \frac{LL \cdot MW_L}{G \cdot MW_G} \cdot \left(\frac{\rho_G}{\rho_L}\right)^{0.5} \qquad F_{LG} = 3.665 \qquad \text{(liquid to gas kinetic energy ratio--use this with GPDC to get Y)}$$

$$F_{LG.ln} := \ln(F_{LG}) \qquad Y_{ln} := -0.117 \cdot F_{LG.ln}^2 - 1.0446 \cdot F_{LG.ln} - 3.8968 \qquad Y := e^{Y_{ln}} \qquad Y = 4.292 \times 10^{-3}$$

The following are additional factors from corresponding GPDC charts, regressed in Excel; see Separations, 331

$$r_\rho := \frac{\rho_w(T_f)}{\rho_L} \qquad r_\rho = 0.842 \qquad f_1 := 1.5306 \cdot r_\rho - 0.459 \qquad f_1 = 0.83$$

$$f_2 := 0.2076 \cdot \ln\left(\frac{\mu_L}{cP}\right) + 1.0126 \qquad f_2 = 1.038$$

Superficial Gas Velocity

$$u_o := \left(\frac{Y}{\frac{\rho_G}{\rho_w(T_f)} \cdot f_1 \cdot f_2} \cdot \frac{g}{F_p}\right)^{0.5} \qquad u_o = 0.032 \frac{m}{s} \qquad \text{(superficial gas velocity at flooding)}$$

Diameter

$$D_T := \left(\frac{4 \cdot G \cdot MW_G}{f \cdot u_o \cdot \pi \cdot \rho_G}\right)^{0.5} \qquad \boxed{D_T = 12.32 \, in} \qquad \text{(Separations, 330)}$$

$$\frac{D_T}{D_P} = 52.156 \qquad \text{(Note: column diameter should be a minimum of 8 times the packing particle diameter to avoid wall effects; Separations)}$$

Section 4: Height

<u>Theory</u>

The height of the column is found by doing a differential balance on the column (Separations, 321):

$$LL \cdot dx = Kxa \cdot \left(x_{eq} - x\right) \cdot A_{cs} \cdot dl$$

($K_x a$ = overall volumetric liquid transfer coefficient, A_{cs} = empty column cross sectional area, and dl = differential height; note, balance is performed on liquid since mass transfer resistance in liquid >> resistance in gas and resistance due to reversible reaction (assumed to be fast))

Separating, integrating, and solving for the column height, l_T, we obtain:

$$l_T = \frac{LL}{Kxa \cdot A_{cs}} \cdot \int_{x_{in}}^{x_{out}} \frac{1}{x_{eq} - x} \, dx$$

(where the first term on the right is H_{OL} (overall height of a transfer unit (HTU)) based on the liquid, and the second is N_{OL} (overall number of transfer units (NTU)) based on the liquid)

$$l_T = H_{OL} \cdot N_{OL}$$

$$H_{OL} = \frac{LL}{Kxa \cdot A_{cs}} = H_L + A \cdot H_G$$

$$H_L = \frac{L}{kxa \cdot A_{cs}} = \frac{u_L}{kLa}$$

($k_x a$ [=] mol/m^{3}s, $k_L a$ [=] s^{-1}, u_L = velocity w/ reference to empty column cross section [=] m/s; A = L/KG)

$$H_G = \frac{G}{kya \cdot A_{cs}} = \frac{u_G}{kGa}$$

(same definitions as above, but with gas)

$$1/K_x a = 1/k_x a + 1/Kk_y a$$

<u>Fluid Properties</u>

$$A := \frac{LL}{K_N \cdot G} \qquad\qquad A = 1.978$$

(absorption factor)

<u>Gas mixture viscosity</u> (<u>Transport Phenomena</u>)--this is based on feed gas composition, but would be more accurate if it were based on average composition through the column--it doesn't make a huge difference.

$$\mu_{N2} := 1.7574 \cdot 10^{-5} \, Pa \cdot s \qquad\qquad \mu_{O2} := 2.0445 \cdot 10^{-5} \, Pa \cdot s \qquad\qquad \text{(viscosities are at 295 K--DIPPR)}$$

$$\mu_{CO2} := 1.4819 \cdot 10^{-5} \, Pa \cdot s \qquad\qquad \mu_{CO} := 1.7533 \cdot 10^{-5} \, Pa \cdot s$$

99

$$\mu_i := \begin{pmatrix} \mu_{CO2} \\ \mu_{CO} \\ \mu_{O2} \\ \mu_{N2} \end{pmatrix} \qquad \mu_{\alpha\_\beta.1} := \frac{\mu_i}{\mu_{i_1}} \qquad \mu_{\alpha\_\beta.2} := \frac{\mu_i}{\mu_{i_2}} \qquad \mu_{\alpha\_\beta.3} := \frac{\mu_i}{\mu_{i_3}} \qquad \mu_{\alpha\_\beta.4} := \frac{\mu_i}{\mu_{i_4}}$$

$$\mu_{\alpha\_\beta} := \text{augment}\left(\mu_{\alpha\_\beta.1}, \mu_{\alpha\_\beta.2}, \mu_{\alpha\_\beta.3}, \mu_{\alpha\_\beta.4}\right)^T$$

$$MW_i := \begin{pmatrix} MW_{CO2} \\ MW_{CO} \\ MW_{O2} \\ MW_{N2} \end{pmatrix} \qquad MW_{\alpha\_\beta.1} := \frac{MW_i}{MW_{i_1}} \qquad MW_{\alpha\_\beta.2} := \frac{MW_i}{MW_{i_2}}$$

$$MW_{\alpha\_\beta.3} := \frac{MW_i}{MW_{i_3}} \qquad MW_{\alpha\_\beta.4} := \frac{MW_i}{MW_{i_4}}$$

$$MW_{\alpha\_\beta} := \text{augment}\left(MW_{\alpha\_\beta.1}, MW_{\alpha\_\beta.2}, MW_{\alpha\_\beta.3}, MW_{\alpha\_\beta.4}\right)^T$$

$$\Phi_{\alpha\beta} := \overrightarrow{\left[\frac{1}{\sqrt{8}} \cdot \left(1 + MW_{\alpha\_\beta}\right)^{-0.5} \cdot \left[1 + \mu_{\alpha\_\beta}^{0.5} \cdot \left(\frac{1}{MW_{\alpha\_\beta}}\right)^{0.25}\right]^2\right]} \qquad y_i := \begin{pmatrix} y_{CO2} \\ y_{in} \\ y_{O2} \\ y_{N2} \end{pmatrix}$$

$$n := 1..4 \qquad sum_n := \overrightarrow{y_i \cdot \Phi_{\alpha\beta}^{\langle n \rangle}} \qquad \mu_{G.mix} := \sum_{n=1}^{4} \frac{\mu_{i_n} \cdot y_{i_n}}{sum_n} \qquad \mu_G := \mu_{G.mix} \qquad \mu_G = 0.017\,cP$$

$$\nu_G := \frac{\mu_G}{\rho_G} \qquad\qquad \nu_G = 0.043 \frac{cm^2}{s} \qquad\qquad \text{(kinematic gas viscosity)}$$

$$\nu_L := \frac{\mu_L}{\rho_L} \qquad\qquad \nu_L = 9.553 \times 10^{-3} \frac{cm^2}{s} \qquad\qquad \text{(kinematic liquid viscosity)}$$

$$\sigma_w := 0.074421 \frac{N}{m} \qquad\qquad \sigma_L := \sigma_w \qquad\qquad \text{(liquid surface tension: assume water, 290.16 K-- DIPPR)}$$

$$A_{cs} := \frac{\pi \cdot D_T^{\,2}}{4} \qquad\qquad A_{cs} = 119.217\ in^2 \qquad\qquad \text{(empty column cross section)}$$

$$u_L := LL \cdot MW_L \cdot \rho_L^{\,-1} \cdot A_{cs}^{\,-1} \qquad u_L = 16.801\ \frac{m^3}{m^2 \cdot hr} \qquad\qquad \text{(superficial liquid velocity)}$$

$$u_G := \frac{V_f}{A_{cs}} \qquad\qquad u_G = 0.073\ \frac{ft}{s} \qquad\qquad \text{(superficial gas velocity)}$$

Diffusion Coefficients

Gas (Chapman-Enskog/Lennard-Jones Parameters from TP text; applies to low density, low pressure gas):
Assumption: valid at 30 psi

$$\kappa := 1.38066 \cdot 10^{-23}\ \frac{J}{K} \qquad \text{(Boltzmann's constant)}$$

$\sigma_{O2} := 3.433 Ang$	$\sigma_{CO} := 3.590 Ang$	$\sigma_{CO2} := 3.996 Ang$	$\sigma_{N2} := 3.667 Ang$
$\varepsilon\_k_{O2} := 113 K$	$\varepsilon\_k_{CO} := 110 K$	$\varepsilon\_k_{CO2} := 190 K$	$\varepsilon\_k_{N2} := 99.8 K$
$\varepsilon_{O2} := \varepsilon\_k_{O2} \cdot \kappa$	$\varepsilon_{CO} := \varepsilon\_k_{CO} \cdot \kappa$	$\varepsilon_{CO2} := \varepsilon\_k_{CO2} \cdot \kappa$	$\varepsilon_{N2} := \varepsilon\_k_{N2} \cdot \kappa$
$T_{c.O2} := 154.4 K$	$T_{c.CO} := 132.9 K$	$T_{c.CO2} := 304.2 K$	$T_{c.N2} := 126.2 K$
$P_{c.O2} := 49.7 atm$	$P_{c.CO} := 34.5 atm$	$P_{c.CO2} := 72.8 atm$	$P_{c.N2} := 33.5 atm$
$V'_{c.O2} := 74.4\ \frac{cm^3}{mol}$	$V'_{c.CO} := 93.1\ \frac{cm^3}{mol}$	$V'_{c.CO2} := 94.1\ \frac{cm^3}{mol}$	$V'_{c.N2} := 90.1\ \frac{cm^3}{mol}$

For CO in CO_2:

$$\sigma_{CO\_CO2} := \frac{1}{2} \cdot \left(\sigma_{CO} + \sigma_{CO2}\right) \qquad \varepsilon_{CO\_CO2} := \left(\varepsilon_{CO} \cdot \varepsilon_{CO2}\right)^{0.5}$$

$$\kappa T\_\varepsilon_{CO\_CO2} := \frac{\kappa \cdot T_f}{\varepsilon_{CO\_CO2}} \qquad\qquad \kappa T\_\varepsilon_{CO\_CO2} = 2.068$$

$$\Omega_{CO\_CO2} := 1.0645 \qquad\qquad \text{(collision integral: assume linear interpolation)}$$

$$D_{CO\_CO2} := 0.0018583 \cdot \left[\left(\frac{T_f}{K} \right)^3 \cdot \left(\frac{1 \cdot \frac{gm}{mol}}{MW_{CO}} + \frac{1 \cdot \frac{gm}{mol}}{MW_{CO2}} \right) \right]^{0.5} \cdot \frac{1}{\frac{P_{tot}}{atm} \cdot \left(\frac{\sigma_{CO\_CO2}}{Ang} \right)^2 \cdot \Omega_{CO\_CO2}} \cdot \frac{cm^2}{s}$$

$$D_{CO\_CO2} = 0.053 \frac{cm^2}{s} \quad \text{(only considers CO in CO}_2\text{ since mixture is ~80\% CO}_2\text{, ~13\% CO)}$$

For CO in N_2:

$$\sigma_{CO\_N2} := \frac{1}{2} \cdot \left(\sigma_{CO} + \sigma_{N2} \right) \qquad \varepsilon_{CO\_N2} := \left(\varepsilon_{CO} \cdot \varepsilon_{N2} \right)^{0.5}$$

$$\kappa T\_\varepsilon_{CO\_N2} := \frac{\kappa \cdot T_f}{\varepsilon_{CO\_N2}} \qquad\qquad \kappa T\_\varepsilon_{CO\_N2} = 2.853$$

$$\Omega_{CO\_N2} := 0.9670 \qquad\qquad \text{(collision integral: assume linear interpolation)}$$

$$D_{CO\_N2} := 0.0018583 \cdot \left[\left(\frac{T_f}{K} \right)^3 \cdot \left(\frac{1 \cdot \frac{gm}{mol}}{MW_{CO}} + \frac{1 \cdot \frac{gm}{mol}}{MW_{N2}} \right) \right]^{0.5} \cdot \frac{1}{\frac{P_{tot}}{atm} \cdot \left(\frac{\sigma_{CO\_N2}}{Ang} \right)^2 \cdot \Omega_{CO\_N2}} \cdot \frac{cm^2}{s}$$

$$D_{CO\_N2} = 0.07 \frac{cm^2}{s} \qquad \text{(only considers CO in N}_2\text{ since mixture is mostly N}_2\text{, not much CO)}$$

$$D_G := \text{if}\left(y_{N2} > y_{CO2}, D_{CO\_N2}, D_{CO\_CO2} \right) \qquad D_G = 0.07 \frac{cm^2}{s} \qquad \text{(gas diffusion variable; typical values between 0.1 and 1 cm}^2\text{/s--\underline{Transport Phenomena}, 518, \underline{Perry's Handbook} 7th ed., 5-48)}$$

Liquid (from Prausnitz text, <u>The Properties of Gases And Liquids (5th ed)</u>, 11.27, Nakanishi Correlation), w = water:

$$I_{CO} := 1 \quad S_{CO} := 1 \quad A_w := 2.8 \quad S_w := 1 \qquad \text{(factors for correlation, Table 11.4, 11.28)}$$

$$V_{CO\_Tb} := 0.0354 \frac{m^3}{kmol} \qquad\qquad \text{(liquid molar volume at boiling point, 81.66 K)}$$

$\beta := 1.065$ (fudge factor: CO is normally gas at 298K and 1 bar)

$V_{CO} := \beta \cdot V_{CO\_Tb}$ $V_{CO} = 37.701 \dfrac{cm^3}{mol}$ (adjusted CO molar volume)

$V_w := 37.4 \dfrac{cm^3}{mol}$ (liquid molar volume of water, 298K, 1 bar; Prausnitz, 11.28)

$$D_{CO\_w} := \left[\frac{9.97 \cdot 10^{-8}}{\left(I_{CO} \cdot \dfrac{V_{CO}}{cm^3 \cdot mol^{-1}}\right)^{\frac{1}{3}}} + \frac{2.40 \cdot 10^{-8} \cdot A_w \cdot S_w \cdot \dfrac{V_w}{cm^3 \cdot mol^{-1}}}{I_{CO} \cdot S_{CO} \cdot \dfrac{V_{CO}}{cm^3 \cdot mol^{-1}}} \right] \cdot \frac{\dfrac{T_f}{K}}{\dfrac{\mu_{wat}(T_f)}{cP}} \cdot \frac{cm^2}{s}$$

(diffusion coefficient of CO in solvent at low concentrations)

$D_L := D_{CO\_w}$ $D_L = 3.213 \times 10^{-5} \dfrac{cm^2}{s}$ (considers only diffusion of CO in water; typical values between 10^{-6} and 10^{-4} cm²/s--Perry's Handbook)

Mass Transfer Coefficient (Onda)

Gas Phase

$Sc_G := \dfrac{\mu_G}{\rho_G \cdot D_G}$ $Sc_G = 0.609$ $Re_G := \dfrac{\rho_G \cdot u_G}{\mu_G \cdot a}$ $Re_G = 8.241$ (Scmidt and Reynolds numbers)

$a_p := a$ (a_p is specific surface area of packing)

$d_p := D_p$ (nominal packing diameter)

$AA := if\left(D_P < 0.012m, 2.0, 5.23\right)$ $AA = 2$ (a constant depending on nominal packing diameter)

$k_{G.O} := AA \cdot Re_G^{0.7} \cdot Sc_G^{0.333} \cdot \left(a_p \cdot d_p\right)^{-2} \cdot a_p \cdot D_G$ $k_{G.O} = 2.292 \times 10^{-3} \dfrac{m}{s}$ (gas mass transfer coefficient)

Liquid Phase

$\sigma_L = 74.421 \dfrac{dyne}{cm}$ (assumed to be water)

$\sigma_c := 33 \dfrac{dyne}{cm}$ (critical surface tension of packing--Bravo and Fair's paper says 61 ceramic, 75 ss, 33 PE--since we are using glass, this is a conservative estimate; one source says for pyrex glass it is 170

$$We_L := \frac{\rho_L \cdot u_L^2}{a_p \cdot \sigma_L} \qquad We_L = 5.485 \times 10^{-4} \qquad Fr_L := \frac{a_p \cdot u_L^2}{g} \qquad Fr_L = 1.399 \times 10^{-3} \quad \text{(Weber and Froude numbers)}$$

$$Re_L := \frac{\rho_L \cdot u_L}{\mu_L \cdot a_p} \qquad Re_L = 7.754 \qquad \text{(Reynolds number)}$$

$$a' := a_p \cdot \left[1 - \exp\left[-1.45 \cdot \left(\frac{\sigma_c}{\sigma_L}\right)^{0.75} \cdot Re_L^{0.1} \cdot Fr_L^{-0.05} \cdot We_L^{0.2}\right]\right] \qquad a' = 162.917 \frac{m^2}{m^3} \qquad \text{(interfacial area density)}$$

$$Re'_L := \frac{\rho_L \cdot u_L}{\mu_L \cdot a'} \qquad Re'_L = 29.986 \qquad \text{(Reynolds number based on a')}$$

$$Sc_L := \frac{\mu_L}{\rho_L \cdot D_L} \qquad Sc_L = 297.339 \qquad \text{(Scmidt number)}$$

$$k_{L.O} := \frac{0.0051 \cdot Re'_L{}^{0.667} \cdot Sc_L{}^{-0.5} \cdot \left(a_p \cdot d_p\right)^{0.4}}{\left(\frac{\rho_L}{\mu_L \cdot g} \cdot \frac{m^3}{s^3}\right)^{0.333}} \cdot \frac{m}{s} \qquad k_{L.O} = 1.029 \times 10^{-4} \frac{m}{s}$$

$$kLa_O := k_{L.O} \cdot a' \qquad\qquad kLa_O = 0.017\,s^{-1}$$

$$kGa_O := k_{G.O} \cdot a' \qquad\qquad kGa_O = 0.373\,s^{-1}$$

Mass Transfer Coefficient (Bravo and Fair)

Bravo and Fair's correlation uses the same equations as Onda's, but the interfacial area density is different. Note that interfacial area density depends on height, which is what we are trying to calculate, so it is iterative.

$$Ca_L := \frac{u_L \cdot \mu_L}{\sigma_L} \qquad Ca_L = 7.073 \times 10^{-5} \qquad\qquad \text{(capillary number)}$$

$$H := 4.5\,ft \qquad\qquad\qquad\qquad \text{(approximate height of the column, a guess--go to end of program, find calculated height, and re-enter it here until they match)}$$

104

$$a' := 19.78 \cdot a_p \cdot \left(Ca_L \cdot Re_G\right)^{0.392} \cdot \frac{\left(\sigma_L \cdot \frac{m}{N}\right)^{0.5}}{\left(H \cdot m^{-1}\right)^{0.4}} \qquad\qquad a' = 161.672 \frac{m^2}{m^3}$$

$$Re'_L := \frac{\rho_L \cdot u_L}{\mu_L \cdot a'} \qquad\qquad Re'_L = 30.217 \qquad\qquad \text{(Reynolds number based on a')}$$

$$k_{L.BF} := \frac{0.0051 \cdot Re'^{0.667}_L \cdot Sc^{-0.5}_L \cdot \left(a_p \cdot d_p\right)^{0.4}}{\left(\frac{\rho_L}{\mu_L \cdot g} \cdot \frac{m^3}{s^3}\right)^{0.333}} \cdot \frac{m}{s} \qquad\qquad k_{L.BF} = 1.035 \times 10^{-4} \frac{m}{s}$$

$$kLa_{BF} := k_{L.BF} \cdot a' \qquad\qquad\qquad kLa_{BF} = 0.017 \, s^{-1}$$

$$kGa_{BF} := kGa_O \qquad\qquad\qquad kGa_{BF} = 0.373 \, s^{-1}$$

Calculate N_{OL}:

From above note that:
$$N_{OL} = \int_{x_{in}}^{x_{out}} \frac{1}{x_{eq} - x} \, dx$$

From linear solute material balance (operating line) and linear equilibrium expression (K value), find expression for $x_{eq} = f(x)$:

$$Y(X) := X \cdot \left(\frac{L'}{G'}\right) + Y_{out} - X_{in} \cdot \left(\frac{L'}{G'}\right) \qquad\qquad X_{eq}(X) := \frac{\dfrac{Y(X)}{K_N \cdot (1 + Y(X))}}{1 - \dfrac{Y(X)}{K_N \cdot (1 + Y(X))}}$$

Assumption: linear operating line (dilute), and ~linear equilibrium curve through origin (see equilibrium plot)

$$N_{OL} := \int_{X_{in}}^{X_{out}} \frac{1}{X_{eq}(X) - X} \, dX \qquad\qquad N_{OL} = 3.495$$

Calculate HOL

$$H_{L.O} := \frac{u_L}{kLa_O} \qquad H_{L.BF} := \frac{u_L}{kLa_{BF}}$$

$$H_{G.O} := \frac{u_G}{kGa_O} \qquad H_{G.BF} := \frac{u_G}{kGa_{BF}}$$

$$H_{OG.O} := H_{G.O} + \frac{1}{A}\cdot H_{L.O} \qquad H_{OG.BF} := H_{G.BF} + \frac{1}{A}\cdot H_{L.BF}$$

$$H_{OL.O} := H_{OG.O}\cdot A \qquad H_{OL.BF} := H_{OG.BF}\cdot A$$

Calculate Height

$$l_{T.O} := N_{OL}\cdot H_{OL.O}$$

$$l_{T.BF} := N_{OL}\cdot H_{OL.BF}$$

$$l_{T.O} = 4.536\,ft$$

$$l_{T.BF} = 4.544\,ft$$

$$\begin{pmatrix} Onda \\ Bravo\_Fair \end{pmatrix}$$

(Note: take the height from BF and substitute it into the H in section "MT Coeff. (Bravo & Fair Corr)" until the values match.)

$$kGa\_kLa_O := \frac{kGa_O}{kLa_O} \qquad kGa\_kLa_O = 22.268$$

$$kGa\_kLa_{BF} := \frac{kGa_{BF}}{kLa_{BF}} \qquad kGa\_kLa_{BF} = 22.325$$

$$D_T = 12.32\,in \qquad \frac{D_T}{D_P} = 52.156 \qquad \rho_L = 1.181\,\frac{gm}{mL} \qquad \frac{LL}{G} = 80.758 \qquad \frac{L'}{G'} = 90.717$$

Section 5: Scale Down to Prototype Size

To build a prototype to test the process we need to scale down. We arbitrarily chose a scrubber with a diameter of 1 in. The following calculations find the corresponding flow rates, etc.

$$D_T = 12.32\,in \qquad D_{Ts} := 1\,in \qquad \text{(actual diameter, prototype diameter (s = small))}$$

106

$$r := \dfrac{D_T^2}{D_{Ts}^2} \qquad\qquad r = 151.792 \qquad\qquad \text{(ratio of areas (diameters))}$$

$$V_{fs} := \dfrac{V_f}{r} \qquad\qquad V_{Ls} := \dfrac{V_L}{r} \qquad\qquad \text{(prototype gas flow rate, prototype liquid flow rate)}$$

$$V_f = 102.275 \dfrac{L}{min} \qquad V_{fs} = 0.674 \dfrac{L}{min} \qquad \text{(actual, prototype gas flow rates)}$$

$$V_L = 21.507 \dfrac{L}{min} \qquad V_{Ls} = 0.037 \dfrac{gal}{min} \qquad \text{(actual, prototype liquid flow rate)}$$

Check

As a check, calculate velocities, which should be the same for actual and prototype columns:

$$v_g := \dfrac{V_f}{A_{cs}} \qquad v_g = 0.073 \dfrac{ft}{s} \qquad\qquad v_L := \dfrac{V_L}{A_{cs}} \qquad v_L = 0.015 \dfrac{ft}{s}$$

$$v_{gs} := \dfrac{V_{fs}}{\dfrac{\pi \cdot D_{Ts}^2}{4}} \qquad v_{gs} = 0.073 \dfrac{ft}{s} \qquad\qquad v_{Ls} := \dfrac{V_{Ls}}{\dfrac{\pi \cdot D_{Ts}^2}{4}} \qquad v_{Ls} = 0.015 \dfrac{ft}{s}$$

Section 6: Miscellaneous

A material balance around the upper portion of the scrubber for a *dilute* solution yields:

$$y(xx) := xx \cdot \dfrac{LL}{G} + y_{out} - x_{in} \cdot \dfrac{LL}{G} \qquad \text{, which is plotted with the equilibrium line below.}$$

CO Equilibrium and Operating Lines

CO Gas Mole Fraction (y-axis) vs CO Liquid Mole Fraction (x-axis)

— CO Equilibrium Line
--- Operating Line
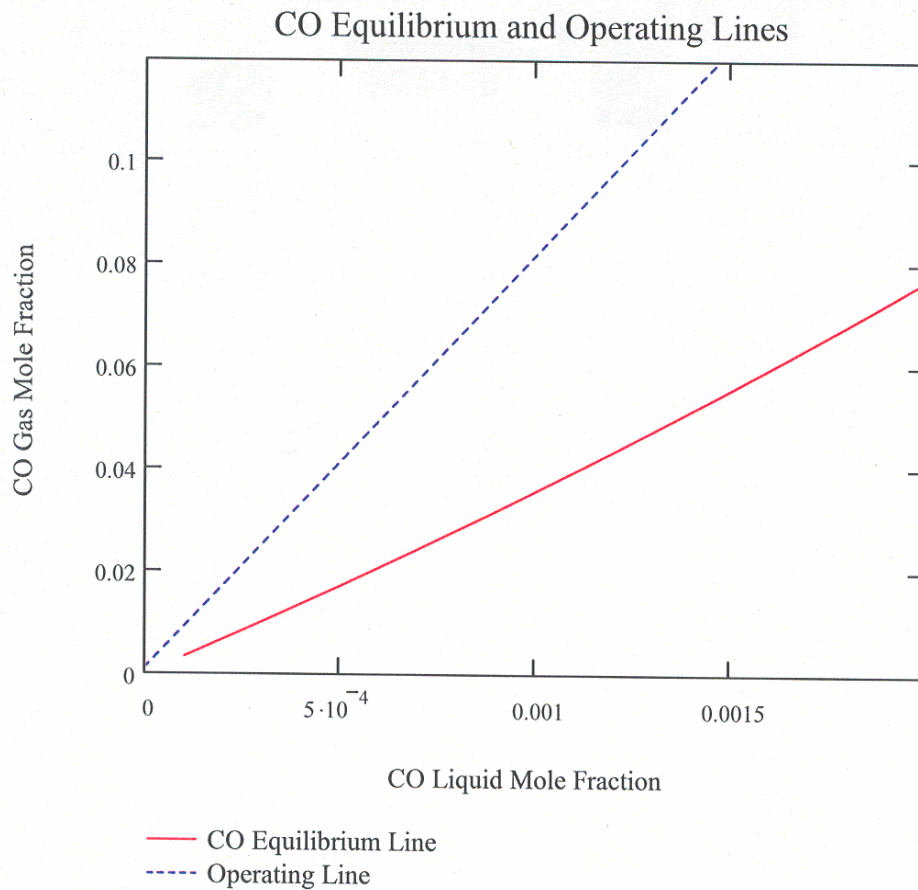
Overall Mass Transfer Coefficient Based on the Liquid

$$LL := V_{Ls} \cdot \rho_L \cdot MW_L^{-1} \qquad A_{cs} := \pi \cdot \frac{D_{Ts}^2}{4} \qquad X_{out} = 1.363 \times 10^{-3} \qquad X_{in} = 0$$

$$Kxa := \frac{LL}{A_{cs}} \cdot \left(\frac{u_L}{kLa_O} + A \cdot \frac{u_G}{kGa_O} \right)^{-1} \qquad Kxa = 530.053 \frac{mol}{m^3 \cdot s}$$

$$Kxa := \frac{LL}{A_{cs}} \cdot \frac{N_{OL}}{l_{T.O}} \qquad Kxa = 530.053 \frac{mol}{m^3 \cdot s} \qquad \frac{CO_{trans}}{CO_{init}} = 0.99038$$

APPENDIX B: Heat Exchanger Design

The overall process consists of three heat exchangers, composing the three sections that follow. The design is based on the latest version of the scrubber design, and uses flow rates corresponding to the scaled down prototype. In general, subscripts contain a number corresponding to heat exchanger, then c or h denoting cold side or hot side stream, followed by any other notations.

This program references the program for calculating column diameter and height:

⤷ Reference:H:\Research\Appendix Material\App\App A Absorber Design.mcd(R)

Fluid properties are calculated according to the following correlations obtained from DIPPR (liquid assumed to be water):

DIPPR Constants/Correlations

$$kmol := 1000mol$$

DIPPR constants and correlations (heat capacity, viscosity, density, thermal conductivity (assumes water for the liquid and pure CO for the gas)) (valid for both HX2 and HX3)

$$D := \begin{pmatrix}
\text{"Cp (liq)"} & \text{"}\mu\text{ (liq)"} & \text{"rho (liq)"} & \text{"k (liq)"} & \text{"Cp (gas)"} & \text{"}\mu\text{ (gas)"} & \text{"k (gas)"} \\
2.7637 \times 10^5 & -52.843 & 17.863 & -0.432 & 2.9108 \times 10^4 & 1.1127 \times 10^{-6} & 5.9882 \times 10^{-4} \\
-2.0901 \times 10^3 & 3.7036 \times 10^3 & 58.606 & 5.7255 \times 10^{-3} & 8.773 \times 10^3 & 0.5338 & 0.6863 \\
8.125 & 5.866 & -95.396 & -8.078 \times 10^{-6} & 3.0851 \times 10^3 & 94.7 & 57.13 \\
-0.014116 & 0 & 213.89 & 1.861 \times 10^{-9} & 8.4553 \times 10^3 & 0 & 501.92 \\
9.3701 \times 10^{-6} & 10 & -141.26 & 0 & 1.5382 \times 10^3 & 0 & 0
\end{pmatrix}$$

Heat Capacity:

$$C_{P.liq}(T, i) := \left[\left(D^{\langle i \rangle}\right)_2 + \left(D^{\langle i \rangle}\right)_3 \cdot \frac{T}{K} + \left(D^{\langle i \rangle}\right)_4 \cdot \left(\frac{T}{K}\right)^2 + \left(D^{\langle i \rangle}\right)_5 \cdot \left(\frac{T}{K}\right)^3 + \left(D^{\langle i \rangle}\right)_6 \cdot \left(\frac{T}{K}\right)^4 \right] \cdot \frac{J}{kmol \cdot K}$$

$$C_{P.gas}(T, i) := \left[\left(D^{\langle i \rangle}\right)_2 + \left(D^{\langle i \rangle}\right)_3 \cdot \left[\frac{\frac{\left(D^{\langle i \rangle}\right)_4}{T \cdot K^{-1}}}{\sinh\left[\frac{\left(D^{\langle i \rangle}\right)_4}{T \cdot K^{-1}}\right]} \right]^2 + \left(D^{\langle i \rangle}\right)_5 \cdot \left[\frac{\frac{\left(D^{\langle i \rangle}\right)_6}{T \cdot K^{-1}}}{\cosh\left[\frac{\left(D^{\langle i \rangle}\right)_6}{T \cdot K^{-1}}\right]} \right]^2 \right] \cdot \frac{J}{kmol \cdot K}$$

Viscosity:

$$\mu_{liq}(T, i) := \exp\left[\left(D^{\langle i \rangle}\right)_2 + \frac{\left(D^{\langle i \rangle}\right)_3 \cdot K}{T} + \left(D^{\langle i \rangle}\right)_4 \cdot \ln\left(\frac{T}{K}\right) + \left(D^{\langle i \rangle}\right)_5 \cdot \left(\frac{T}{K}\right)^{\left(D^{\langle i \rangle}\right)_6}\right] \cdot Pa \cdot s$$

$$\mu_{gas}(T, i) := \frac{\left(D^{\langle i \rangle}\right)_2 \cdot \left(\frac{T}{K}\right)^{\left(D^{\langle i \rangle}\right)_3}}{1 + \frac{\left(D^{\langle i \rangle}\right)_4}{T \cdot K^{-1}} + \frac{\left(D^{\langle i \rangle}\right)_5}{\left(\frac{T}{K}\right)^2}} \cdot Pa \cdot s$$

Thermal Conductivity:

$$k_{liq}(T, i) := \left[\left(D^{\langle i \rangle}\right)_2 + \left(D^{\langle i \rangle}\right)_3 \cdot \frac{T}{K} + \left(D^{\langle i \rangle}\right)_4 \cdot \left(\frac{T}{K}\right)^2 + \left(D^{\langle i \rangle}\right)_5 \cdot \left(\frac{T}{K}\right)^3 + \left(D^{\langle i \rangle}\right)_6 \cdot \left(\frac{T}{K}\right)^4\right] \cdot \frac{W}{m \cdot K}$$

$$k_{gas}(T, i) := \frac{\left(D^{\langle i \rangle}\right)_2 \cdot \left(\frac{T}{K}\right)^{\left(D^{\langle i \rangle}\right)_3}}{1 + \frac{\left(D^{\langle i \rangle}\right)_4}{T \cdot K^{-1}} + \frac{\left(D^{\langle i \rangle}\right)_5}{\left(\frac{T}{K}\right)^2}} \cdot \frac{W}{m \cdot K}$$

Density:

$$T_c := 647.096K \qquad T_r(T) := \frac{T}{T_c} \qquad t(T) := 1 - T_r(T)$$

$$\rho_{liq}(T, i) := \left[\left(D^{\langle i \rangle}\right)_2 + \left(D^{\langle i \rangle}\right)_3 \cdot t(T)^{0.35} + \left(D^{\langle i \rangle}\right)_4 \cdot t(T)^{\frac{2}{3}} + \left(D^{\langle i \rangle}\right)_5 \cdot t(T) + \left(D^{\langle i \rangle}\right)_6 \cdot t(T)^{\frac{4}{3}}\right] \cdot \frac{kmol}{m^3}$$

110

Section 1: HEAT EXCHANGER ONE (HX1)

This heat exchanger consists of 5 heating ropes (3/16" diameter by 10' long) wrapped in series in a spiral around the 3/8" copper tubing. The copper tubing is coiled a little over 2 times in coils that are about 1 foot in diameter. The CO-containing liquid is heated as it travels upwards through the coils, ensuring that CO bubbles released from solution travels upwards to the CO stream. The original flow rate used to calculate the number of ropes required was too large--the following calculations show the heat addition required.

Heat Exchanger One

$T_{1c.in} := (16 + 273.16)K \quad T_{1c.out} := (75 + 273.16)K$ (inlet, outlet solution temperatures)

$\Delta T_{1c} := T_{1c.out} - T_{1c.in} \quad T_{1c} := \dfrac{T_{1c.in} + T_{1c.out}}{2}$ (temperature change and average temperature)

$V_{1c} := 0.05 \dfrac{gal}{min} \quad MW_L = 26.241 \dfrac{gm}{mol} \quad \rho_L = 1.181 \dfrac{gm}{mL} \quad m_{1c} := V_{1c} \cdot \rho_L$ (mass flow rate, other liquid properties)

$C_{p.1c} := C_{P.liq}(T_{1c}, 1) \cdot MW_L^{-1} \qquad C_{p.1c} = 2.867 \dfrac{J}{gm \cdot K}$

$Q_1 := m_{1c} \cdot C_{p.1c} \cdot \Delta T_{1c} \qquad\qquad Q_1 = 630.082 \text{ watt}$

$\boxed{Q_1 = 630.082 \text{ W}}$ Heat addition required to heat liquid from 16 ºC to 75 ºC.

Section 2: HEAT EXCHANGER TWO (HX2)

User Inputs Required For Program

$D_o := 0.25in \qquad t_w := 0.030in$ (copper tubing dimensions)

$T_{2h.in} := T_{1c.out} \qquad\qquad T_{2h.out} := (16 + 273.16)K$ (hot side inlet and outlet temperatures)

$T_{2c.in} := (15 + 273.16)K \qquad T_{2c.out} := (20 + 273.16)K$ (cold side inlet and outlet temperatures)

$\varepsilon_f := 0.00152mm$ (e_f from Perry's, Table 6-1)

Copper Tubing Properties (both HX2 and HX3);(dimensions from
www.kembla.com.au/astm_b280.html)

$$k_c := 401 \frac{W}{m \cdot K}$$ (thermal conductivity)

$$D_i := D_o - 2t_w$$ (outer diameter, wall thickness, inner diameter)

Tubing Type	OD	Wall Thickness
1/4"	0.25	0.030
3/8"	0.375	0.032

Hot Process Stream Properties (Aqueous Liquid)

$$\Delta T_{2h} := T_{2h.in} - T_{2h.out}$$ $\Delta T_{2h} = 59\ K$ (temperture difference from inlet to outlet)

$$T_{2h} := (T_{2h.in} + T_{2h.out}) \cdot 0.5$$ $T_{2h} = 318.66\ K$ (average T, used for stream properties)

$$m_{2h} := m_{1c}$$ $m_{2h} = 0.493 \frac{lb}{min}$ (mass flow rate)

$$C_{P.2h} := C_{P.liq}(T_{2h}, 1)$$ $C_{P.2h} = 75.236 \frac{J}{mol \cdot K}$ (molar heat capacity: assumption--water)

$$C_{p.2h} := \frac{C_{P.2h}}{MW_L}$$ $C_{p.2h} = 2.867 \frac{J}{gm \cdot K}$ (mass heat capacity: liquid MW rather than water)

$$\rho_{2h} := \rho_L$$ $\rho_{2h} = 1.181 \frac{gm}{mL}$ (density: liquid)

$$\mu_{2h} := \mu_{liq}(T_{2h}, 2)$$ $\mu_{2h} = 0.606\ cP$ (viscosity: water)

$$k_{2h} := k_{liq}(T_{2h}, 4)$$ $k_{2h} = 0.632 \frac{W}{m \cdot K}$ (thermal conductivity: water)

Required Heat Removal

$$Q_2 := m_{2h} \cdot C_{p.2h} \cdot \Delta T_{2h}$$ $Q_2 = 630.082\ watt$

Cooling Water Properties

$$\Delta T_{2c} := T_{2c.out} - T_{2c.in}$$ (temperature difference)

$$T_{2c} := (T_{2c.in} + T_{2c.out}) \cdot 0.5$$ $T_{2c} = 290.66\ K$ (average T, used for stream properties)

Copper Tubing Properties (both HX2 and HX3);(dimensions from
www.kembla.com.au/astm_b280.html)

$$k_c := 401 \frac{W}{m \cdot K}$$ (thermal conductivity)

$$D_i := D_o - 2t_w$$ (outer diameter, wall thickness, inner diameter)

Tubing Type	OD	Wall Thickness
1/4"	0.25	0.030
3/8"	0.375	0.032

Hot Process Stream Properties (Aqueous Liquid)

$$\Delta T_{2h} := T_{2h.in} - T_{2h.out}$$ $\Delta T_{2h} = 59\ K$ (temperture difference from inlet to outlet)

$$T_{2h} := (T_{2h.in} + T_{2h.out}) \cdot 0.5$$ $T_{2h} = 318.66\ K$ (average T, used for stream properties)

$$m_{2h} := m_{1c}$$ $m_{2h} = 0.493\ \dfrac{lb}{min}$ (mass flow rate)

$$C_{P.2h} := C_{P.liq}(T_{2h}, 1)$$ $C_{P.2h} = 75.236\ \dfrac{J}{mol \cdot K}$ (molar heat capacity: assumption--water)

$$C_{p.2h} := \frac{C_{P.2h}}{MW_L}$$ $C_{p.2h} = 2.867\ \dfrac{J}{gm \cdot K}$ (mass heat capacity: liquid MW rather than water)

$$\rho_{2h} := \rho_L$$ $\rho_{2h} = 1.181\ \dfrac{gm}{mL}$ (density: liquid)

$$\mu_{2h} := \mu_{liq}(T_{2h}, 2)$$ $\mu_{2h} = 0.606\ cP$ (viscosity: water)

$$k_{2h} := k_{liq}(T_{2h}, 4)$$ $k_{2h} = 0.632\ \dfrac{W}{m \cdot K}$ (thermal conductivity: water)

Required Heat Removal

$$Q_2 := m_{2h} \cdot C_{p.2h} \cdot \Delta T_{2h}$$ $Q_2 = 630.082\ watt$

Cooling Water Properties

$$\Delta T_{2c} := T_{2c.out} - T_{2c.in}$$ (temperature difference)

$$T_{2c} := (T_{2c.in} + T_{2c.out}) \cdot 0.5$$ $T_{2c} = 290.66\ K$ (average T, used for stream properties)

$$C_{P.2c} := C_{P.liq}(T_{2c}, 1) \qquad C_{p.2c} := \frac{C_{P.2c}}{MW_w} \qquad C_{p.2c} = 4.192 \frac{J}{gm \cdot K} \qquad \text{(heat capacity: water)}$$

$$\rho_{2c} := \rho_{liq}(T_{2c}, 3) \cdot MW_w \qquad \rho_{2c} = 0.998 \frac{gm}{mL} \qquad \text{(density)}$$

$$\mu_{2c} := \mu_{liq}(T_{2c}, 2) \qquad \mu_{2c} = 1.083 \, cP \qquad \text{(viscosity)}$$

$$k_{2c} := k_{liq}(T_{2c}, 4) \qquad k_{2c} = 0.595 \frac{W}{m \cdot K} \qquad \text{(thermal conductivity)}$$

$$m_{2c} := \frac{Q_2}{C_{p.2c} \cdot \Delta T_{2c}} \qquad m_{2c} = 3.977 \frac{lb}{min} \qquad \text{(mass flow rate)}$$

$$V_{2c} := m_{2c} \cdot \rho_{2c}^{-1} \qquad V_{2c} = 0.478 \frac{gal}{min} \qquad \text{(volumetric flow rate)}$$

<u>Cooling Water Check</u>

Velocity and Re through tubing before and after HX2 to test reasonableness

$$v_2 := V_{2c} \cdot 4 \cdot \left(\pi \cdot D_i^2 \right)^{-1} \qquad v_2 = 5.405 \frac{ft}{s}$$

$$Re_2 := \frac{\rho_{2c} \cdot v_2 \cdot D_i}{\mu_{2c}} \qquad Re_2 = 7.324 \times 10^3$$

<u>Overall Heat Transfer Coefficient</u> (using LMTD, Heat & Mass Text)

$$\Delta T_{2.1} := T_{2h.in} - T_{2c.out} \qquad \Delta T_{2.1} = 55 \, K$$

$$\Delta T_{2.2} := T_{2h.out} - T_{2c.in} \qquad \Delta T_{2.2} = 1 \, K$$

$$\Delta T_{2.lm} := \frac{\Delta T_{2.1} - \Delta T_{2.2}}{\ln\left(\frac{\Delta T_{2.1}}{\Delta T_{2.2}} \right)} \qquad \Delta T_{2.lm} = 13.475 \, K \qquad \text{(log mean temperature difference, LMTD)}$$

$$UA_2 := \frac{Q_2}{\Delta T_{2.lm}} \qquad UA_2 = 46.758 \frac{W}{K} \qquad \text{(overall heat transfer coefficient)}$$

Hot Side Heat Transfer Coefficient

$$v_{2h} := \frac{4V_{1c}}{\pi \cdot D_i^2}$$
$$v_{2h} = 0.566 \frac{ft}{s}$$
(velocity)

$$Re_{2h} := \frac{\rho_{2h} \cdot v_{2h} \cdot D_i}{\mu_{2h}}$$
$$Re_{2h} = 1.621 \times 10^3$$
(Reynolds number)

$$Pr_{2h} := \frac{C_{p.2h} \cdot \mu_{2h}}{k_{2h}}$$
$$Pr_{2h} = 2.748$$
(Prandtl number)

Friction factor, f (Table 8.4, 8.21, Heat and Mass Transfer text):

$$f_{2h} := if\left[Re_{2h} > 3000, \left(0.790 \cdot \ln\left(Re_{2h}\right) - 1.64\right)^{-2}, \frac{64}{Re_{2h}}\right]$$
$$f_{2h} = 0.039$$

Friction factor, f (Fluids text)--comparison:

$$Roughness := \frac{\varepsilon_f}{D_i}$$

Guess: $f_h := 0.03$
$$f_h := root\left[\left[\left(-2.0 \cdot \log\left(\frac{\frac{\varepsilon_f}{D_i}}{3.7} + \frac{2.51}{Re_{2h} \cdot f_h^{0.5}}\right)\right) - \frac{1}{f_h^{0.5}}\right], f_h\right]$$
$$f_h = 0.053$$

Calculate Nusselt Number:

$$Nu_{2h} := if\left[\left(0.5 < Pr_{2h} < 2000\right) \wedge \left(3000 < Re_{2h} < 5 \cdot 10^6\right), \frac{\frac{f_{2h}}{8} \cdot \left(Re_{2h} - 1000\right) \cdot Pr_{2h}}{1 + 12.7 \cdot \left(\frac{f_{2h}}{8}\right)^{0.5} \cdot \left(Pr_{2h}^{\frac{2}{3}} - 1\right)}, 3.66\right]$$

(valid for fully developed, L/D > 10, and conditions specified above; laminar valid for fully developed, uniform Ts)

$$h_{2h} := \frac{Nu_{2h} \cdot k_{2h}}{D_i}$$
$$h_{2h} = 479.632 \frac{W}{m^2 \cdot K}$$
(hot side heat transfer coefficient; typical values between 50 and 500 W/(m2·K)--Transport Phenomena, 425)

<u>Cold Side Heat Transfer Coefficient</u>

$D_{2ci} := 6\text{in}$ (inner diameter of heat exchanger shell)

$$v_{2c} := \frac{4 \cdot V_{2c}}{\pi \cdot D_{2ci}^2} \qquad v_{2c} = 5.42 \times 10^{-3} \frac{\text{ft}}{\text{s}} \quad \text{(velocity)}$$

$$Re_{2c} := \frac{\rho_{2c} \cdot v_{2c} \cdot D_o}{\mu_{2c}} \qquad Re_{2c} = 9.664 \qquad \text{(flow across cylinder)}$$

$$Pr_{2c} := \frac{C_{p.2c} \cdot \mu_{2c}}{k_{2c}} \qquad Pr_{2c} = 7.624 \qquad \text{(Prandtl number)}$$

$$T_{2c.f}(T_{2cs}) := (T_{2cs} + T_{2c}) \cdot 0.5 \qquad \text{(film temperature, as a function of surface temperature)}$$

$$\beta_{2c} := 257 \cdot 10^{-6} \cdot K^{-1} \qquad \text{(thermal expansion coefficient (T = 290 K))}$$

$$\nu_{2c} := \frac{\mu_{2c}}{\rho_{2c}} \qquad \nu_{2c} = 0.011 \frac{\text{cm}^2}{\text{s}} \qquad \text{(kinematic viscosity)}$$

$$Gr_{2c}(T_{2cs}) := \frac{g \cdot \beta_{2c} \cdot |T_{2cs} - T_{2c}| \cdot D_o^3}{\nu_{2c}^2} \qquad \text{(Grashof number)}$$

$$Ra_{2c}(T_{2cs}) := Gr_{2c}(T_{2cs}) \cdot Pr_{2c} \qquad \text{(Raleigh number)}$$

$$Nu_{2c}(T_{2cs}) := \text{if}\left[Ra_{2c}(T_{2cs}) < 10^{12}, \left[0.60 + \frac{0.387 \cdot Ra_{2c}(T_{2cs})^{\frac{1}{6}}}{\left[1 + \left(\frac{0.559}{Pr_{2c}}\right)^{\frac{9}{16}}\right]^{\frac{8}{27}}}\right]^2, \text{"invalid"} \right] \qquad \text{(Nusselt number)}$$

$$h_{2c}(T_{2cs}) := \frac{k_{2c} \cdot Nu_{2c}(T_{2cs})}{D_o} \qquad \text{(natural convection heat transfer coefficient)}$$

116

Size of HX2

Initial guess: $x_2 := 30.4\text{ft}$ (changing guess value slightly changes answer)

$$xx := \begin{vmatrix} T_{2cs} \leftarrow T_{2h} - Q_2 \cdot \left(\dfrac{1}{\pi \cdot D_i \cdot h_{2h} \cdot x_2} + \dfrac{\ln\left(\dfrac{D_o}{D_i}\right)}{2 \cdot \pi \cdot k_c \cdot x_2} \right) \\[2em] x \leftarrow \text{root}\left[UA_2 - \left(\dfrac{1}{h_{2h} \cdot \pi \cdot D_i \cdot x_2} + \dfrac{\ln\left(\dfrac{D_o}{D_i}\right)}{2 \cdot \pi \cdot k_c \cdot x_2} + \dfrac{1}{h_{2c}(T_{2cs}) \cdot \pi \cdot D_o \cdot x_2} \right)^{-1} \right], x_2 \right] \\[2em] out \leftarrow \begin{pmatrix} T_{2cs} \cdot K^{-1} \\ x \cdot \text{ft}^{-1} \end{pmatrix} \end{vmatrix}$$

$T_{2cs} := xx_1 \cdot K$ $\qquad T_{2cs} = 309.301 \text{ K}$

$h_{2c}(T_{2cs}) = 831.724 \dfrac{W}{m^2 K}$ (heat transfer coefficient; typical values between 100 and 600 W/(m²·K)--Transport Phenomena)

$x_2 := \text{if}\left(\dfrac{Gr_{2c}(T_{2cs})}{Re_{2c}^2} > 5, xx_2 \cdot \text{ft}, "oops" \right)$ $\qquad \boxed{x_2 = 30.358 \text{ f}}$

Test validity of natural convection assumption:

$\dfrac{Gr_{2c}(T_{2cs})}{Re_{2c}^2} = 109.311$ Since this is >> 1, forced convection can be neglected.

117

Section 3: HEAT EXCHANGER THREE (HX3)

User Inputs Required For Program

$D_{ow} := 0.25in$ $t_w := 0.030in$ (copper tubing dimensions)

$T_{3h.in} := (75 + 273.16)K$ $T_{3h.out} := (20 + 273.16)K$ (hot side inlet and outlet temperatures)

$T_{3c.in} := (14 + 273.16)K$ (cold side inlet temperature)

$T_{3c.out} := (15 + 273.16)K$ (intitial guess for outlet temperature of cooling water)

$\varepsilon_f := 0.00152mm$ (e_f from Perry's, Table 6-1)

$m_{3c} := m_{2c}$ $m_{3c} = 3.977\dfrac{lb}{min}$ (reasonable mass flow rate of cooling water)

$D_{3hi} := 3in$ (inside diameter of out tube)

Hot Process Stream Properties

$T_{3h} := \left(T_{3h.in} + T_{3h.out}\right)\cdot 0.5$ $T_{3h} = 320.66\ K$ (average temperature, used for properties)

$\Delta T_{3h} := T_{3h.in} - T_{3h.out}$ $\Delta T_{3h} = 55\ K$ (temperature change through HX3)

$n_{3h} := \dfrac{CO_{trans}}{r}$ $n_{3h} = 0.521\dfrac{mol}{hr}$ (molar flow rate of hot gas (CO))

$\rho_{3h.in} := \dfrac{P_{tot}\cdot MW_{CO}}{R_g\cdot T_{3h.in}}$ $\rho_{3h.out} := \dfrac{P_{tot}\cdot MW_{CO}}{R_g\cdot T_{3h.out}}$ (inlet and outlet densities)

$\rho_{3h}(T) := \dfrac{P_{tot}\cdot MW_{CO}}{R_g\cdot T}$ $\rho_{3h} := \rho_{3h}\left(T_{3h}\right)$ (average density)

$V_{3h.in} := \dfrac{n_{3h}\cdot R_g\cdot T_{3h.in}}{P_{tot}}$ $V_{3h.out} := \dfrac{n_{3h}\cdot R_g\cdot T_{3h.out}}{P_{tot}}$ (inlet and outlet volumetric flow rates)

$V_{3h}(T) := \dfrac{n_{3h}\cdot R_g\cdot T}{P_{tot}}$ $V_{3h} := V_{3h}\left(T_{3h}\right)$ (average volumetric flow rate)

118

$m_{3h} := \rho_{3h} \cdot V_{3h}$ $m_{3h} = 5.367 \times 10^{-4} \dfrac{lb}{min}$ (mass flow rate)

$C_{P.3h} := C_{P.gas}(T_{3h}, 5)$ $C_{p.3h} := \dfrac{C_{P.3h}}{MW_{CO}}$ $C_{p.3h} = 1.041 \dfrac{J}{gm \cdot K}$ (heat capacity)

$\mu_{3h} := \mu_{gas}(T_{3h}, 6)$ $\mu_{3h} = 0.019\,cP$ (viscosity)

$k_{3h} := k_{gas}(T_{3h}, 7)$ $k_{3h} = 0.027 \dfrac{W}{m \cdot K}$ (thermal conductivity)

Calculate Required Heat Removal

$Q_3 := m_{3h} \cdot C_{p.3h} \cdot \Delta T_{3h}$ $Q_3 = 0.232\,W$

Cool Process Stream Properties

$T_{3c.out} :=$

$\left|\begin{array}{l} T_{3c} \leftarrow (T_{3c.in} + T_{3c.out}) \cdot 0.5 \\[2mm] \rho_{3c} \leftarrow \rho_{liq}(T_{3c}, 3) \cdot MW_w \\[2mm] V_{3c} \leftarrow m_{3c} \cdot \rho_{3c}^{-1} \\[2mm] C_{p.3c} \leftarrow \dfrac{C_{P.liq}(T_{3c}, 1)}{MW_w} \\[4mm] \Delta T_{3c} \leftarrow \dfrac{Q_3}{C_{p.3c} \cdot m_{3c}} \\[4mm] T_{3c.out} \leftarrow T_{3c.in} + \Delta T_{3c} \end{array}\right.$

    (average temperature, used for stream properties)

    (average water density)

    (average volumetric flow rate)

    (average heat capacity)

    (temperature difference through HX3)

    (outlet water temperature)

$T_{3c.out} = 287.162\,K$

$T_{3c} := (T_{3c.in} + T_{3c.out}) \cdot 0.5$ $T_{3c} = 287.161\,K$

$\rho_{3c} := \rho_{liq}(T_{3c}, 3) \cdot MW_w$ $C_{p.3c} := \dfrac{C_{P.liq}(T_{3c}, 1)}{MW_w}$ $\mu_{3c} := \mu_{liq}(T_{3c}, 2)$ $k_{3c} := k_{liq}(T_{3c}, 4)$

$V_{3c} := m_{3c} \cdot \rho_{3c}^{-1}$ $V_{3c} = 0.477 \dfrac{gal}{min}$

Overall Heat Transfer Coefficient (using LMTD, Heat & Mass Text)

$\Delta T_{3.1} := T_{3h.in} - T_{3c.out}$ $\Delta T_{3.1} = 60.998\,K$

119

$$\Delta T_{3.2} := T_{3h.out} - T_{3c.in} \qquad \Delta T_{3.2} = 6 \text{ K}$$

$$\Delta T_{3.lm} := \frac{\Delta T_{3.1} - \Delta T_{3.2}}{\ln\left(\dfrac{\Delta T_{3.1}}{\Delta T_{3.2}}\right)} \qquad \Delta T_{3.lm} = 23.715 \text{ K} \qquad \text{(log mean temperature difference, LMTD)}$$

$$UA_3 := \frac{Q_3}{\Delta T_{3.lm}} \qquad UA_3 = 9.796 \times 10^{-3} \frac{W}{K} \qquad \text{(overall heat transfer coefficient)}$$

Cold Side Heat Transfer Coefficient

$$v_{3c} := \frac{V_{3c}}{\pi \cdot D_i^2 \cdot 0.25} \qquad v_{3c} = 5.399 \frac{ft}{s} \qquad \text{(velocity)}$$

$$Re_{3c} := \frac{\rho_{3c} \cdot v_{3c} \cdot D_i}{\mu_{3c}} \qquad Re_{3c} = 6.733 \times 10^3 \qquad \text{(flow through cylinder)}$$

$$Pr_{3c} := \frac{C_{p.3c} \cdot \mu_{3c}}{k_{3c}} \qquad Pr_{3c} = 8.379 \qquad \text{(Prandtl)}$$

Calculate friction factor, f (correlation from Fluids):

$$\text{Roughness} := \frac{\varepsilon_f}{D_i}$$

Guess: $f_{3c} := 0.03$

$$f_{3c} := \text{root}\left[\left[\left(-2.0 \cdot \log\left(\frac{\dfrac{\varepsilon_f}{D_i}}{3.7} + \frac{2.51}{Re_{3c} \cdot f_{3c}^{0.5}}\right)\right) - \frac{1}{f_{3c}^{0.5}}\right], f_{3c}\right] \qquad f_{3c} = 0.035$$

Calculate Nusselt Number:

$$Nu_{3c} := \text{if}\left[(0.5 < Pr_{3c} < 2000) \wedge (3000 < Re_{3c} < 5 \cdot 10^6), \frac{\dfrac{f_{3c}}{8} \cdot (Re_{3c} - 1000) \cdot Pr_{3c}}{1 + 12.7 \cdot \left(\dfrac{f_{3c}}{8}\right)^{0.5} \cdot \left(Pr_{3c}^{\frac{2}{3}} - 1\right)}, \text{"problem"}\right]$$

(valid for fully developed, L/D > 10, and conditions specified above) $\qquad Nu_{3c} = 57.732$

$$h_{3c} := \frac{Nu_{3c} \cdot k_{3c}}{D_i}$$

$$h_{3c} = 7.059 \times 10^3 \frac{W}{m^2 \cdot K}$$

(heat transfer coefficient; typical values between 500 and 10000 W/(m2·K)--<u>Transport Phenomena</u>)

Hot Side Heat Transfer Coefficient

$$v_{3h} := \frac{4 V_{fs}}{\pi \cdot D_{3hi}^2}$$

$$v_{3h} = 8.079 \times 10^{-3} \frac{ft}{s}$$

(velocity)

$$Re_{3h} := \frac{\rho_{3h} \cdot v_{3h} \cdot D_o}{\mu_{3h}}$$

$$Re_{3h} = 2.563$$

(across a cylinder)

$$Pr_{3h} := \frac{C_{p.3h} \cdot \mu_{3h}}{k_{3h}}$$

$$Pr_{3h} = 0.733$$

(Prandtl number)

$$T_{3h.f}(T_{3hs}) := (T_{3hs} + T_{3h}) \cdot 0.5$$

(film temperature, as a function of surface temperature)

$$\beta_{3h}(T_{3hs}) := \frac{1}{T_{3h.f}(T_{3hs})}$$

(thermal expansion coefficient)

$$\nu_{3h} := \frac{\mu_{3h}}{\rho_{3h}}$$

(kinematic viscosity)

$$Gr_{3h}(T_{3hs}) := \frac{g \cdot \beta_{3h}(T_{3hs}) \cdot \left| T_{3hs} - T_{3h} \right| \cdot D_o^3}{\nu_{3h}^2}$$

(Grashof number)

$$Ra_{3h}(T_{3hs}) := Gr_{3h}(T_{3hs}) \cdot Pr_{3h}$$

(Raleigh number)

$$Nu_{3h}(T_{3hs}) := \left[0.60 + \frac{0.387 \cdot Ra_{3h}(T_{3hs})^{\frac{1}{6}}}{\left[1 + \left(\frac{0.559}{Pr_{3h}} \right)^{\frac{9}{16}} \right]^{\frac{8}{27}}} \right]^2$$

(Nusselt number)

$$h_{3h}(T_{3hs}) := \frac{k_{3h} \cdot Nu_{3h}(T_{3hs})}{D_o}$$

(natural convection heat transfer coefficient)

121

Size of HX3

Initial guess: $x_3 := 3\,\text{ft}$

$$xxx := \left| \begin{array}{l} T_{3hs} \leftarrow T_{3c} + Q_3 \cdot \left(\dfrac{1}{\pi \cdot D_i \cdot h_{3c} \cdot x_3} + \dfrac{\ln\left(\dfrac{D_o}{D_i}\right)}{2 \cdot \pi \cdot k_c \cdot x_3} \right) \\[3em] x \leftarrow \text{root}\left[UA_3 - \left(\dfrac{1}{h_{3c} \cdot \pi \cdot D_i \cdot x_3} + \dfrac{\ln\left(\dfrac{D_o}{D_i}\right)}{2 \cdot \pi \cdot k_c \cdot x_3} + \dfrac{1}{h_{3h}(T_{3hs}) \cdot \pi \cdot D_o \cdot x_3} \right)^{-1}, x_3 \right] \\[3em] \text{out} \leftarrow \begin{pmatrix} T_{3hs} \cdot K^{-1} \\[1em] x \cdot \text{ft}^{-1} \end{pmatrix} \end{array} \right.$$

$T_{3hs} := xxx_1 \cdot K$ $T_{3hs} = 287.163\ K$

$h_{3h}(T_{3hs}) = 15.919\,\dfrac{W}{m^2 K}$ (heat transfer coefficient; typical
                                                                                       values between 3 and 20
                                                                                       W/(m^2·K)--Transport Phenomena)

$x_3 := \text{if}\left(\dfrac{Gr_{3h}(T_{3hs})}{Re_{3h}^2} > 5, xxx_2 \cdot \text{ft}, "oops" \right)$ $\boxed{x_3 = 0.102\,\text{ft}}$

Test validity of natural convection assumption:

$\dfrac{Gr_{3h}(T_{3hs})}{Re_{3h}^2} = 1.132 \times 10^3$ Since this is >> 1, forced convection can be neglected.

122

APPENDIX C: Detailed Process Schematics
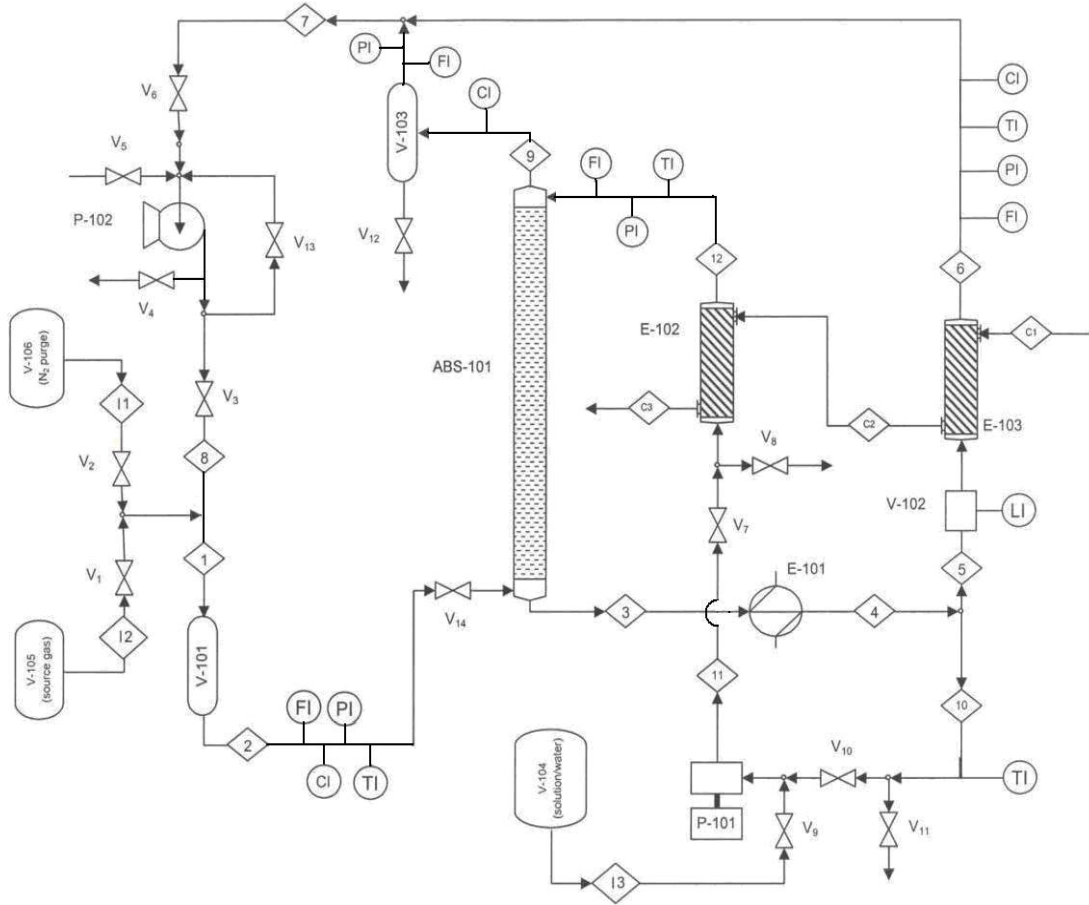
Figure 19. Detailed Process Flow and Instrumentation Diagram, Version 1.
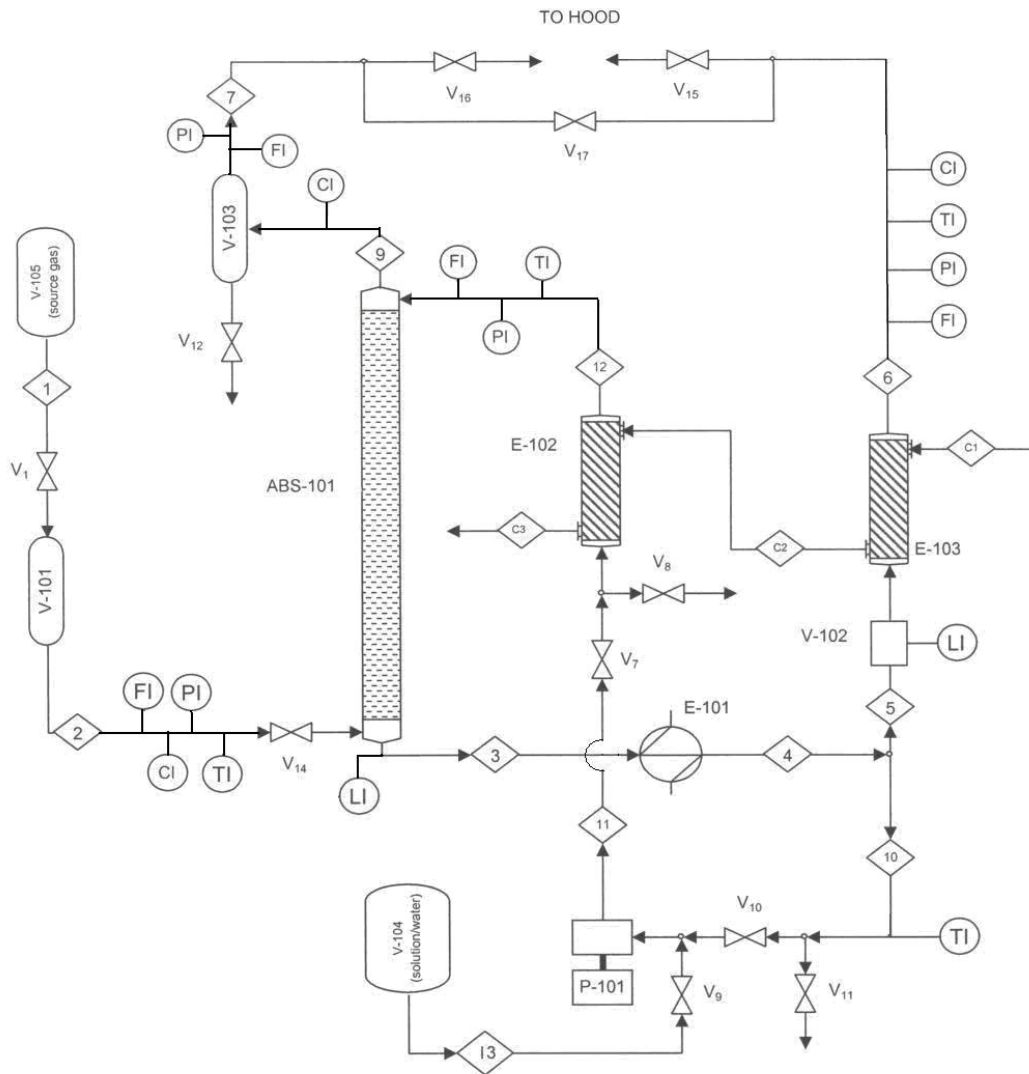
Figure 20. Detailed Process Flow and Instrumentation Diagram, Version 2.

Following is an explanation of symbols used: FI, CI, PI, TI, and LI are flow, composition, pressure, temperature, and level indicators, respectively; ABS, E, V, and P represent absorber, heat exchanger, vessel or valve, and pump respectively; and the numbered diamonds refer to stream names (the numbers preceded by "I" or "c" are inlet and cooling streams, respectively).

124

APPENDIX D: Other Equipment

Several other pieces of equipment were used to allow the prototype to operate, and are included in this section.

Pumps

Figure 21 and Figure 22 show the liquid pump and gas pump, respectively.

Figure 21. Liquid Pump, P-101.

The liquid pump (P-101) was a variable-speed pump drive rated for 0 to 40 ºC, with a 5000 maximum rpm, and was obtained from Cole-Parmer Instrument Co. The pump head is a gear pump head, also obtained from Cole-Parmer (product of

Micropump, Inc.), and supplies 0.91 mL/rev, for a maximum flow rate of about 4.6 liters per minute (LPM) or ~73 gallons per hour (GPH). Its maximum allowable system pressure is 300 psi with a maximum differential pressure of 80 psi. The allowable temperature range is -46 to 121 ºC.

Figure 22. Vacuum/Pressure Pump, P-102.

The pump used to circulate the gas (P-102) was a laboratory, oil-less diaphragm vacuum pump and compressor and is a product of Gast Manufacturing, Inc. (obtained through Cole-Parmer). It can be operated between 0 and 40 ºC, at a maximum pressure of 60 psi, maximum vacuum of 25.5 inches Hg, and has a free air capacity of 1.1 CFM (31.2 LPM). It included regulators and valves, and vented to atmosphere. Note that this pump was not used with Version 2 of the prototype.

126

Vessels

The first vessel (V-101) in the process is a ballast tank and allows some "give" in the process. It is a stainless steel tank and has a volume of approximately 1 gallon, as shown in Figure 23 (center tank).

Figure 23. Ballast tank, V-101.

The second vessel (V-102) was a sight glass, with the glass being 1 in. in diameter and 2 in. tall, allowing the operator to monitor and maintain the proper level. It was borosilicate glass, with the main body made of brass, and was rated for a maximum of 130 psi and 212 ºF. It was supplied by McMaster-Carr (see Figure 24). This was later changed to PVC tubing encased in a polycarbonate tube, shown in Figure 25. A similar PVC sight tube was attached to the bottom of the column to help monitor liquid levels—this is shown in Figure 26.

Figure 24. Sight glass, V-102.

Figure 25. Sight tube.

Figure 26. Sight tube at the bottom of the column, above "p trap"

The third vessel (V-103) was constructed of galvanized steel, and used as a liquid trap, should the column become fully entrained. This prevented the liquid from traveling with the gas and entering the gas pump. Any captured liquid does not re-enter the process, but can be drained through a valve at the bottom of the trap. Figure 27 shows this liquid trap.

Figure 27. Liquid trap, V-103.

The fifth vessel (V-105) was the 14-liter Scotty Gas cylinder containing the gas mixture (see Figure 23, left side). As mentioned, this gas mixture (15% CO_2, 7% CO, 5% O_2, balance N_2) was used during process identification and Version 1 of the prototype.

The final vessel (V-106) was a standard gas cylinder from the BYU central stores containing N_2. It was used to practice with the project, and to purge the process following experiments.

Valves

In Version 1 of the prototype, the first two valves were high pressure gate valves. All other valves in the process were 2-way ball valves (except Valve 14), the majority being necessary primarily during start-up and shut-down of the process. Although this type of valve is not ideal for flow control, Valves 3 and 6 were satisfactory in controlling the gas flow rate, along with Valve 13 used in the bypass line, allowing a significantly reduced flow rate of gas. Valve 14, used in both versions, was a check valve (added after some experiments) used to prevent flow of liquid into the gas inlet. In Version 2, Valves 15, 16, and 17 (on the offgas and CO streams) were gate valves which allow fine-tune control of the flow rates and pressure in the system.

Measurement Devices

As can be seen in Figure 15, five types of gages were used in various locations throughout the process to indicate flow, pressure, temperature, composition, and level.

The flow rates of the inlet gas (stream 2), separated CO (stream 6), offgas (stream 9), and cooled liquid (stream 12) were all measured using rotameters (FI 2, 6, 9, 12) obtained from Cole-Parmer. Table 11 shows the specifications for these flow meters.

Table 11. Flow meter specifications.

| Stream | Flow Meter Calibrations | | | | Operation Limits | |
	Pressure	Temp.	Material	Range	Temp.	Pressure
2	14.7 psi	70 °F	Air	0.2 – 14 LPM	-	75 psig[a]
6	14.7 psi	70 °F	Air	6 – 60 SCFH	149 °F	100 psig
9	14.7 psi	70 °F	Air	6 – 60 SCFH	149 °F	100 psig
12	-	-	Water	0.025 – 0.25 GPM	212 °F[b]	150 psig[c]

[a] Working pressure.
[b] At 0 pressure.
[c] At 70 °F.

Note that during application, the floats in some meters bounced up and down, reducing the accuracy of the measurement. In addition to this inaccuracy, the meters were calibrated for air and water, but were used with a gas other then air, and a liquid other than water. Some adjustments were made to the values indicated by the gas rotameters to account for the differences in gas type, temperature, and pressure as follows.

The indicated flow rate was converted to the actual flow rate at process conditions by the following equation:

$$\frac{V_A}{V_I} = \sqrt{\frac{\rho_I(\rho_f - \rho_A)}{\rho_A(\rho_f - \rho_I)}} \tag{D-1}$$

where V is volumetric flow rate, ρ is density, A refers to actual conditions, f refers to the float in the rotameter, and I refers to the value associated with the indicated reading, or the condition for which it is calibrated (usually 70 °F, 14.7 psi). Since the density of the float is much greater than the density of the gas, the quantities (ρ_f- ρ_A) and ($\rho_f - \rho_I$) can be approximated as ρ_f. In addition, substituting (P·MW)/(R·T) for the density (where P is pressure, MW is molecular weight, R is the universal gas constant, and T is temperature) resulted in the following equation:

$$V_A = V_I \sqrt{\frac{P_I MW_I T_A}{T_I P_A MW_A}} \qquad \textbf{(D-2)}$$

This could further be converted to the flow rate at standard temperature and pressure by using the ideal gas law; however, values in this paper are reported as actual flow rates at the current conditions. No adjustments were made for the liquid rotameter reading, which was calibrated for water.

Pressure gauges were obtained from Grainger and have a 60 psi range with 1 psi graduations. Pressures were monitored on the absorber inlet gas (stream 2), separated CO (stream 6), offgas (stream 9), and cooled liquid (stream 12).

Temperatures were monitored on the absorber inlet gas (stream 2), separated CO (stream 6), heated liquid (stream 10), cooled liquid (stream 12), and 4 locations on the surface of the heating ropes on E-101.

The four process stream temperatures were measured with Type K thermocouples (aluminum and chromium alloys). A thermowell made of copper

tubing and soldered at one end was inserted into the process line so that the end of the thermowell did not significantly hinder flow. The thermocouple sits in the bottom of the thermowell, which is filled with oil, against the solder. Once the system reached steady state, the temperature drop from the process stream across the solder to the thermocouple was not significant.

The thermocouples used to monitor surface temperature of E-101 were also Type K thermocouples, and were located in potential hot spots in E-101. The surface temperature of the heating ropes was monitored to ensure that the maximum allowable temperature (482 °C) was not reached. A multimeter measured the voltage generated by the thermocouples, and the voltage was converted to temperature using equations provided by Omega Engineering, Inc. A schematic of the thermocouple measurements was obtained from the Omega website[43] and is shown in Figure 28.
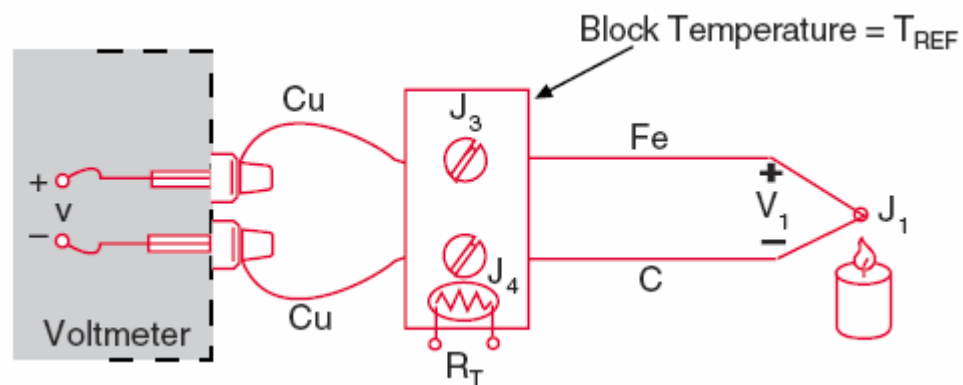
Figure 28. Schematic of thermocouple measurement (Omega).

The terminal strip was fastened to the prototype framework where ambient temperature was also measured and used to correct the process temperature. A source of error for the temperature measured in the thermowells arises from any temperature

drop from the stream across the solder of the thermowell (solder is lead, and approximately 1/8 in. thick) and into the oil where the thermocouple junction was located. Once the system reached steady state, this error was small. Finally, Omega reports that the error in a Type K thermocouple is approximately 2 ºC[43], so overall the temperature measurement is probably within a few degrees centigrade. This causes no problem in temperature measurement of E-101 since the surface temperature of the ropes never approaches the maximum allowable temperature. The error is more significant for the actual process streams as they should operate between approximately 20 and 75 ºC. The process was heated until the temperature indicated approximately 80 ºC to ensure maximum CO release, even though the majority should be released at approximately 70 ºC.[24] It should be noted that this 70 ºC applies to the solid CO compound formed in a concentrated solution. Since no temperature was reported for a dilute solution, this same value had to be assumed for the cases using dilute solution.

Compositions of inlet and outlet gases were analyzed using a Gow-Mac Gas Chromatograph (GC) and Carboxen 1000 packed column. Syringe adaptors containing replaceable septa were placed in the lines of each stream to be measured. The needle of a gas tight, 2.5 mL syringe was injected into the syringe adaptor and used to withdraw a sample of gas (typically 600 µL) which was then injected into the GC. The GC detector and injection port were maintained at approximately 225 ºC, while the oven temperature started at 90 ºC, then after 4.5 minutes of operation ramped up to 225 ºC at a rate of 25 ºC/min where it remained for 1 minute prior to cooling back to 90 ºC. The O_2 and N_2 peaks had a retention time of approximately 3

minutes, while the CO and CO_2 peaks had retention times of approximately 4 and almost 10 minutes, respectively. Peak areas of CO_2 and CO were then used to assist in determining the separation.

Chemicals

The process used de-ionized water in the solution, obtained from laboratories in the Clyde building, where experiments were performed. The CuCl was 97% pure and supplied by Sigma-Aldrich. The $MgCl_2 \cdot 6H_2O$ was $\geq 99\%$ pure and was also obtained from Sigma-Aldrich.

The gas mixture originally used in the process (7% CO, 5% O_2, 15% CO_2, balance N_2) came in a 14 liter (L) Scotty Gas cylinder and was supplied by Supelco. When the gas supply changed, the new supply (11% CO, 2.6% O_2, 30% CO_2, balance N_2) came in a size 200 cylinder (approximately 55 ft^3), and was obtained through Central Stores at BYU. These mixtures differ from the industrial process gas in that they contain a high percentage of N_2 due to laboratory safety constraints. The percent of gas in the 14 L cylinder was accurate to $\pm 5\%$, and the percent of gas obtained through Central Stores was accurate to $\pm 2\%$.

Tubing and Fittings

The majority of tubing in the process was ¼ inch copper tubing. The portion through which the column liquid drained and was heated was 3/8 inch copper tubing. In Version 2 of the prototype a portion of the offgas and CO stream at the very end consisted of 1/8 inch copper tubing. The copper tubing in theory helps to slow disproportionation of Cu^+ to Cu^{++} and Cu^o. Other tubing in the process that was not

required to maintain high pressure and temperature streams (gas exhaust, cooling water) consisted of PVC. Fittings consisted primarily of brass, expect at the more heated portions of the process where stainless steel or CPVC was used.

APPENDIX E: Raw Results

Detailed Summary of Cases 1 through 6

    Case 1: This experiment used Version 1 (recycle) of the prototype. Upon mixing, the solution was light tan-brown, with a slight greenish tint—a significant amount of CuCl did not dissolve into solution, and much remained in the mixing vessels as well as the feed vessel to the apparatus. When solution started flowing through the apparatus, large reddish brown flakes and chunks appeared in the sight glass, plugging up the equipment. The system had not been exposed to the solution before this point, and it was realized that the zinc in the galvanized steel parts reacted with copper according to the reaction(s):

$$2Cu^+ + Zn \Leftrightarrow Zn^{2+} + 2Cu^o \qquad\qquad \text{(E-1)}$$

and/or

$$Cu^{2+} + Zn \Leftrightarrow Zn^{2+} + Cu^o \qquad\qquad \text{(E-2)}$$

causing the copper in solution to precipitate. The solution also reacted with other materials in the process (brass fittings, aluminum floats in the flow meters, and aluminum heat exchanger), but not as rapidly as with the galvanized steel. This led to

the following improvements: all galvanized parts (except the liquid trap) were replaced with 316 stainless steel or CPVC, and a coating of high-temperature, water-resistant paint was applied to the inside of the aluminum heat exchanger. A bypass line was added to the gas pump so the flow rate of gas to the column could be reduced, and a check valve was added to the gas inlet of the column to prevent solution from flowing back up the gas line. Other improvements included replacing the gas inlet and liquid flow meters (which had slightly corroded) with different meters to measure reduced flows, and the sight glass and heat exchanger number three were lowered to allow better liquid drainage from the column

Case 2: Again, not all of the CuCl dissolved—some remained in the flask bottom, some in the feed vessel bottom. The solution was tan-milky looking, with some green forming in some areas. During operation, system pressure continually dropped from the desired 30 psig, requiring re-pressurization; the float in the liquid flow meter was stuck until very end; and the solution continually turned darker rusty red over time until the level could not be seen in the sight glass. All stream compositions measured with the GC looked the same, indicating no separation taking place. It was realized that because liquid drained downward from the column while being heated, any released CO may have traveled back to the column. It was also discovered that the inlet gas was exiting through the bottom of the column rather than traveling up through the column—this required other minor experiments as it was not noticeable with just the sight glass or the flow meters. The following adjustments were made: the sight glass was placed above the separation point, something similar to a p-trap was put in place at the bottom of the column, and the coils of the first heat

exchanger (E-101) were adjusted so that the liquid would drain from the column and then travel upwards through the heat exchanger to the separation point. Since the liquid to gas ratio was not as large as it should be, it was also necessary to reduce the gas and increase the liquid flow to the column in the next case.

Case 3: This time the solution, which was dark brown-black, was continuously stirred with a magnetic stirrer. Although some insolubles remained, more of the solute was dissolved than in the previous two cases. During operation, the system continued to have difficulty in maintaining the desired pressure. Composition measurements were less than ideal since only one sample could be analyzed at a time (and required ~15 minutes), and composition continually changed. It was realized that since the offgas stream from the column was connected to the product stream, and the flow rate of the product was smaller than that of the column offgas, the CO accumulated in the product stream, which was initially full of the original gas mixture. The system was therefore not at steady state, and the composition measurement of this stream did not accurately represent the amount of CO separated. Despite these imperfections, chromatograms of the stream compositions indicated that separation was taking place. As in Case 2, the solution became red over time, but occurred more slowly in this case. Due to limitations noted in this case and new discoveries, the following changes were made: since it was found that the system lost pressure through the gas pump, this portion was eliminated, and the system was converted to a non-recycle system; a new, cheaper gas mixture was found (with slightly different composition); the sight glass was replaced with a long, clear tube made of PVC encased in a polycarbonate tube for

added support; and a similar sight tube (without the polycarbonate) was added to the bottom of the column to allow observation of the process at that point.

Case 4: With the recycle portion eliminated from the process, the inlet gas to the column required a fresh feed—since the composition of this feed was known, only an initial measurement needed to be taken, rather than continual measurements as in previous cases. As with previous cases, the measured composition of the CO stream was not accurate, as this stream was still connected to the column offgas stream prior to being vented. The solution in this case also turned orange-red over time, probably indicating disproportionation. Once the solution was heated, bubbles could be seen rising through the liquid, making it appear to be boiling. The experiment eventually had to be stopped because the solution became dark enough that the liquid flow meter could not be read. At this point the temperature of the heated liquid started to rise, while the liquid level began rising up the sight tube toward the aluminum heat exchanger, possibly indicating that the system was beginning to be plugged. Again, composition measurements indicated that separation was occurring, even at the time the experiment had to be stopped. The major change to this system involved adding a piece of 1/8 inch copper tubing to the very end of the first heat exchanger, immediately before the heated solution entered the sight tube chamber where gas and liquid were separated. This line extended vertically upward approximately 3 feet and ended with syringe adaptor. The line would initially be filled with gas mixture, but during the process, a syringe would be used to withdraw the gas allowing the line to fill with heated solution. As CO (and any other gas absorbed into solution) was released from solution, the line would eventually fill back up with gas. Although not

completely accurate, a measurement of the composition at this point would at least verify whether it was really CO being released from the solution.

Case 5: Before running the process with concentrated solution it was desired to "break-in" the new fittings and tubing with a dilute solution, and also practice measurement with the new CO measurement line. This experiment was not originally intended to be a quantitative experiment included in the major cases, but was included because of the information that it provided. The solution in this case was also unique—to not use up too much of the remaining $MgCl_2 \cdot 6H_2O$, NaCl was added to provide chloride ions to the solution. A smaller concentration of CuCl was used in this case than in previous experiments. Because of difficulties in measuring the CO stream composition, only one reasonable measurement was taken.

Case 6: A new bottle of CuCl was used for this case. Unfortunately, the normal light, tan-brown color of the powder had a greenish hue, indicating some kind of contamination. This brings into question how much Cu^+ was really present in the solution—if there were not really 3 moles per liter, the solution may not have really been concentrated ($Cl^- > 10$ mol/L). However, the concentration of Cl^- from the $MgCl_2 \cdot 6H_2O$ source was 9.6 mol/L, requiring only 0.4 mol/L to come from the CuCl source. It is unlikely that of the 3 mol/L of CuCl thought to be added to the solution, less than 0.4 mol/L was actually present. The solution took longer to dissolve in this case as it was initially more of a sludge or slurry. Once mixed, the solution somewhat resembled thick, dirty engine oil, and it may have been more of a suspension than a solution (on the ternary diagram, it was very close to the solution/suspension line). This particular prototype does not seem to handle thick fluids very well, which led to

some difficulties during operation. It was very difficult to obtain a steady state operation in this case—the liquid level would start to rise in the sight tube on the heated solution side and then drop, while the temperature would rapidly rise much too high (>>75 ºC), and it appeared at times that no solution was draining from the column. Besides the solution being thick, another implication is that according to Katsumoto,[24] in the concentrated solutions the absorbed CO forms a solid particle (which is what increases the absorption in the concentrated solutions)—if these solid particles were formed, they would likely have not been able to pass through the heat exchanger, but contribute to plugging it up instead. One last implication is that the solution was so dark in this case (and not with the red color noticed in other cases) that the liquid flow meter could not be read—the flow-control dial was set to the exact position which indicated 0.05 gal/min in previous cases and was assumed to be the same in this case. As with other cases, stream composition measurement indicated separation, but it was not increased, as was expected—this is discussed later. The new line that was installed to measure CO released from the solution did not work accurately in this case and contained a large amount of moisture.

Raw Experimental Data

The following tables show the raw data taken during Cases 3, 4, and 6. There are two tables for each case; the first shows temperatures, pressures, and flow rates, and the second shows the gas chromatograph analysis for gas compositions. The room temperature in each case was taken at the thermocouple junction, which was located above heat exchanger one. The temperatures T_1 through T_4 represent the surface

142

temperature at various locations of heat exchanger one. In all cases, TI represents

temperature (note that most temperatures are reported in millivolts, mV), PI represents

pressure, FI represents flow rate, and time is the actual time each set of measurements

started to be collected. In the tables containing GC measurements, the first column

containing "time" represents the time the sample was collected, and the second and

third columns with "time" represent the peak retention time of the peaks. Whenever a

flow rate column indicates a "0," it does not necessarily mean there was no flow rate,

but the flow rate was too small to be detected by the meter.

Table 12. Case 3 (0.65M CuCl, 2.92M MgCl$_2$) Experimental Raw Data.

Time	T_{room} (°C)	T_1 (mV)	T_2 (mV)	T_3 (mV)	T_4 (mV)	TI_{10} (mV)	TI_6 (mV)	TI_2 (mV)	TI_{12} (mV)	PI_2 (psig)	PI_{12} (psig)	PI_6 (psig)	PI_9 (psig)	FI_2 (SLPM)	FI_{12} (GPM)	FI_6 (SCFH)	FI_9 (SCFH)
13:50	22.6	0															
14:03	22.8	0	2.6	4.1	5.2	1.1	0	0	0	11	12	10	10	1.25	0.04	0	6
14:10	23.0	0	2.4	3.8	5.1	2.2	0	0	-0.1	9.5	11	8.5	9	1.25	0.04	0	6
14:20	23.3	0	2	3.3	4.5	2.1	0	0	-0.3	8	9.5	7	8	1.25	0.04	0	6
14:31	23.3	0	1.9	3.3	4.6	2.3	0	0	-0.4	7	8.5	6	7	1.25	0.025	0	5
14:42	23.3	0	2	3.4	4.8	2.1	0	0.1	-0.3	6	7.5	6	6	1.2	0.025	0	5
14:58	23.6	0	1.9	3.3	4.6	2.3	0	0.1	-0.3	5	7	4.5	5	1.05	0.025	0	5
15:07	23.5	0	1.9	3.2	4.5	2.3	0	0.1	-0.3	6.5	8	6	6.5	1.1	0.025	0	5
15:16	23.5	0	1.9	3.3	4.8	2.3	0	0	-0.3	6	7	5.5	5.5	1.1	0.025	0	5
15:26	23.6	0	1.9	3.2	4.6	2.3	0	0	-0.3	5	6.5	4.5	5	1.05	0.025	0	5
15:38	23.6	0	1.9	3.3	4.6	2.3	0	0	-0.3	4.5	6	4	4.5	1.05	0.025	0	5
15:48	23.7	0	1.9	3.1	4.5	2.2	0	0	-0.3	4	5.5	3.5	4	1	0.025	0	5

Table 13. Case 3 (0.65M CuCl, 2.92M MgCl$_2$) Experimental Raw Data.

Time	Stream	N_2+O_2 Area	CO Area	Time (min)	CO_2 Area	Time (min)
	Standard	162160	20318	5.8	46501	10.7
14:00	2	162880	14485	5.8	33312	10.7
14:20	6	168869	3598	5.8	9206	10.7
14:42	9	164972	5608	5.8	29410	10.7
15:07	2	166701	7450	5.8	32392	10.7
15:26	6	160333	27619	5.8	14856	10.7
15:46	9	166547	4471	5.8	29758	10.7

Table 14. Case 4 (0.81M CuCl, 2.01M MgCl$_2$) Experimental Raw Data.

Time	T$_{room}$ (ºC)	T$_1$ (mV)	T$_2$ (mV)	T$_3$ (mV)	T$_4$ (mV)	TI$_{10}$ (mV)	TI$_6$ (mV)	TI$_2$ (mV)	TI$_{12}$ (mV)	PI$_2$ (psig)	PI$_{12}$ (psig)	PI$_6$ (psig)	PI$_9$ (psig)	FI$_2$ (SLPM)	FI$_{12}$ (GPM)	FI$_6$ (SCFH)	FI$_9$ (SCFH)
14:31	24.8																
14:55	25.8	3.2	4.5	5.6	6.6	2.1	0	0	-0.4	30	31	29	30	0.5	0.053	0	0
15:12	26.3	1.9	3.7	3.6	4.4	2	0	0	-0.4	30	30	29	30	0.5	0.053	0	0
15:34	26.4	3.1	4.3	5	5.9	2.1	0	0	-0.5	30	31	29	30	0.45	0.05	0	0
16:04	26.9	1.1	3.8	4	4.7	1.7	0	0	-0.5	30	30	29	29	0.5	0.053	0	0
16:45	27	2.9	4.3	5.3	6.3	2.1	0	0	-0.5	30	31	29	30	0.45	0.053	0	0
17:38	27.6	-	-	-	-	2.8	-	-	-	-	-	-	-	0.5	-	-	-

Table 15. Case 4 (0.81M CuCl, 2.01M MgCl$_2$) Experimental Raw Data.

Time	Stream	N$_2$+O$_2$ Area	CO Area	Time (min)	CO$_2$ Area	Time (min)
	2	78047	5350	4.09	16525	9.48
	2	71588	7292	3.52	21583	9.39
14:31	9	59304	10224	4.07	33492	9.43
14:55	9	64481	2088	4.1	35247	9.42
14:55	6	64607	5752	3.6	31745	9.39
15:34	9	64091	3005	4.08	34563	9.42
15:34	6	64301	4832	4.01	33983	9.4
16:04	2	57602	11412	3.59	35306	9.4
16:43	9	65249	2686	4.1	34286	9.44
16:44	6	66957	3009	4.05	33971	9.41
17:38	9	62719	2524	4.11	35867	9.43

Table 16. Case 6 (3.0M CuCl, 4.8M MgCl$_2$) Experimental Raw Data.

Time	T$_{room}$ (ºC)	T$_1$ (mV)	T$_2$ (mV)	T$_3$ (mV)	T$_4$ (mV)	TI$_{10}$ (mV)	TI$_6$ (mV)	TI$_2$ (mV)	TI$_{12}$ (mV)	PI$_2$ (psig)	PI$_{12}$ (psig)	PI$_6$ (psig)	PI$_9$ (psig)	FI$_2$ (SLPM)	FI$_{12}$ (GPM)	FI$_6$ (SCFH)	FI$_9$ (SCFH)
14:00	21.6																
14:39	22.2	0	1.4	3.3	4.4	0.9	0	0	-0.2	31	31	29	30	0.2	0.05	0	0
15:17	23.4	0	2.8	5.7	7.8	1.2	0	0	-0.1	30	29	27	28	0.5	0.05	0	0
15:26	23.6	0	2.6	5.4	7.1	2.2	0	0	-0.2	30	30	28	29	0.5	0.05	0	0

Table 17. Case 6 (3.0M CuCl, 4.8M MgCl$_2$) Experimental Raw Data.

Time	Stream	N$_2$+O$_2$ Area	CO Area	Time (min.sec)	CO$_2$ Area	Time (min)
	2	59196	11300	3.51	34851	9.36
	2	58672	11162	3.58	34303	9.38
14:25	2	57956	11390	4.04	34775	9.4
14:43	9	62973	3876	3.53	35616	9.35
15:20	9	61737	2607	4.10	36446	9.41
15:25	6a	68981	2945	3.6	14470	9.52

APPENDIX F: Results Analysis—Material Balance

This program uses experimental measurements combined with theory (to account for physical absorption of CO_2, O_2, and N_2 into solution) to calculate stream compositions.
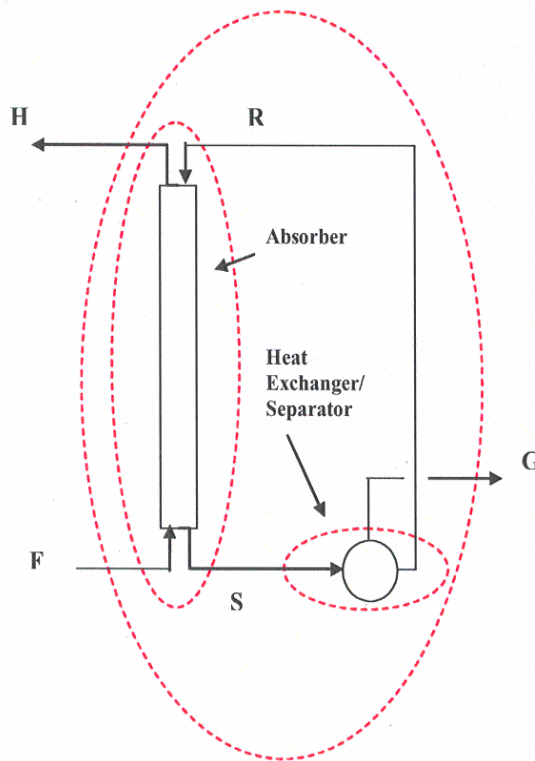
Notation: F = feed gas, H = column offgas, G = separated CO offgas, S = exiting column liquid (cool), R = heated liquid (R is cooled before re-entering the column in the actual process).

ORIGIN := 1

147

Henry's Constants (Perry's Handbook) for N_2, O_2, and CO_2 in Water (t = temperature, ℃)

$$t_1 := \begin{pmatrix} 0 \\ 5 \\ 10 \\ 15 \\ 20 \\ 25 \\ 30 \\ 35 \\ 40 \\ 45 \\ 50 \\ 60 \\ 70 \\ 80 \\ 90 \\ 100 \end{pmatrix} \quad H_{N2} := \begin{pmatrix} 5.29 \\ 5.97 \\ 6.68 \\ 7.38 \\ 8.04 \\ 8.65 \\ 9.24 \\ 9.85 \\ 10.4 \\ 10.9 \\ 11.3 \\ 12 \\ 12.5 \\ 12.6 \\ 12.6 \\ 12.6 \end{pmatrix} \cdot 10^4 \, atm \quad H_{O2} := \begin{pmatrix} 2.55 \\ 2.91 \\ 3.27 \\ 3.64 \\ 4.01 \\ 4.38 \\ 4.75 \\ 5.07 \\ 5.35 \\ 5.63 \\ 5.88 \\ 6.29 \\ 6.63 \\ 6.87 \\ 6.99 \\ 7.01 \end{pmatrix} \cdot 10^4 \, atm \quad t_2 := \begin{pmatrix} 0 \\ 5 \\ 10 \\ 15 \\ 20 \\ 25 \\ 30 \\ 35 \\ 40 \\ 45 \\ 50 \\ 60 \end{pmatrix} \quad H_{CO2} := \begin{pmatrix} 0.728 \\ 0.876 \\ 1.04 \\ 1.22 \\ 1.42 \\ 1.64 \\ 1.86 \\ 2.09 \\ 2.33 \\ 2.57 \\ 2.83 \\ 3.41 \end{pmatrix} \cdot 10^3 \, atm$$

Fit the Data

$vs1 := pspline(t_1, H_{N2})$ $Hen_{N2}(x) := interp(vs1, t_1, H_{N2}, x)$

$vs2 := pspline(t_1, H_{O2})$ $Hen_{O2}(x) := interp(vs2, t_1, H_{O2}, x)$

$vs3 := pspline(t_2, H_{CO2})$ $Hen_{CO2}(x) := interp(vs3, t_2, H_{CO2}, x)$

$i := 1 .. 101 \qquad tt_i := (i - 1) \cdot 1$

Henry's Constant (N2, O2)

H (atm) vs Temperature (°C)

——— H (N2)
- - - - H (O2)

Henry's Constant (CO2)

H (atm) vs Temperature (°C)

——— H (CO2)

149
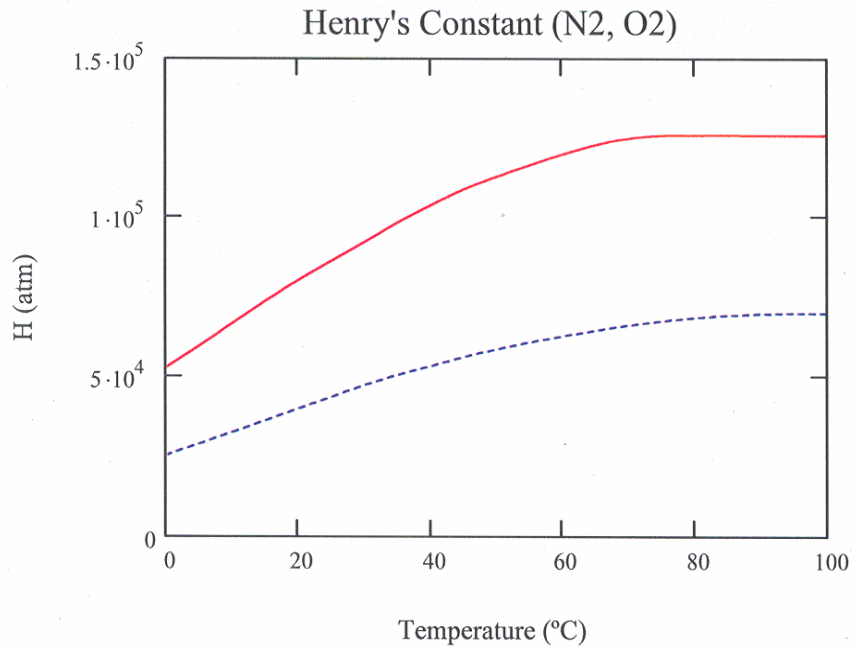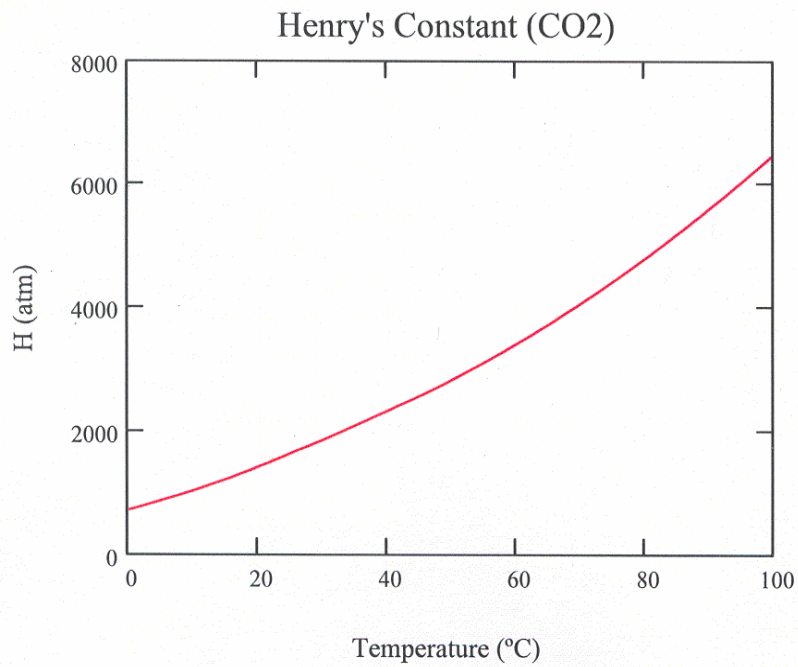
User Input

Indicated gauge pressures: $P_{g.F} := 30\text{psi}$ $P_{g.H} := 30\text{psi}$ $P_{g.G} := 29\text{psi}$ $P_{g.R} := 31\text{psi}$

Indicated temperatures (ºC): $T_{FF} := 25.8$ $T_{RR} := 77.7$ $T_{SS} := 15.8$

Indicated flow rates: $V_{F.I} := 0.5\dfrac{L}{min}$ $V_{LL} := 0.053\dfrac{gal}{min}$

Peak areas (column offgas): $k_{CO2\_CO} := 0.889$ $A_{CO2} := 35247$ $A_{CO} := 2088$

Composition: $y_{CO.F} := 0.111$ $y_{CO2.F} := 0.2999$ $y_{O2.F} := 0.02647$ $y_{N2.F} := 0.5626$

Composition check: $y := y_{CO.F} + y_{CO2.F} + y_{O2.F} + y_{N2.F}$ $y = 1.0000$

Constants

$R_g := 0.08206 L \cdot atm \cdot mol^{-1} \cdot K^{-1}$ (universal gas constant)

$P_{atm} := 12.3\text{psi}$ (atmospheric pressure)

Absolute Pressure

$P_F := P_{g.F} + P_{atm}$ $P_H := P_{g.H} + P_{atm}$ $P_G := P_{g.G} + P_{atm}$ $P_R := P_{g.R} + P_{atm}$

Absolute Temperature

$T_F := \left(T_{FF} + 273.15\right)K$ $T_S := \left(T_{SS} + 273.15\right)K$ $T_R := \left(T_{RR} + 273.15\right)K$

Actual Flow of feed gas at process conditions (adjusts for pressure, temperature, and molecular gas differences between actual process gas and what the gauge was calibrated for)

$$V_F := V_{F.I}\left(\dfrac{14.7\text{psi}}{P_F} \cdot \dfrac{T_F}{294.26K} \cdot \dfrac{29\dfrac{gm}{mol}}{33\dfrac{gm}{mol}}\right)^{0.5}$$ $V_F = 0.2785\dfrac{L}{min}$ (volumetric flow rate)

$n_F := P_F \cdot V_F \cdot R_g^{-1} \cdot T_F^{-1}$ $n_F = 0.0327\dfrac{mol}{min}$ (molar flow rate)

Calculate CO$_2$/CO molar ratio in column offgas

150

$$y_{CO2\_CO} := k_{CO2\_CO} \cdot \frac{A_{CO2}}{A_{CO}} \qquad y_{CO2\_CO} = 15.0070 \qquad \text{(response constant)}$$

Liquid Information

Reference:H:\Research\Appendix Material\App\App A Absorber Design.mcd(R)

$$V_L := V_{LL} \qquad\qquad V_L = 0.0530 \frac{gal}{min} \qquad\qquad \text{(redefine volumetric flow rate)}$$

$$\rho_L = 1.1808 \frac{gm}{mL} \qquad\qquad MW_L = 26.2413 \frac{gm}{mol} \qquad\qquad \text{(density, molecular weight of solution)}$$

$$n_L := V_L \cdot \rho_L \cdot MW_L^{-1} \qquad n_L = 9.0277 \frac{mol}{min} \qquad\qquad \text{(molar flow rate)}$$

$$n_{H2O} := n_L \cdot \frac{n_w}{n_{Tot}} \qquad n_{H2O} = 8.5498 \frac{mol}{min} \qquad \text{(molar flow rate of water--this is used in the material balance rather than total liquid since gases absorb into water)}$$

Calculate molar flow rate and partial pressures of feed stream:

$$n_{CO.F} := y_{CO.F} \cdot n_F \qquad n_{CO2.F} := y_{CO2.F} \cdot n_F \qquad n_{O2.F} := y_{O2.F} \cdot n_F \qquad n_{N2.F} := y_{N2.F} \cdot n_F$$

$$P_{CO.F} := y_{CO.F} \cdot P_F \qquad P_{CO2.F} := y_{CO2.F} \cdot P_F \qquad P_{O2.F} := y_{O2.F} \cdot P_F \qquad P_{N2.F} := y_{N2.F} \cdot P_F$$

Calculate mole fraction of gases physically absorbed into liquid in column (assumes: Henry's Law, gas absorption not affected by other gases (pure gas), gas achieves equilibrium with absorbed gas, and absorption into pure water)

$$x_{CO2.S} := \frac{P_{CO2.F}}{Hen_{CO2}(T_{SS})} \qquad x_{O2.S} := \frac{P_{O2.F}}{Hen_{O2}(T_{SS})} \qquad x_{N2.S} := \frac{P_{N2.F}}{Hen_{N2}(T_{SS})}$$

$$n_{CO2.S} := \frac{x_{CO2.S} \cdot n_{H2O}}{1 - x_{CO2.S}} \qquad n_{O2.S} := \frac{x_{O2.S} \cdot n_{H2O}}{1 - x_{O2.S}} \qquad n_{N2.S} := \frac{x_{N2.S} \cdot n_{H2O}}{1 - x_{N2.S}}$$

Assume a separation to calculate an initial guess for CO chemically absorbed into solution:

$$Sep := 0.9 \qquad\qquad n_{CO.S} := Sep \cdot n_{CO.F}$$

Assume all CO desorbs upon heating the liquid:

$$n_{CO.R} := 0 \frac{mol}{min}$$

Initial guess values for compositions of streams G and H:

$$n_{CO.G} := n_{CO.S} \qquad n_{CO2.G} := n_{CO2.S} \qquad n_{O2.G} := n_{O2.S} \qquad n_{N2.G} := n_{N2.S}$$

151

$$n_{CO.H} := n_{CO.F} \qquad n_{CO2.H} := n_{CO2.F} \qquad n_{O2.H} := n_{O2.F} \qquad n_{N2.H} := n_{N2.F}$$

$$n_G := n_{CO2.G} + n_{O2.G} + n_{N2.G} + n_{CO.G}$$

The following equations come from combining multiple material balance equations.

Given

$$n_{CO2.G} = \frac{P_{CO2.F} \cdot \dfrac{n_{H2O}}{Hen_{CO2}(T_{SS})}}{1 - \dfrac{P_{CO2.F}}{Hen_{CO2}(T_{SS})}} - \frac{n_{CO2.G} \cdot \dfrac{P_G}{n_G} \cdot \dfrac{n_{H2O}}{Hen_{CO2}(T_{RR})}}{1 - \dfrac{n_{CO2.G}}{Hen_{CO2}(T_{RR})} \cdot \dfrac{P_G}{n_G}}$$

$$n_{O2.G} = \frac{P_{O2.F} \cdot \dfrac{n_{H2O}}{Hen_{O2}(T_{SS})}}{1 - \dfrac{P_{O2.F}}{Hen_{O2}(T_{SS})}} - \frac{n_{O2.G} \cdot \dfrac{P_G}{n_G} \cdot \dfrac{n_{H2O}}{Hen_{O2}(T_{RR})}}{1 - \dfrac{n_{O2.G}}{Hen_{O2}(T_{RR})} \cdot \dfrac{P_G}{n_G}}$$

$$n_{N2.G} = \frac{P_{N2.F} \cdot \dfrac{n_{H2O}}{Hen_{N2}(T_{SS})}}{1 - \dfrac{P_{N2.F}}{Hen_{N2}(T_{SS})}} - \frac{n_{N2.G} \cdot \dfrac{P_G}{n_G} \cdot \dfrac{n_{H2O}}{Hen_{N2}(T_{RR})}}{1 - \dfrac{n_{N2.G}}{Hen_{N2}(T_{RR})} \cdot \dfrac{P_G}{n_G}}$$

$$n_G = n_{CO.G} + n_{CO2.G} + n_{O2.G} + n_{N2.G} \qquad n_{CO.G} = n_{CO.F} - n_{CO.H} \qquad n_{CO.G} = n_{CO.S}$$

$$n_{CO2.H} = n_{CO2.F} + \frac{n_{CO2.G} \cdot \dfrac{P_G}{n_G} \cdot \dfrac{n_{H2O}}{Hen_{CO2}(T_{RR})}}{1 - \dfrac{n_{CO2.G}}{Hen_{CO2}(T_{RR})} \cdot \dfrac{P_G}{n_G}} - \frac{P_{CO2.F} \cdot \dfrac{n_{H2O}}{Hen_{CO2}(T_{SS})}}{1 - \dfrac{P_{CO2.F}}{Hen_{CO2}(T_{SS})}}$$

$$n_{O2.H} = n_{O2.F} + \frac{n_{O2.G} \cdot \dfrac{P_G}{n_G} \cdot \dfrac{n_{H2O}}{Hen_{O2}(T_{RR})}}{1 - \dfrac{n_{O2.G}}{Hen_{O2}(T_{RR})} \cdot \dfrac{P_G}{n_G}} - \frac{P_{O2.F} \cdot \dfrac{n_{H2O}}{Hen_{O2}(T_{SS})}}{1 - \dfrac{P_{O2.F}}{Hen_{O2}(T_{SS})}}$$

152

$$n_{N2.H} = n_{N2.F} + \frac{n_{N2.G} \cdot \dfrac{P_G}{n_G} \cdot \dfrac{n_{H2O}}{Hen_{N2}(T_{RR})}}{1 - \dfrac{n_{N2.G}}{Hen_{N2}(T_{RR})} \cdot \dfrac{P_G}{n_G}} - \frac{P_{N2.F} \cdot \dfrac{n_{H2O}}{Hen_{N2}(T_{SS})}}{1 - \dfrac{P_{N2.F}}{Hen_{N2}(T_{SS})}}$$

$$n_{CO.H} = \frac{n_{CO2.H}}{y_{CO2\_CO}}$$

$$Ans := Find\left(n_{CO.G}, n_{CO2.G}, n_{O2.G}, n_{N2.G}, n_G, n_{CO.H}, n_{CO2.H}, n_{O2.H}, n_{N2.H}, n_{CO.S}\right)$$

Remaining Stream Values

Using the solution, calculate remaining stream values:

$n_{CO.G} := Ans_1$ $\qquad n_{CO2.G} := Ans_2$ $\qquad n_{O2.G} := Ans_3$ $\qquad n_{N2.G} := Ans_4$ $\qquad n_G := Ans_5$

$n_{CO.H} := Ans_6$ $\qquad n_{CO2.H} := Ans_7$ $\qquad n_{O2.H} := Ans_8$ $\qquad n_{N2.H} := Ans_9$ $\qquad n_{CO.S} := Ans_{10}$

$n_{CO2.R} := n_{CO2.S} - n_{CO2.G}$ $\qquad n_{O2.R} := n_{O2.S} - n_{O2.G}$ $\qquad n_{N2.R} := n_{N2.S} - n_{N2.G}$

$$y_{CO.G} := \frac{n_{CO.G}}{n_G} \qquad y_{CO2.G} := \frac{n_{CO2.G}}{n_G} \qquad y_{O2.G} := \frac{n_{O2.G}}{n_G} \qquad y_{N2.G} := \frac{n_{N2.G}}{n_G}$$

$$P_{CO.G} := y_{CO.G} \cdot P_G \qquad P_{CO2.G} := y_{CO2.G} \cdot P_G \qquad P_{O2.G} := y_{O2.G} \cdot P_G \qquad P_{N2.G} := y_{N2.G} \cdot P_G$$

$$Sep_{CO} := \frac{n_{CO.G}}{n_{CO.F}} \qquad Sep_{CO2} := \frac{n_{CO2.G}}{n_{CO2.F}} \qquad Sep_{O2} := \frac{n_{O2.G}}{n_{O2.F}} \qquad Sep_{N2} := \frac{n_{N2.G}}{n_{N2.F}}$$

$$n_R := n_{CO.R} + n_{CO2.R} + n_{O2.R} + n_{N2.R}$$

$$n_H := n_{CO.H} + n_{CO2.H} + n_{O2.H} + n_{N2.H}$$

$$n_S := n_{CO.S} + n_{CO2.S} + n_{O2.S} + n_{N2.S}$$

Results

$$F := stack\left(n_{CO.F}, n_{CO2.F}, n_{O2.F}, n_{N2.F}, n_F\right)$$

$$S := stack\left(n_{CO.S}, n_{CO2.S}, n_{O2.S}, n_{N2.S}, n_S\right)$$

$$R := stack\left(n_{CO.R}, n_{CO2.R}, n_{O2.R}, n_{N2.R}, n_R\right)$$

$$G := stack\left(n_{CO.G}, n_{CO2.G}, n_{O2.G}, n_{N2.G}, n_G\right)$$

$$H := stack\left(n_{CO.H}, n_{CO2.H}, n_{O2.H}, n_{N2.H}, n_H\right)$$

153

$P_{GG} := \text{stack}\left(P_{CO.G}, P_{CO2.G}, P_{O2.G}, P_{N2.G}\right)$

$y_G := \text{stack}\left(y_{CO.G}, y_{CO2.G}, y_{O2.G}, y_{N2.G}\right)$

$Sep := \text{stack}\left(Sep_{CO}, Sep_{CO2}, Sep_{O2}, Sep_{N2}\right)$

$P_{FF} := \text{stack}\left(P_{CO.F}, P_{CO2.F}, P_{O2.F}, P_{N2.F}\right)$

$\text{Pressures} := \text{augment}\left(P_{FF}, P_{GG}\right)$

$\text{Molar\_Flows} := \text{augment}(F, S, G, R, H)$

$$
\begin{array}{ccccc}
F & S & G & R & H
\end{array}
$$

$$
\text{Molar\_Flows} =
\begin{pmatrix}
3.6272 \times 10^{-3} & 3.1961 \times 10^{-3} & 3.1961 \times 10^{-3} & 0.0000 & 4.3109 \times 10^{-4} \\
9.7999 \times 10^{-3} & 5.9061 \times 10^{-3} & 3.3306 \times 10^{-3} & 2.5755 \times 10^{-3} & 6.4693 \times 10^{-3} \\
8.6497 \times 10^{-4} & 1.7608 \times 10^{-5} & 1.6732 \times 10^{-5} & 8.7611 \times 10^{-7} & 8.4824 \times 10^{-4} \\
0.0184 & 1.8488 \times 10^{-4} & 1.7978 \times 10^{-4} & 5.1001 \times 10^{-6} & 0.0181 \\
0.0327 & 9.3047 \times 10^{-3} & 6.7232 \times 10^{-3} & 2.5814 \times 10^{-3} & 0.0259
\end{pmatrix}
\frac{mol}{min}
\begin{pmatrix}
CO \\ CO2 \\ O2 \\ N2 \\ Tot
\end{pmatrix}
$$

$$
\begin{array}{cc}
F & G
\end{array}
$$

$$
\text{Pressures} =
\begin{pmatrix}
4.6953 & 19.6333 \\
12.6858 & 20.4595 \\
1.1197 & 0.1028 \\
23.7980 & 1.1044
\end{pmatrix} psi
\qquad
y_G =
\begin{pmatrix}
0.4754 \\
0.4954 \\
0.0025 \\
0.0267
\end{pmatrix}
\qquad
Sep =
\begin{pmatrix}
88.12 \\
33.99 \\
1.93 \\
0.98
\end{pmatrix} \%
\begin{pmatrix}
CO \\ CO2 \\ O2 \\ N2
\end{pmatrix}
$$

Calculate the experimental $K_x a$ (this will be less than design):

$$
A_{cs} := \pi \cdot \frac{(1\,in)^2}{4} \qquad p := 1..5 \qquad G' := \sum_{p=2}^{4} \left(\text{Molar\_Flows}^{\langle 1 \rangle}\right)_p \qquad G' = 0.0290 \frac{mol}{min}
$$

$$
L' := n_L \qquad L' = 9.0277 \frac{mol}{min}
$$

$$
y_{out} := \frac{n_{CO.H}}{n_H} \qquad y_{out} = 0.0166 \qquad Y_{out} := \frac{y_{out}}{1 - y_{out}} \qquad Y_{out} = 0.0169
$$

$$
x_{out} := \frac{n_{CO.S}}{n_L} \qquad x_{out} = 0.0004 \qquad X_{out} := \frac{x_{out}}{1 - x_{out}} \qquad X_{out} = 0.0004
$$

154

$$Y(X) := X \cdot \left(\frac{L'}{G'}\right) + Y_{out} - X_{in} \cdot \left(\frac{L'}{G'}\right)$$

$$X_{eq}(X) := \frac{\dfrac{Y(X)}{K_N \cdot (1+Y(X))}}{1 - \dfrac{Y(X)}{K_N \cdot (1 + Y(X))}}$$

$$N_{OL} := \int_{X_{in}}^{X_{out}} \frac{1}{X_{eq}(X) - X}\, dX \qquad N_{OL} = 0.3037$$

$$Kxa\_predict := Kxa \qquad Kxa\_predict = 530.0527\ \frac{mol}{m^3 \cdot s}$$

$$Kxa\_exp := \frac{n_L}{A_{cs}} \cdot \frac{N_{OL}}{4ft} \qquad Kxa\_exp = 73.9679\ \frac{mol}{m^3 \cdot s}$$

Use the experimental $K_x a$ to predict height required to remove 99% CO:

$$CO_{sep} := 0.99$$

$$x_{out} := \frac{CO_{sep} \cdot n_{CO.F}}{n_L + CO_{sep} \cdot n_{CO.F}} \qquad x_{out} = 0.0004 \qquad X_{out} := \frac{x_{out}}{1 - x_{out}} \qquad X_{out} = 0.0004$$

$$y_{out} := \frac{\left(1 - CO_{sep}\right) \cdot n_{CO.F}}{n_H + \left(1 - CO_{sep}\right) \cdot n_{CO.F}} \qquad y_{out} = 0.0014 \qquad Y_{out} := \frac{y_{out}}{1 - y_{out}} \qquad Y_{out} = 0.0014$$

Operating line and equilibrium equations:

$$Y(X) := X \cdot \left(\frac{L'}{G'}\right) + Y_{out} - X_{in} \cdot \left(\frac{L'}{G'}\right)$$

$$X_{eq}(X) := \frac{\dfrac{Y(X)}{K_N \cdot (1+Y(X))}}{1 - \dfrac{Y(X)}{K_N \cdot (1 + Y(X))}}$$

Predicted height:

$$N_{OL} := \int_{X_{in}}^{X_{out}} \frac{1}{X_{eq}(X) - X}\, dX \qquad N_{OL} = 0.6791 \qquad l_T := \frac{n_L}{A_{cs} \cdot Kxa\_exp} \cdot N_{OL} \qquad l_T = 8.9444\ ft$$

$$n_{CO.S} := x_{out} \cdot n_L \qquad \frac{n_{CO.S}}{n_{CO.F}} = 0.9896$$

Check

$$\varepsilon := 10^{-3} \frac{mol}{min}$$

$$c_1 := if\left[\left|\left(n_{CO.F} + n_{CO.R}\right) - \left(n_{CO.H} + n_{CO.S}\right)\right| < \varepsilon, 1, 0\right] \qquad\qquad c_1 = 1.0000$$

$$c_2 := if\left[\left|\left(n_{CO2.F} + n_{CO2.R}\right) - \left(n_{CO2.H} + n_{CO2.S}\right)\right| < \varepsilon, 1, 0\right] \qquad\qquad c_2 = 1.0000$$

$$c_3 := if\left[\left|\left(n_{O2.F} + n_{O2.R}\right) - \left(n_{O2.H} + n_{O2.S}\right)\right| < \varepsilon, 1, 0\right] \qquad\qquad c_3 = 1.0000$$

$$c_4 := if\left[\left|\left(n_{N2.F} + n_{N2.R}\right) - \left(n_{N2.H} + n_{N2.S}\right)\right| < \varepsilon, 1, 0\right] \qquad\qquad c_4 = 1.0000$$

$$c_5 := if\left[\left|n_{CO.S} - \left(n_{CO.R} + n_{CO.G}\right)\right| < \varepsilon, 1, 0\right] \qquad\qquad c_5 = 1.0000$$

$$c_6 := if\left[\left|n_{CO2.S} - \left(n_{CO2.R} + n_{CO2.G}\right)\right| < \varepsilon, 1, 0\right] \qquad\qquad c_6 = 1.0000$$

$$c_7 := if\left[\left|n_{O2.S} - \left(n_{O2.R} + n_{O2.G}\right)\right| < \varepsilon, 1, 0\right] \qquad\qquad c_7 = 1.0000$$

$$c_8 := if\left[\left|n_{N2.S} - \left(n_{N2.R} + n_{N2.G}\right)\right| < \varepsilon, 1, 0\right] \qquad\qquad c_8 = 1.0000$$

$$c_9 := if\left[\left|n_{CO.F} - \left(n_{CO.H} + n_{CO.G}\right)\right| < \varepsilon, 1, 0\right] \qquad\qquad c_9 = 1.0000$$

$$c_{10} := if\left[\left|n_{CO2.F} - \left(n_{CO2.H} + n_{CO2.G}\right)\right| < \varepsilon, 1, 0\right] \qquad\qquad c_{10} = 1.0000$$

$$c_{11} := if\left[\left|n_{O2.F} - \left(n_{O2.H} + n_{O2.G}\right)\right| < \varepsilon, 1, 0\right] \qquad\qquad c_{11} = 1.0000$$

$$c_{12} := if\left[\left|n_{N2.F} - \left(n_{N2.H} + n_{N2.G}\right)\right| < \varepsilon, 1, 0\right] \qquad\qquad c_{12} = 1.0000$$

$$c_{13} := if\left(\left|n_{CO2.H} - y_{CO2\_CO} \cdot n_{CO.H}\right| < \varepsilon, 1, 0\right) \qquad\qquad c_{13} = 1.0000$$

$$c_{14} := if\left[\left|\left(y_{CO.G} + y_{CO2.G} + y_{O2.G} + y_{N2.G}\right) - 1\right| < \varepsilon \cdot \frac{min}{mol}, 1, 0\right] \qquad\qquad c_{14} = 1.0000$$

$$Check := \left(c_1 \wedge c_2 \wedge c_3 \wedge c_4 \wedge c_5 \wedge c_6 \wedge c_7 \wedge c_8 \wedge c_9 \wedge c_{10} \wedge c_{11} \wedge c_{12} \wedge c_{13}\right)$$

$$Check = 1.0000$$

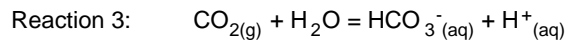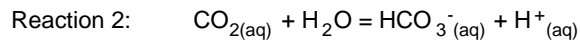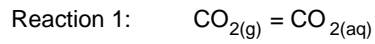$$Check := if(Check = 1, "converged", "oops!")$$

This checks that all equations are satisfied, not whether values are reasonable (i.e., negative values).

APPENDIX G: Absorption of CO_2 and Solution Acidity

This program calculates the acidity of the process solution due to the dissolved CO_2, and determines whether increasing the acidity of the solution would decrease the amount of CO_2 dissolved.

Definitions: $\quad ORIGIN := 1 \qquad molal := mol \cdot (1000gm)^{-1} \qquad bar := 0.98692atm \qquad i := 1..12$

Data (from ASME Handbook on Water Technology for Thermal Power Systems):

Reaction 1: $\quad CO_{2(g)} = CO_{2(aq)}$

Reaction 2: $\quad CO_{2(aq)} + H_2O = HCO_{3\ (aq)}^{-} + H^{+}_{(aq)}$

Reaction 3: $\quad CO_{2(g)} + H_2O = HCO_{3\ (aq)}^{-} + H^{+}_{(aq)}$

$$
t := \begin{pmatrix} 25 \\ 50 \\ 75 \\ 100 \\ 125 \\ 150 \\ 175 \\ 200 \\ 225 \\ 250 \\ 275 \\ 300 \end{pmatrix}
\qquad
K_1 := \begin{pmatrix} 0.034 \\ 0.019 \\ 0.013 \\ 0.01 \\ 8.67 \times 10^{-3} \\ 8.16 \times 10^{-3} \\ 7.98 \times 10^{-3} \\ 8.7 \times 10^{-3} \\ 9.62 \times 10^{-3} \\ 0.011 \\ 0.013 \\ 0.016 \end{pmatrix} \frac{molal}{bar}
\qquad
pK_2 := \begin{pmatrix} 6.366 \\ 6.311 \\ 6.343 \\ 6.433 \\ 6.569 \\ 6.742 \\ 6.948 \\ 7.188 \\ 7.460 \\ 7.763 \\ 8.098 \\ 8.465 \end{pmatrix}
$$

$$K_2 := 10^{-pK_2} \cdot molal$$

$$K_3 := \overrightarrow{(K_1 \cdot K_2)}$$

$\text{Hen} := K_1^{-1}$ $P_{CO2.F} := 0.2999(30\text{psi} + 12.4\text{psi})$

<u>Find the pH</u> of initially neutral water in contact with CO_2:

$m_{CO2} := \dfrac{P_{CO2.F}}{\text{Hen}}$ (molality of CO2 in water)

Initial guesses: $H_{ion} := 10^{-6}\text{molal}$ $HCO3 := 0.003\text{molal}$ $OH := 10^{-8}\text{molal}$

Convert to log to help mathcad's given block:

$x_H := \ln\left(H_{ion}\cdot\text{molal}^{-1}\right)$ $x_{HCO3} := \ln\left(HCO3\cdot\text{molal}^{-1}\right)$ $x_{OH} := \ln\left(OH\cdot\text{molal}^{-1}\right)$

Given

$x_H + x_{OH} = \ln\left(10^{-14}\right)$ (water hydrolysis equation)

$x_{HCO3} + x_H - \ln\left(P_{CO2.F}\text{bar}^{-1}\right) = \ln\left(K_{3_1}\cdot\text{bar}\cdot\text{molal}^{-2}\right)$ (equilibrium relation of reaction 3)

$-\exp\left(x_{OH}\right) + \exp\left(x_H\right) - \exp\left(x_{HCO3}\right) = 0$ (charge balance)

$\text{Ans} := \text{Find}\left(x_{OH}, x_H, x_{HCO3}\right)$

$\text{Ans} = \begin{pmatrix} -23.151 \\ -9.086 \\ -9.086 \end{pmatrix}$ $m_c := \exp(\text{Ans})\cdot\text{molal}$ $m_c = \begin{pmatrix} 8.827\times 10^{-11} \\ 1.133\times 10^{-4} \\ 1.133\times 10^{-4} \end{pmatrix}\text{molal}$

$pH := -\log\left(m_{c_2}\cdot\text{molal}^{-1}\right)$ $pH = 3.946$ (note: molality ~ molarity for H$^+$)

Because this pH is far from neutral, the following procedure can be used to calculate pH:

	initial moles	final moles
CO_2	m_{CO2}	$m_{CO2} - \xi$
HCO_3^-	0	ξ
H+	0	ξ

The molality of CO_2, m_{CO2}, is calculated from the Henry's constant.

At equilibrium (final moles): $K_2 = \dfrac{m_{HCO3}\cdot m_H}{m_{CO2}} = \dfrac{\xi^2}{m_{CO2} - \xi}$

158

Solve for ξ ($\xi = m_H$) and pH:

$$m_H := \frac{-K_2 \cdot molal^{-1} + \sqrt{\left(K_2 \cdot molal^{-1}\right)^2 - 4 \cdot -m_{CO2} \cdot K_2 \cdot molal^{-2}}}{2} \cdot molal$$

$$pH := -\log\left(m_H \cdot molal^{-1}\right) \qquad pH =$$

	1
1	3.947
2	4.046
3	4.144
4	4.246
5	4.345
6	4.445
7	4.552
8	4.653
9	4.767
10	4.89
11	5.021
12	5.159

<u>Calculate the total molality as a function of pH and temperature</u>

$j := 1 .. 70 \qquad pH_j := 1 + 0.1 \cdot j$ (pH range)

$k := 1 .. 61 \qquad vs1 := cspline(t, K_1) \qquad k_1(x) := interp(vs1, t, K_1, x)$ (fits an equation to the data above, as a function of temperature)

$vs2 := cspline(t, K_2) \qquad k_2(x) := interp(vs2, t, K_2, x)$

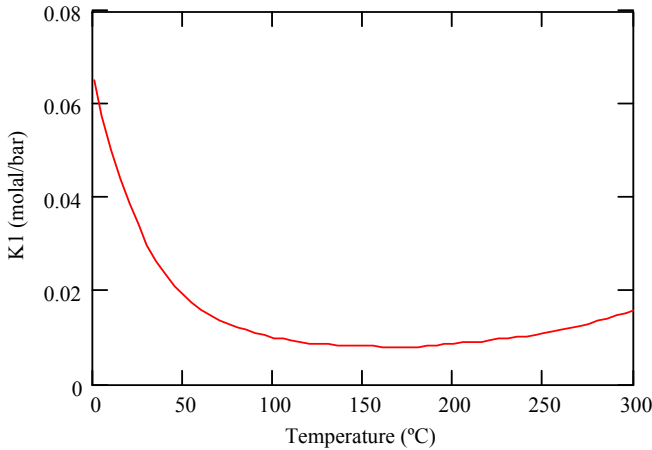$vs3 := cspline(t, K_3) \qquad k_3(x) := interp(vs3, t, K_3, x)$

$tt_k := 5 \cdot (k - 1)$ (temperature range)

Total molality as a function of CO $_2$ partial pressure, pH, and temperature:

$$m_{tot}\left(ph,p_{CO2},x\right) := p_{CO2} \cdot k_1(x) + \frac{k_3(x) \cdot p_{CO2}}{\left(10^{-ph}\right) \cdot molal} \qquad\qquad p_{CO2} := P_{CO2.F}$$

Molality = f(pH, T, CO2)
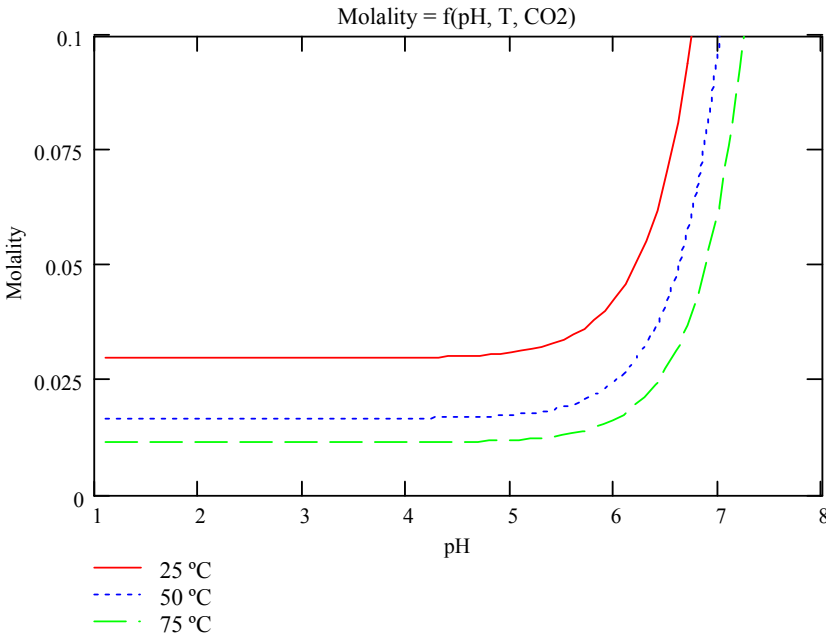
The plot shows that once the solution has reached a pH of about 5 (and this system is at least that low), the molality changes very little upon increasing the acidity.